RESEARCH REPORT

HEALTH EFFECTS INSTITUTE

Number 147
April 2010

Atmospheric Transformation of Diesel Emissions

Barbara Zielinska, Shar Samy, Jacob D. McDonald, and JeanClare Seagrave

Atmospheric Transformation of Diesel Emissions

Barbara Zielinska, Shar Samy, Jacob D. McDonald, and JeanClare Seagrave

with a Critique by the HEI Health Review Committee

Research Report 147

Health Effects Institute

Boston, Massachusetts

Trusted Science • Cleaner Air • Better Health

Publishing history: The Web version of this document was posted at *www.healtheffects.org* in April 2010.

Citation for document:

Zielinska B, Samy S, McDonald JD, Seagrave J. 2010. Atmospheric Transformation of Diesel Emissions. HEI Research Report 147. Health Effects Institute, Boston, MA.

 Asterisk Typographics, Barre, Vt., Compositor. Printed by Recycled Paper Printing, Boston, Mass. Library of Congress Catalog Number for the HEI Report Series: WA 754 R432.

Cover paper: made with at least 55% recycled content, of which at least 30% is post-consumer waste; free of acid and elemental chlorine. Text paper: made with 100% post-consumer waste recycled content; acid free; no chlorine used in processing. The book is printed with soy-based inks and is of permanent archival quality.

CONTENTS

Research Report 147

ABOUT HEI

The Health Effects Institute is a nonprofit corporation chartered in 1980 as an independent research organization to provide high-quality, impartial, and relevant science on the effects of air pollution on health. To accomplish its mission, the institute

- Identifies the highest-priority areas for health effects research;
- Competitively funds and oversees research projects;
- Provides intensive independent review of HEI-supported studies and related research;
- Integrates HEI's research results with those of other institutions into broader evaluations; and
- Communicates the results of HEI research and analyses to public and private decision makers.

HEI receives half of its core funds from the U.S. Environmental Protection Agency and half from the worldwide motor vehicle industry. Frequently, other public and private organizations in the United States and around the world also support major projects or certain research programs. HEI has funded more than 280 research projects in North America, Europe, Asia, and Latin America, the results of which have informed decisions regarding carbon monoxide, air toxics, nitrogen oxides, diesel exhaust, ozone, particulate matter, and other pollutants. These results have appeared in the peer-reviewed literature and in more than 200 comprehensive reports published by HEI.

HEI's independent Board of Directors consists of leaders in science and policy who are committed to fostering the public–private partnership that is central to the organization. The Health Research Committee solicits input from HEI sponsors and other stakeholders and works with scientific staff to develop a Five-Year Strategic Plan, select research projects for funding, and oversee their conduct. The Health Review Committee, which has no role in selecting or overseeing studies, works with staff to evaluate and interpret the results of funded studies and related research.

All project results and accompanying comments by the Health Review Committee are widely disseminated through HEI's Web site (*www.healtheffects.org*), printed reports, newsletters, and other publications, annual conferences, and presentations to legislative bodies and public agencies.

ABOUT THIS REPORT

Research Report 147, *Atmospheric Transformation of Diesel Emissions*, presents a research project funded by the Health Effects Institute and conducted by Dr. Barbara Zielinska of the Division of Atmospheric Sciences, Desert Research Institute, Reno, Nevada, and her colleagues. This report contains three main sections.

The HEI Statement, prepared by staff at HEI, is a brief, nontechnical summary of the study and its findings; it also briefly describes the Health Review Committee's comments on the study.

The Investigators' Report, prepared by Zielinska and colleagues, describes the scientific background, aims, methods, results, and conclusions of the study.

The Critique is prepared by members of the Health Review Committee with the assistance of HEI staff; it places the study in a broader scientific context, points out its strengths and limitations, and discusses remaining uncertainties and implications of the study's findings for public health and future research.

This report has gone through HEI's rigorous review process. When an HEI-funded study is completed, the investigators submit a draft final report presenting the background and results of the study. This draft report is first examined by outside technical reviewers and a biostatistician. The report and the reviewers' comments are then evaluated by members of the Health Review Committee, an independent panel of distinguished scientists who have no involvement in selecting or overseeing HEI studies. During the review process, the investigators have an opportunity to exchange comments with the Review Committee and, as necessary, to revise their report. The Critique reflects the information provided in the final version of the report.

HEI STATEMENT

Synopsis of Research Report 147

Atmospheric Transformation of Diesel Emissions

BACKGROUND

Diesel exhaust (DE) is an important contributor to air pollution and consists of a complex mixture of hundreds of compounds in either gas or particle form. After emission, DE undergoes chemical and physical transformations, or "aging," in the atmosphere as well as dispersion and transport. The aging process depends on the environment into which the DE is emitted; the atmosphere contains many compounds, including oxidizing and nitrating radicals, as well as organic and inorganic compounds from sources other than diesel engines. These compounds can influence the chemical composition and toxicity of DE as well as how long its various components remain in the atmosphere. Because of substantial changes in diesel engine technology and after-treatment over the past decade, there is a need to evaluate the newer technologies, including their emissions, the atmospheric processing of their emissions, and the corresponding health effects.

In response to Request for Preliminary Applications 98-6, "Health Effects of Air Pollution," Dr. Barbara Zielinska of the Desert Research Institute in Reno, Nevada, and her colleagues submitted an application to study the effects of photochemical transformations on DE constituents and whether such changes in chemical and physical form would be reflected in changes in toxicity. The investigators' atmospheric aging experiments would be conducted at the European Photoreactor (EUPHORE) outdoor simulation chamber in Valencia, Spain. Samples would then be shipped to Dr. Zielinska's laboratory in the United States for detailed chemical analyses and to her collaborator Dr. JeanClare Seagrave at the Lovelace Respiratory Research Institute in Albuquerque, New Mexico, for toxicologic experiments in rodents. The HEI Health Research Committee thought that Dr. Zielinska's approach to studying the photochemical transformations of DE and their potential effects on its toxicity was novel and likely to produce interesting results. The Committee recommended the proposed study for funding, with a strong recommendation that the investigators use a modern diesel engine.

APPROACH

DE was generated at EUPHORE using a 2003-model-year Ford light-duty diesel engine that was run on a dynamometer at about 50% load. EUPHORE has two outdoor simulation chambers with a volume of about 200 m^3 and a retractable cover that allows atmospheric reactions to take place in daylight (allowing photochemical reactions to occur) or in the dark, simulating nighttime conditions. In addition to DE, several compounds (precursors to hydroxyl [OH] or nitrate [NO_3] radicals, toluene, or a mixture of volatile organic compounds [VOCs]) were added to the atmospheric mixture to create various aging conditions. The mixture was then allowed to react for 3 to 5 hours; after completion of the reactions, the chamber cover was closed (if open), and integrated air samples were collected overnight using Teflon filters to collect particles and XAD adsorbent-resin cartridges to collect gaseous species. Parallel samples were collected for detailed chemical analyses and in vivo toxicologic experiments.

Zielinska and colleagues conducted three sampling campaigns, in January 2005, May 2005, and May and June 2006. During the first campaign, the investigators found that high concentrations of nitrogen oxides (NO_x) were interfering with the experiments and therefore decided to develop a NO_x denuder to remove the majority of NO_x from the engine exhaust before its injection into the chamber. A particular challenge was to find an efficient method of removing NO_x without substantially altering the concentrations and properties of the particulate matter (PM) in the exhaust. In the end, cobalt

This Statement, prepared by the Health Effects Institute, summarizes a research study funded by HEI and conducted by Dr. Barbara Zielinska of the Division of Atmospheric Sciences, Desert Research Institute, Reno, NV, and colleagues. Research Report 147 contains both the detailed Investigators' Report and a Critique of the study prepared by the Institute's Health Review Committee.

oxide was selected for use as the absorption material to capture the NO_x from the exhaust stream. After the second sampling campaign, the design of the NO_x denuder was improved further to allow even more efficient removal of NO_x for use in the third, final campaign.

The investigators measured a large number of compounds known to be present in DE, including alkanes, polycyclic aromatic hydrocarbons (PAHs), nitro-PAHs, and polar compounds, as well as hopanes and steranes that are known to be present in lubricating oil. They also measured elemental carbon (EC) and organic carbon (OC), NO_3, and sulfate.

Two series of toxicologic experiments were conducted. The investigators used rats initially but, after the third sampling campaign, switched to mice because the sample masses were insufficient for intratracheal instillation in rats (mice require less sample mass because of their much lower body weight compared with that of rats). The animals were killed 24 hours after intratracheal instillation for evaluation of markers of inflammation in blood and lung lavage fluid as well as signs of inflammation, cytotoxicity, and parenchymal changes in lung tissue. The mice, in addition, were evaluated for markers of oxidative stress and macrophage phagocytosis in lung tissue and lavage fluid cells, respectively.

RESULTS AND INTERPRETATION

The investigators reported that most of the exposures in daylight as well as the exposures in the dark with added NO_3-radical precursors led to particle formation and increased concentrations of semivolatile organic compounds. These results were evident in the increased fraction of OC in the samples and the increased ratios of OC to EC compared with atmospheres containing only DE. The addition of toluene or VOC in daylight led to the highest increases in organic compounds, including the formation of pyrolized OC, which is indicative of the presence of highly polar or oligomeric organic compounds. The investigators reported increased concentrations of many organic compounds, such as 9-fluorenone and other oxy-PAHs; nitro-naphthalene and other nitro-PAHs; certain nitropyrenes and nitrofluoranthenes; and polar compounds, such as heptanoic acid and oxalic acid. In addition, exposures in daylight led to the formation of ozone (O_3) and formic acid. On the other hand, concentrations of primary pollutants such as alkanes were reduced, indicating that these compounds had reacted to form secondary organics.

The investigators examined toxicologic outcomes using samples collected in the second and third campaigns. Some general patterns appeared that were consistent in both rats and mice. For example, the investigators observed increased cytotoxicity after the addition of toluene to DE in daylight, increased histopathologic indications of inflammation after the addition of OH radicals or toluene to DE in daylight, and increased concentrations of polymorphonuclear neutrophils in lavage fluid (also an indicator of inflammation) after the addition of OH radicals to DE in daylight. Other results were less consistent. Concentrations of protein in lavage fluid, for example, increased in rats but to a lesser extent in mice exposed to DE aged in daylight. Markers of oxidative stress in mice yielded mixed results: significant changes were observed under some exposure conditions but not others, and in some cases the changes were the opposite of those that would have been expected. The investigators concluded that the addition of toluene and, to a lesser extent, OH-radical precursors to DE in daylight increased the toxic potential of the samples compared with DE aged in daylight without any additional compounds.

In its independent review of the study, the HEI Health Review Committee stated that Dr. Zielinska and colleagues had successfully conducted a complex study to characterize the atmospheric transformations of DE under the influence of sunlight, O_3, radicals, and organic compounds. The report presented novel results on the atmospheric aging of DE derived from a 2003-model-year light-duty engine under a variety of conditions. Strengths of the study design included the use of state-of-the-art atmospheric chamber facilities, the use of a realistic set of atmospheric aging conditions, and the analysis of a large number of organic compounds. The Committee noted that a minor criticism might be that the use of a light-duty engine could be considered less relevant to the United States, which has a much lower percentage of light-duty diesel engines than Europe does.

The Committee commended the investigators' efforts to develop an efficient NO_x denuder but concluded that the additional work had led to a reduced number of experiments and a set of somewhat disparate results that remain predominantly descriptive and qualitative in nature. The results of the first sampling campaign, conducted without a

NO_x denuder, were not representative of reactions that might take place in ambient air. In addition, results from the second and third sampling campaigns are difficult to compare because of the use of two different denuders and rodent species.

The Committee agreed with the investigators' conclusion that exposing DE to daylight (with or without additional VOCs), as well as adding NO_3-radical precursors to DE in the dark, resulted in increased particle mass concentrations and the formation of secondary organic compounds, such as oxy-PAHs and nitro-PAHs. The Committee thought that the list of compounds analyzed was extensive but agreed with the investigators that future studies could further characterize the formation of secondary products by, for example, analyzing additional organic compounds in PM and measuring additional carbonyls, such as glyoxal and acetaldehyde. One of the limiting factors of the study was the variable number of replicate experiments. Some atmospheric aging conditions were tested only once; others were tested up to four times. It thus remains difficult to assess the extent of variability in the formation of certain compounds within and among the experimental conditions. Although the investigators were appropriately cautious in their interpretations, further research will be needed to obtain a more complete, systematic, and quantitative set of results.

The assessment of the toxicity of aged DE samples was considered well designed. Samples to be tested were collected using filters and XAD cartridges to capture both particles and gaseous components, an important improvement over many older studies of DE that assessed the effects of diesel particles only. The investigators observed increased inflammation under some conditions; changes in biochemical measures correlated fairly well with changes in histopathologic findings. The Committee noted that several endpoints were used as indicators of oxidative stress and that some of these have been shown to be more reliable than others. This variation could account for certain discrepancies in the results, such as changes in heme oxygenase-1 and oxidized glutathione but not in thiobarbituric-acid–reacting substances. It remains difficult to draw firm conclusions other than that atmospheric aging of DE generally seemed to increase the toxicity of the samples. Further research will be needed to evaluate which of the atmospheric reaction products might be contributing to the increased toxicity.

In summary, this study has generated a large, complex data set on the detailed chemical composition of samples collected under a variety of experimental conditions intended to simulate real-world atmospheric aging of DE. The investigators observed that atmospheric aging under certain conditions, such as in daylight (which facilitates photochemical reactions) or with the addition of radical precursors (which facilitates chemical reactions), led to the formation of particles and secondary organic compounds. Atmospheric-aging conditions generally also increased the toxicity of samples, as indicated by increased concentrations of markers of inflammation and oxidative stress in exposed rodents. However, it remains difficult to relate specific chemical-reaction products to increases in toxicity. Further systematic research on the composition and toxicity of DE and other pollution mixtures after atmospheric transformation is needed to provide more quantitative answers. Importantly, such research should cover the most recent diesel engine technologies that comply with the 2007 and 2010 PM and NO_x standards in the United States and that have much lower emissions compared with those of older technologies, including the 2003 engine used in this study.

INVESTIGATORS' REPORT

Atmospheric Transformation of Diesel Emissions

Barbara Zielinska, Shar Samy, Jacob D. McDonald, and JeanClare Seagrave

Division of Atmospheric Sciences, Desert Research Institute, Reno, Nevada (B.Z., S.S.), and Lovelace Respiratory Research Institute, Albuquerque, New Mexico (J.D.M., J.S.)

ABSTRACT

The hypothesis of this study was that exposing diesel exhaust (DE*) to the atmosphere transforms its composition and toxicity. Our specific aims were (1) to characterize the gas- and particle-phase products of atmospheric transformations of DE under the influence of daylight, ozone (O_3), hydroxyl (OH) radicals, and nitrate (NO_3) radicals; and (2) to explore the biologic activity of DE before and after the transformations took place. The study was executed with the aid of the EUPHORE (European Photoreactor) outdoor simulation chamber facility in Valencia, Spain. EUPHORE is one of the largest and best-equipped facilities of its kind in the world, allowing investigation of atmospheric transformation processes under realistic ambient conditions (with dilutions in the range of 1:300). DE was generated on-site using a modern light-duty diesel engine and a dynamometer system equipped with a continuous emission-gas analyzer. The engine (a turbocharged, intercooled model with common-rail direct injection) was obtained from the Ford Motor Company. A first series of experiments was carried out in January 2005 (the winter 2005 campaign), a second in May 2005 (the summer 2005 campaign), and a third in May and June 2006 (the summer 2006 campaign). The diesel fuel that was used closely matched the one currently in use in most of the United States (containing 47 ppm sulfur and 15% aromatic compounds). Our experiments examined the effects on the composition of DE aged in the dark with added NO_3 radicals and of DE aged in daylight with added OH radicals both with and without added volatile organic compounds (VOCs). In order to remove excess nitrogen oxides (NO_x), a NO_x denuder was devised and used to conduct experiments in realistic low-NO_x conditions in both summer campaigns. A scanning mobility particle sizer was used to determine the particle size and the number and volume concentrations of particulate matter (PM) in the DE. O_3, NO_x, and reactive nitrogen oxides (NO_y) were monitored using chemiluminescence and Fourier transform infrared instruments. At the end of the exposures, samples of particle-associated and semivolatile organic compounds (SVOCs) were collected from the chamber for chemical analysis using an XAD-coated annular denuder followed by a filter and XAD cartridge. (XAD is an adsorbent polystyrene divinylbenzene resin used in sampling cartridges.) Samples for toxicity testing were collected using Teflon filters followed by two XAD cartridges. The chemical analyses included determination of organic carbon (OC), elemental carbon (EC), carbon fractions, inorganic ions (e.g., sulfate and nitrate), and speciated organic compounds (polycyclic aromatic hydrocarbons [PAHs], nitro-PAHs, polar compounds, alkanes, hopanes, and steranes). The toxicity tests were performed with extracts of PM combined with the SVOCs. The biologic activity of these extracts was evaluated in vivo by instilling them into the tracheas of rodents and measuring pulmonary toxicity, inflammation, and oxidative-stress responses. Results from the chemical analyses indicated that aging DE in the dark with added NO_3 radicals and aging DE in daylight with and without additions led to the formation of additional particles and SVOC mass caused by reactions of VOCs, SVOCs, and inorganic gases. The greatest increase in mass occurred with the addition of VOCs as co-reactants. The proportions of the pyrolized OC (POC) fraction increased in the organic mass, which suggested that highly polar and oligomeric compounds had been formed. Results from the toxicity testing were

This Investigators' Report is one part of Health Effects Institute Research Report 147, which also includes a Critique by the Health Review Committee and an HEI Statement about the research project. Correspondence concerning the Investigators' Report may be addressed to Dr. Barbara Zielinska, Division of Atmospheric Sciences, Desert Research Institute, 2215 Raggio Parkway, Reno, Nevada 89512-1905.

Although this document was produced with partial funding by the United States Environmental Protection Agency under Assistance Award CR–83234701 to the Health Effects Institute, it has not been subjected to the Agency's peer and administrative review and therefore may not necessarily reflect the views of the Agency, and no official endorsement by it should be inferred. The contents of this document also have not been reviewed by private party institutions, including those that support the Health Effects Institute; therefore, it may not reflect the views or policies of these parties, and no endorsement by them should be inferred.

*A list of abbreviations and other terms appears at the end of the Investigators' Report.

consistent with the hypothesis that the toxicity of the samples had been affected by changes in their composition (caused both by the atmospheric aging and by changes in the initial composition of the DE presumably associated with changes in the engine, which was new at the outset and accrued wear during the study).

INTRODUCTION

A wide range of gas- and particle-phase organic and inorganic compounds are emitted from diesel engines. Once released into the atmosphere, these compounds (and other combustion emissions) are dispersed, transported, and transformed over time by various physical and chemical processes that determine their ultimate fate in the environment. The time scales of these atmospheric transformations vary widely; atmospheric lifetimes range from less than a minute for some highly reactive organic compounds to months for less reactive constituents (with the result that they can sometimes be transported over large distances). Some gaseous species contribute to the formation of secondary particle aerosols by a series of chemical transformations; sulfates and nitrates are common examples of such aerosols. Some fraction of particulate OC results from the oxidation of VOCs by way of atmospheric reactions with reactive gaseous species, such as OH radicals, NO_3 radicals, or O_3. Substantial data now exist on the physical and chemical nature of primary DE. But our understanding of the physical and chemical changes that primary DE undergoes in the atmosphere is still limited, an understanding that would clearly be important in assessing the true effects of DE on human health and welfare.

ATMOSPHERIC TRANSFORMATION OF COMPLEX MIXTURES IN DIESEL EXHAUST

Complete and incomplete combustion of fuel in diesel engines results in the formation of a complex mixture of emissions containing hundreds of organic and inorganic constituents in the gas and particle phases. To meet current and future diesel emission standards, new control technologies have been gradually introduced over the past 20 years. The new technologies focus on improvements in engine design, development of oxidation catalysts and efficient trap systems, recirculation of exhaust gas, and modification of fuel composition and fuel-additive effects. As a result, the character of diesel emissions has changed, and will continue to change, over time.

In the laboratory, emissions from motor vehicles are measured using engine or chassis dynamometers. The emissions are diluted by a factor of approximately 10 in dilution tubes before measurement. The relevance of these measurements to realistic conditions in the atmosphere is open to question, because emissions from actual vehicles on the road typically have much higher dilution factors (~10^3), have longer residence times (from seconds to days compared with fractions of a second) before collection or measurement, undergo photochemical transformations in the atmosphere, and are collected at lower temperatures. As will be discussed below, they also interact with other ambient air pollutants, including the exhaust of other vehicles.

Although a number of laboratory studies have been carried out to elucidate photochemical and oxidative processes that can lead to the formation of secondary products, including secondary organic aerosols, most of these studies have investigated single precursor compounds or simplified chemical mixtures in smog chamber experiments. The reactions of aromatic hydrocarbons and PAHs that are important constituents of motor vehicle emissions, for example, have been studied in a series of smog chamber experiments (Zielinska et al. 1989a,b; Atkinson and Arey 1994; Arey 1998; Volkamer et al. 2001; Kalberer et al. 2004; Martin-Reviejo and Wirtz 2005; Zielinska 2005). However, comparing the results obtained from these laboratory studies with the results obtained from analyses of real ambient aerosol particles is not straightforward. This difficulty might be attributable to the simplified chemical mixtures in which the laboratory reactions occurred compared with those found in the actual atmosphere (Graber and Rudich 2006). There is a need, then, to investigate photochemical processes in real mixtures emitted from diesel engines and other combustion sources. One way of doing this is to inject the emissions into a modern outdoor smog chamber (with dilutions in the range of 1:300 or more), as we have done in the study described in this report.

Chemical reactions in the atmosphere can occur in the gas (homogeneous) or particle (heterogeneous) phase. The rates and mechanisms of these two types of reactions can be very different. In the gas phase, the chief atmospheric reaction pathways include the following (Atkinson 1988):

- reaction with gaseous NO_3 radicals in the dark,
- reaction in daylight (photolysis),
- reaction with OH radicals in daylight, and
- reaction with O_3 in daylight or in the dark.

Reactive gaseous species, such as NO_3 radicals, OH radicals, and O_3, are present in the atmosphere at night (NO_3 radicals), by day (OH radicals), and at both times (O_3). For the routes of formation of these species and their concentrations in the troposphere, see Finlayson-Pitts and Pitts (2000).

In the atmosphere, higher-molecular-weight organic compounds present in DE are partitioned into the particle phase. The atmospheric lifetimes of these particle-bound compounds are not well known, partly because the chemical processes associated with them depend on the nature of the particle substrate (Behymer and Hites 1985, 1988) and because many of the laboratory studies pertaining to them were done using unrealistic adsorbents, such as glass-fiber or Teflon-coated glass-fiber filters, silica gel, or alumina. Extrapolation of the sometimes contradictory results reported by various laboratories to realistic conditions in the atmosphere presents major problems. Still, in the particle phase, the chief atmospheric reaction pathways for these compounds probably include photolysis; reactions with O_3; and nitration with NO_2, nitric acid (HNO_3), and dinitrogen pentoxide (N_2O_5).

For more detailed discussions of the atmospheric transformations of DE in the gas and particle phases, see Winer and Busby (1995) and Zielinska (2005).

A particularly important class of compounds found in motor vehicle emissions is the polycyclic aromatic compounds (which include PAHs) and their oxygenated and nitrated derivatives (oxy-PAHs and nitro-PAHs). Many of these compounds are mutagenic or carcinogenic and are designated as hazardous air pollutants (listed in the polycyclic-organic-matter class of compounds) in the Clean Air Act Amendments of 1990 (U.S. Congress 1990). It has been shown that PAHs with two to four rings (distributed between the gas and particle phases) are highly abundant in DE (Zielinska et al. 2004a,b). For PAHs present in the gas phase, the reaction with OH radicals is predominant, leading to atmospheric lifetimes of a few hours or less. The reaction with NO_3 radicals in the dark is usually of minor significance as a PAH-loss process but might prove to be important as a formation route for mutagenic nitro-PAHs. Albrechcinski and colleagues (1988), for example, studied changes in the mutagenicity of DE as determined by the Ames test. Mixtures of O_3, NO_x, and other compounds were added to diluted DE in a simulation chamber. Some of the mixtures were aged in the dark; others were aged in daylight. The largest increases in the mutagenicity of particle samples from the chamber occurred for mixtures of O_3 and NO_2 that had been aged in the dark. Although the products of these reactions were not characterized, the increases in mutagenicity were presumably caused by reactions of PAHs with NO_3 radicals and the formation of nitro-PAHs.

Relatively few data on reaction products are available for gas-phase reactions. It has been shown that, in the presence of NO_x, OH-radical reactions with naphthalene, 1- and 2-methylnaphthalene, acenaphthylene, biphenyl, fluoranthene, pyrene, and acephenanthrylene lead to the formation of nitro-PAHs (Arey et al. 1986, 1989; Atkinson et al. 1987, 1990; Zielinska et al. 1988, 1989a; Arey 1998). In addition, two- to four-ring PAHs in the gas phase are observed to react in mixtures of N_2O_5, NO_3 radicals, NO_2, and air, in which NO_3 radicals are generated by the thermal decomposition of N_2O_5, leading to the formation of nitro-PAHs (Zielinska et al. 1986, 1989a; Atkinson et al. 1987, 1990; Arey et al. 1989).

HEALTH EFFECTS OF DIESEL EXHAUST

DE has been the subject of many studies of health effects over the past several decades. The studies have investigated (1) mutagenicity in bacterial systems; (2) toxicity, oxidative stress, and pro-inflammatory effects on cultured eukaryotic cells; (3) similar effects on, as well as alterations in, innate immune response and allergic responses caused by inhalation or intratracheal instillation (often using only the particle fraction) in animals; (4) controlled human exposure; and (5) epidemiologic patterns of health effects. Most of the studies reported adverse health effects, ranging from mutagenicity to overt toxicity. Only a few, however, have explicitly investigated the effects (primarily mutagenicity) associated with alterations in the chemical composition of DE after atmospheric aging (Claxton and Barnes 1981; Takeda et al. 1984; Stark et al. 1985). Instillation into rat lungs of DE particles combined with O_3 produced changes in toxicity related to the O_3 concentration (Madden et al. 2000). Photochemical effects on the toxicologic responses to various chemicals, including those associated with DE, have been observed in cultured cells (Jaspers et al. 2003; Doyle et al. 2004; Sexton et al. 2004). However, most of the studies of DE were conducted with freshly generated exhaust or with particulate fractions. Recent studies comparing several sources of collected particles have emphasized that, even within this one type of material, differences in composition have vastly different effects on biologic responses (DeMarini et al. 2004; Singh et al. 2004). Given the known potential for atmospheric transformations of DE constituents and the fact that most human exposures do not occur at the tailpipe, the current study undertook to assess the toxicity of collected particulate and semivolatile fractions from DE aged in various ways. We used methods that were similar to those used in an earlier study (Seagrave et al. 2002, 2005a,b), which assessed differences in the toxicity of emission samples from the combustion of gasoline, diesel fuel, and compressed natural gas.

SPECIFIC AIMS

The objective of this study was to test the hypothesis that photochemical transformations of DE in the atmosphere result in changes in its toxicity. Our specific aims were the following:

1. to characterize the gas- and particle-phase products of the atmospheric transformations of DE under the influence of daylight, O_3, OH radicals, and NO_3 radicals; and
2. to explore the biologic effects of DE before and after the atmospheric transformations take place.

We conducted a systematic evaluation of the composition and toxicity of DE aged in a range of atmospheric conditions. Test atmospheres were developed to represent key differences in the major pathways that might affect DE reactions in both the presence and absence of daylight. State-of-the-art methods for the characterization of the chemical and physical transformations of DE were used. These included analyses of the decay of compounds emitted in exhaust and of the formation of new products along each of the respective reaction pathways. After instillation of the atmospheric constituents into rodent lungs, the resulting changes in in vivo toxicity were evaluated for each of the test atmospheres.

METHODS AND STUDY DESIGN

SYSTEM UPDATES AND MODIFICATIONS

Significant steps were taken to ensure that the experiments made use of test atmospheres that were highly relevant to the reactions of contemporary diesel emissions in a realistic ambient atmosphere. Our timeline (Figure 1) includes the steps that were taken throughout the program to optimize test conditions to meet this aim. The chamber experiments were conducted in chamber B of the EUPHORE outdoor simulation chamber facility in Valencia, Spain, which is currently among the largest (200 m^3) and best-equipped facilities of its kind in the world (Becker 1996). Our first task was to update EUPHORE with a modern (circa 2003) diesel engine, because the HEI Research Committee had required the use of such an engine (i.e., a turbocharged, intercooled model with common-rail direct injection). After inquiring about the possibility of obtaining an engine from various manufacturers, we learned in May 2003 that Ford Motor Company's Dagenham Engine Plant in Dagenham, United Kingdom, would be willing to donate one of its current-model diesel engines, the 1.8-L Lynx derivative (a V277 90 PS Stage 3 fixed-geometry turbo diesel with a Delphi fuel system) used in the company's Focus and Transit Connect models. The decision was made to obtain the engine, and arrangements were made to ship it directly to Valencia.

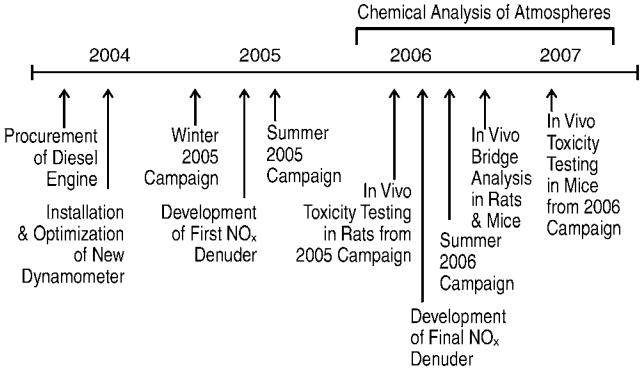

Figure 1. A timeline of the study's principal events.

The new engine was installed, EUPHORE's dynamometer system was upgraded, and a continuous emission-gas analyzer (MEXA-7170D, Horiba Instruments, Irvine, CA) was added to the dynamometer to permit continuous monitoring of the engine's gaseous emissions (carbon monoxide [CO], carbon dioxide [CO_2], NO_x, total hydrocarbons, and oxygen [O_2]). The engine and dynamometer were made operational in late fall 2004.

A final step toward the production of realistic atmospheres in the EUPHORE chamber was discovering and reducing the engine's high output of NO_x, which had been inhibiting the intended photochemical reactions. Indeed, the specific aims of the study could not have been achieved without removing the excess NO_x. The magnitude of the NO_x problem was discovered during our first aging experiments, in January 2005, when high NO_x concentrations and much-lower-than-anticipated vapor and particulate emissions were found. In these experiments, DE was injected into the reaction chamber for a few minutes, and the concentrations of the resulting exhaust constituents were measured in the chamber. Injecting DE into the chamber for 2 minutes produced approximately 30 $\mu g/m^3$ of diesel PM, a few ppb of VOCs, and nearly 1 ppm of NO_x (30% of this as NO_2). At such high concentrations of NO_x, any photochemistry that might occur does not reflect real-world tropospheric chemistry. Under these conditions, the formation of OH radicals and O_3 is extremely low, and any OH radicals or O_3 formed are rapidly removed from the system through reactions with nitric oxide (NO) to form NO_2 and nitric acid (Finlayson-Pitts and Pitts 2000). In addition, the photochemical transformation of organic compounds in daylight is effectively shut down. To solve this problem in time for the summer 2005 campaign (in May 2005), we undertook to develop and optimize a NO_x denuder that would be able to reduce the high NO_x concentrations.

The first version of the NO_x denuder was developed between February and April 2005 and was in fact used in the summer 2005 campaign (see section on NO_x Denuder, below). Although this denuder worked relatively well in

removing NO_x, it led to rather high particle losses as the DE was passed through it, which resulted in low PM concentrations in the chamber. Our next goal, then, was to improve the NO_x denuder to increase its capacity for NO_x removal while decreasing its particle losses. As described below in the NO_x Denuder section and in Appendix B (available on the Web at *www.healtheffects.org* or from HEI upon request), a new, improved denuder was developed in fall 2005 and winter 2005–2006 and was used in the summer 2006 campaign (in May and June 2006).

EXPERIMENTAL DESIGN

Figure 2 shows the principal steps in the experiment. The first step was the injection of DE (and in some cases co-reactants, such as volatile hydrocarbons or O_3, to help create targeted atmospheres) into the chamber. The DE was injected through the NO_x denuder in order to reduce NO_x in the chamber to appropriately low concentrations. Some experiments were conducted without the denuder in place; these yielded DE essentially without atmospheric reactions and thus served as a baseline for comparison with DE after atmospheric reactions and to show the resulting changes in composition and toxicity. In our final experiments, all atmospheres were generated with the denuder in place in order to create realistic atmospheric conditions. After injection, the reactants were allowed to age for 4 to 5 hours either in the dark or in natural daylight (depending on the target atmosphere). During this time, several real-time analyzers (as described below in EUPHORE Chamber Exposures) were used to characterize the resulting changes in the chemical and physical composition of the atmospheres.

At the conclusion of the aging period, the atmospheric reactions in daylight were terminated (by closing the chamber's protective cover), and integrated samples were collected for detailed chemical analysis and in vivo toxicity testing. Chemical analyses included determination of OC, EC, carbon fractions (the mass of carbon in all forms relative to the total particle mass), inorganic ions (e.g., sulfate and nitrate), and speciated organic compounds (PAHs, nitro-PAHs, polar compounds, alkanes, hopanes, and steranes). These analytes are the key species in DE that result from combustion (PAHs and polar compounds), fuel and lubrication-oil emissions (alkanes, hopanes, and steranes), and atmospheric reactions (nitro-PAHs and polar compounds). The in vivo toxicity tests were performed with extracts of PM combined with the SVOCs. The SVOCs were important to include because they account for a majority of the mass of DE and have been shown to contribute substantially to its toxicity (Seagrave et al. 2002). The biologic activity of these atmospheric constituents was evaluated by instilling them into the tracheas of rodents and measuring pulmonary toxicity, inflammation, and oxidative-stress responses. This approach has been used in several previous studies to compare the relative toxicity of engine emissions (Seagrave et al. 2002, 2005a,b) and ambient air (Seagrave et al. 2006).

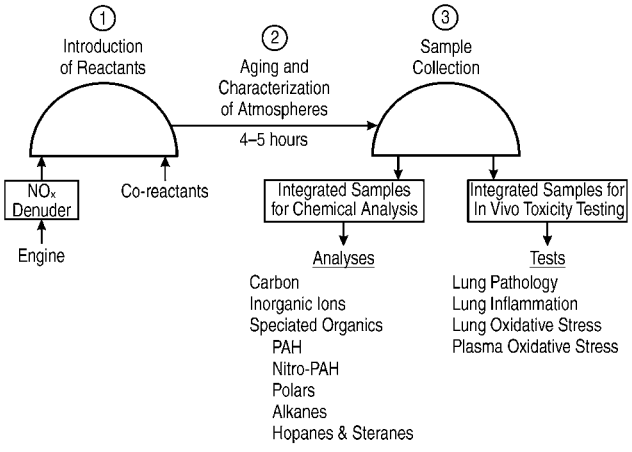

Figure 2. The principal components of the study's experimental set-up.

Details of our experimental procedures, including the chamber atmosphere selection and development, chemical analysis of atmospheres, and conduct of in vivo toxicity tests, are given below.

EUPHORE CHAMBER FACILITY

The EUPHORE outdoor simulation chamber facility in Valencia, Spain, is currently among the largest and best-equipped in the world, allowing investigation of atmospheric transformation processes under realistic ambient conditions. The construction of EUPHORE's two simulation chambers (chambers A and B) was completed in 1995. Each chamber (see Figure 3) consists of a transparent hemispheric Teflon bag with a volume of about 204 m^3. The chambers are made of a fluorinated ethylene propylene (FEP) Teflon foil, with a thickness of 127 µm, made by DuPont. The Teflon FEP foil transmits more than 80% of solar radiation in the wavelength range of 280 to 640 nm into the chambers. Each chamber is protected against adverse weather conditions by a retractable hemispheric housing. The floor of each chamber consists of 32 symmetrically arranged aluminum panels covered with Teflon FEP foil. To compensate for the heating of the chambers by solar radiation, the panels are cooled by a refrigeration system (Becker 1996).

Inlet and outlet ports and other accessories, such as mixing fans, analytic systems, and excess-pressure valves, are located on the chamber floor so that the hemispheric surface remains unobstructed. Integrated into the chamber

Figure 3. EUPHORE (European Photoreactor) outdoor-simulation chamber facility in Valencia, Spain.

flanges are ports for the input of reactants and sampling lines for the various analytic instruments. To mix reactants, two mixing fans with an air throughput of 4000 m^3/hr each are installed in each chamber. A White mirror system for a long-path Fourier transform infrared spectrometer is situated in chamber B for in situ measurements of VOCs and inorganic gases. Numerous analytic instruments — including, for example, NO and NO_2 detectors, gas chromatographs (GCs) with various detectors, a formaldehyde detector, a GC–mass spectrometer (MS) system, a scanning mobility particle sizer, an O_3 detector, and others (see Table 1) — are mounted on a platform under the chamber floor. The sampling lines for these instruments are connected directly to the chamber. Our DE exposures were carried out in chamber B. In addition, a novel instrument from the University of Wuppertal (Wuppertal, Germany) for the measurement of nitrous acid (HONO) was also available for part of the study; it can detect HONO in the range of 5 parts per trillion (ppt) to 10 ppm.

Diesel Engine

DE was generated on-site using a modern, light-duty diesel engine and a dynamometer system. The engine (a turbocharged, intercooled model with common-rail direct injection) was a 1.8-L Lynx V277 obtained from Ford Motor Company. It was mounted on the dynamometer, which was equipped with a continuous emission-gas analyzer to allow continuous monitoring of the engine's emissions of gaseous CO, CO_2, NO_x, total hydrocarbons, and O_2. The engine test rig was situated under the EUPHORE chamber (Figure 4). The engine exhaust was guided in heated tubes under the chamber and injected into the chamber by means of a three-way valve that can tolerate temperatures up to 200°C. In general, a separate, smaller line was used that allowed approximately 20% of the total engine exhaust to enter the chamber; the rest was vented to the outside. Inside the chamber, very fast dilution was achieved by fans that mixed the exhaust gas with clean chamber air. (This also prevented the agglomeration of particles and the condensation of water.)

The engine was generally operated at approximately 2000 rpm under a load of approximately 60 Nm (Newton-meter), representing approximately 50% of the engine's total power. Before each injection of exhaust into the chamber, the engine was warmed up to reach a steady state. The diesel fuel that was used closely matched the one that is currently used (or will be used in the near future) in most of the United States (containing 47 ppm sulfur and 15% aromatic compounds). Appendix A gives a summary of engine conditions; a detailed description of

Table 1. Analytic Instruments Connected to EUPHORE Chamber B

Instrument[a]	Compound or Parameter	Detection Limit	Sampling Method	Analysis Type
Magna 550 FTIR	VOCs, NO_x, SO_2, HNO_3	10 ppb	In situ White mirror system (553-m optical path)	Online
Fison 8000 GC-FID/PID	VOCs, carbonyls	20 ppb, 10 ppb	5 mL sampling loop	Online Online
Fison 80 GC/ECD	Peroxyacetyl nitrate	0.2 ppb	Cryogenic enrichment	Online
Aerolaser AL4021	Formaldehyde	0.1 ppb by Hantzsch reaction	Direct line from the chamber	Online
SMPS	PM size and number distribution	< 20 nm	Direct line from the chamber	Online, 5-min averages
Eco Physics NO_x monitor	NO, NO_2	< 1 ppb	Teflon line	Online Online
Monitor Labs NO_x monitor	NO, NO_y	1 ppb, 1 ppb	Teflon line	Online
TE48C CO monitor	CO	20 ppb	Teflon line	Online
Ozone monitor (UV 254 nm)	O_3	1 ppb	Teflon line	Online
Spectral radiometer	Solar flux	—	Inside the reactor, 50 cm above the ground	6-min averages
Thermometer	Temperature	—	Below fan in the shadow	1-min averages
Pressure gauge	Pressure	—	Teflon line	1-min averages
TS-2 dewpoint mirror	Humidity	−50°C	Teflon line	1-min averages

[a]FTIR indicates Fourier-transform infrared spectrometer; FID indicates flame ionization detector; PID indicates plasma ionization detector; ECD indicates electron-capture device; SMPS indicates scanning mobility particle sizer.

engine conditions during each injection is available upon request. Between campaigns, the engine remained mounted on the dynamometer at the EUPHORE facility. It was operated for approximately 43 hours from the start of the winter 2005 campaign (in January 2005) to the end of the summer 2005 campaign. Hours of operation before the summer 2006 were rather minimal (approximately 8 hours logged), and the total operation time of the engine to date is approximately 100 hours (including experimental operation times under load).

In the summer 2006 campaign, because the engine was overheating as a result of longer run times under load, we performed two or three separate injections of exhaust into the chamber for most of the runs. In general, we continued each injection until the engine's water temperatures reached 95°C to 96°C. At that point, the valve leading to the chamber was closed, and the engine was run on idle for 10 to 15 minutes, until its water temperature returned to approximately 80°C to 85°C. Afterward, the engine was returned to 2000 rpm and a 60-Nm load, and we repeated the process for one or two additional injections. This procedure usually increased the PM concentrations in the chamber by no more than a few $\mu g/m^3$ in the subsequent injections.

NO_x DENUDER

As explained above (in System Updates and Modifications), development of an efficient NO_x denuder was a necessary component of the chamber experiments. The experiments used exhaust from a modern light-duty diesel engine at a flow rate of approximately 180 L/min. To allow investigation of atmospheric transformations under realistic ambient conditions (i.e., with dilutions in the range of 1:300 to 1:400), more than 90% of the NO_x had to be removed from the DE before injection. The development of a denuder capable of absorbing this much NO_x (at concentrations greater than 300 ppm) from an exhaust stream for at least 7 minutes (the minimum length of an injection) necessitated experimentation with a variety of configurations and absorption materials.

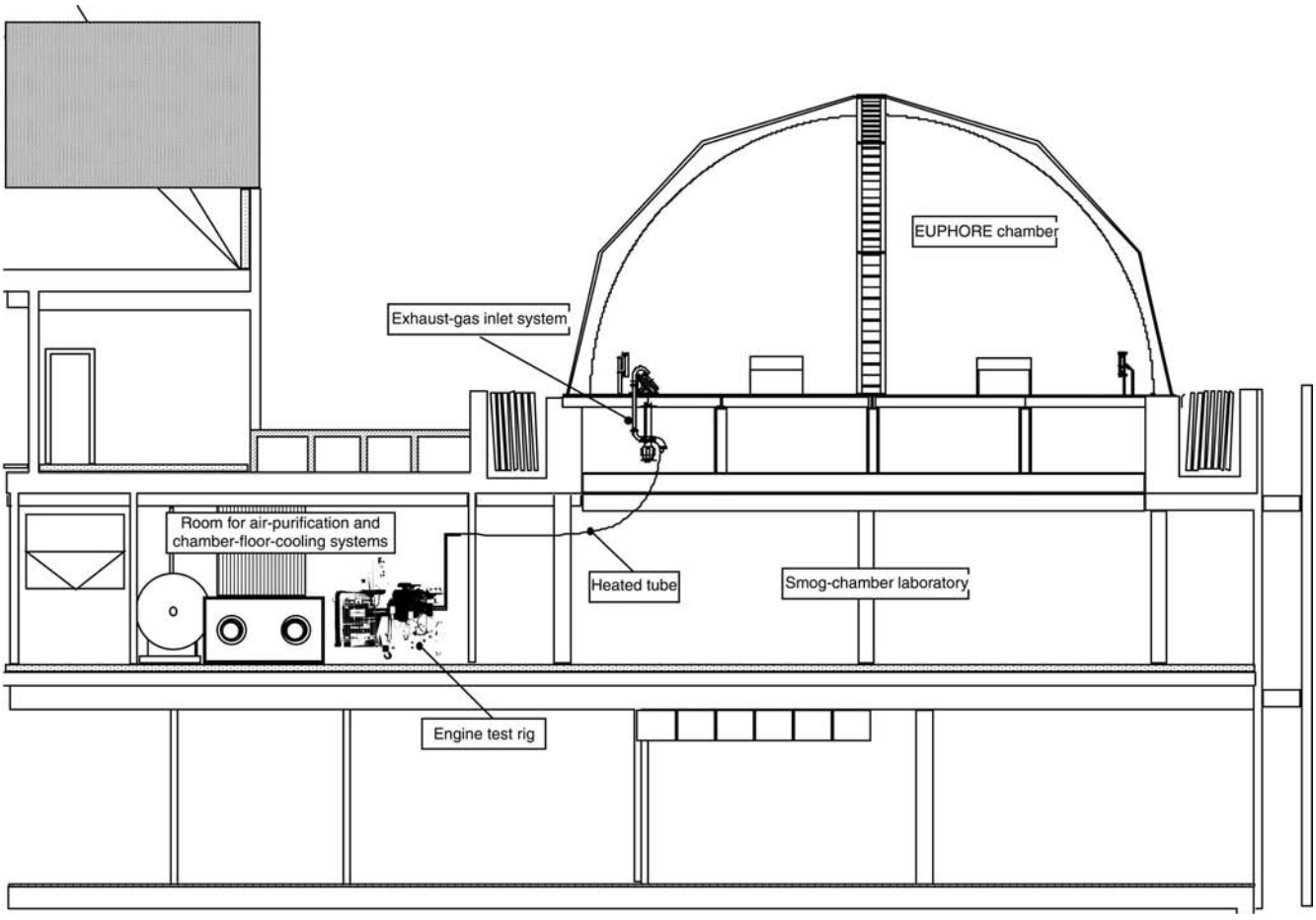

Figure 4. Set-up of the engine test rig at EUPHORE.

The following section describes the results of experiments we conducted at the Desert Research Institute in Reno, Nevada, in 2005 to develop and evaluate such a NO_x denuder. The results of these efforts guided the design of the final, efficient denuder used in the 2006 summer campaign. Additional details are provided in Appendix B.

Denuder Channel Configurations and Materials

In recent years, a variety of researchers have used cobalt(II,III) oxide (Co_3O_4) as an absorption material to remove NO_x species (NO, NO_2, and HNO_3) from exhaust streams (e.g., Braman et al. 1986; Ammann 2001; Arens et al. 2001; Saathof et al. 2003; Vijay et al. 2005). The Co_3O_4 was applied as a coating on the walls of cylindrical- or rectangular-channel denuders or on the ceramic granules that surround denuder screen tubes. These coatings can be regenerated by heating and flushing with air or oxygen at about 400°C, resulting in the release of the absorbed NO_x and thus allowing the materials to be used again. In an earlier study of emissions from gasoline-powered vehicles, we constructed a small denuder using Co_3O_4 coatings on the inner walls of the denuder's stainless steel tubes. However, we discovered in winter 2005 that this design was unable to handle the higher NO_x concentrations found in DE, and because we also needed to design for higher exhaust flow rates and NO_x concentrations than had been encountered in some of the previous studies, we realized that our remaining campaigns were going to require a novel approach. New experimentation in spring 2005 led to the construction of a denuder with cordierite ceramic cylinders that allowed us to transport the denuder in sections and assemble it easily on-site (see Appendix B). The cylinders (Applied Ceramics, Doraville, GA) were 5.7 inches in diameter and 3 inches long, with a honeycomb of 16 channels (0.19 inches in internal diameter [i.d.]) per square inch, and were used for the summer 2005 campaign. Up to 12 of these cylinders were soaked in a nearly saturated aqueous solution of cobalt nitrate hexahydrate; between

1 and 2 kg of the solution were taken up by the cylinders. The cylinders were then baked in an oven at 400°C for at least 12 hours. Unfortunately, instability of the resulting coating led to material loss through flaking. Nevertheless, a denuder with cylinders prepared in this way was used in the summer 2005 campaign; it was effective in removing NO_x during short injections of DE (4 minutes or less) but could not handle longer injections. These difficulties, along with the relatively high particle losses of the denuder even during short injections and the resulting low concentrations of diesel PM in the chamber, made it clear that the design of a truly effective NO_x denuder remained as a challenge (although the maximized surface area was an attractive feature of the honeycomb configuration).

Several initial experiments were conducted at the Desert Research Institute in fall and winter 2005 using a denuder with a simple four-channel annular design and stainless steel mesh as a surface substrate. Constructed by the Lovelace Respiratory Research Institute of Albuquerque, New Mexico, this denuder was further modified by us for several experiments at the Desert Research Institute. The channels were 39 cm long and 2.5 cm wide. An additional 15-cm pre-chamber was constructed to establish laminar flow in the exhaust before it entered the channels. Absorbent material was packed on the outside of the main interior channels to allow convenient transport and replacement (or regeneration) of the packed material. Once exhaust flow was established, gaseous diffusion through the mesh apertures (~1 mm in diameter) allowed the NO_x to be removed efficiently. The channel pathways were left completely open along the line-of-sight axis to reduce particulate loss caused by impaction. In comparison with the honeycomb channels, at 0.48 cm in diameter, the annular denuder channels were significantly larger, at 2.5 cm in diameter, and relatively lower particle losses caused by impaction were expected.

Substrate Selection and Preparation

Use of an aluminum oxide (Al_2O_3) substrate in the preparation of NO_x absorbents has been shown to be effective and beneficial for absorbent stability (Hendershot 2004). However, after evaluation of several types of Al_2O_3, it became obvious that, for our purposes, the material would not be practical to prepare, handle, and regenerate. Further investigation led to a firebrick material with the industrial reference name of Grog. Grog is composed of silica (approximately 50%), Al_2O_3 (approximately 40%), iron oxide (approximately 2%), titanium oxide (approximately 2%), and several other earth metals (e.g., sodium and potassium). It can be purchased in particle form in various particle-size ranges and is readily available through the firebrick industry. Because the Grog-coating process we were attempting was novel, it was necessarily undertaken without benefit of guidance from the experience of other researchers.

An effective coating process should allow in-field regeneration (by way of thermal desorption) or replacement (from prepared stock) of the absorbent surface. Complete oxidation of cobalt nitrate to Co_3O_4 depends on several factors. The high oxidizing capacity of Co_3O_4, which affects NO_x storage sites, appears to depend on a consistent preparation procedure and substrate. The purchased Grog was first sifted with a coarse, 1-mm metallic mesh to make certain that smaller particles were not present. A saturated solution of cobalt nitrate was applied to the Grog until incipient wetness was obtained. To achieve the desired weight loading and uniform coating, the Grog was then dried at approximately 300°C, crushed, and recoated. A final weight loading of 500 g cobalt nitrate hexahydrate per liter of Grog was achieved. The coated Grog was then reacted at 400°C in a flushing flow (> 10 L/min) of a 1:3 mixture of oxygen and air for 6 to 8 hours. The presence of cobalt in the form of Co_3O_4 has been demonstrated by X-ray diffraction analysis in a similarly produced absorbent material using a different substrate (Vijay et al. 2005). The presence and influence of Co_3O_4, cobalt(II) oxide (CoO), and cobalt(III) oxide (Co_2O_3) (in varying concentrations) on NO_x storage capacity is not well understood. One of the objectives of the fall 2005 experiments was to develop a consistent procedure for producing the absorbent material while evaluating the performance of the straight cylindrical-channel denuder configuration. Appendix B includes descriptions and data results for these experiments, addressing issues of thermal desorption, regeneration, and optimal absorbent depth.

The data and material logistics provided by these experiments were important for successful application on larger scales in the 2006 summer campaign. The Co_3O_4 coating now had the capacity to remove NO_x efficiently, and the Grog acted as an effective substrate. The addition of barium to the cobalt–Grog absorbent did not appear to substantially enhance its capacity to remove NO_x (see Appendix B). The regenerative properties of the cobalt–Grog were sufficient for multiple uses.

Evaluation of several materials for the construction of the channels (e.g., stainless steel mesh and laser-punched stainless steel sheets) led to the decision to use stainless steel type-304 perforated tubes with 24-gauge (approximately 1-mm) apertures. This spiral-seamed tubing was 167 cm (66 inches) long, with a 2.54-cm (1-inch) outer diameter. The channels were straight cylinders. The internal channel configuration allowed for a minimum of 1.5 cm of space for cobalt–Grog between all channels.

A mixing chamber of 30.5 cm preceded the packed channel section of the denuder. The exhaust channel was expanded to approximately 9 cm before the connection point to the main denuder body (the elbow section in the drawing shown in Figure 13, Appendix B). The output section consisted of a 30.5-cm hollow section. Several alignment plates (at least three) inserted in the channel section ensured proper alignment of the channels. Because cobalt–Grog has a relatively high density (1.28 g/cm^3), the embedded perforated-tube channels had to be aligned before filling (see Appendix B). The total volume of the packed section (after subtraction of the channel sections) was 132 L. This gave a total weight of 169 kg (372 lb) just for the cobalt–Grog in the denuder body, which necessitated shipping the cobalt–Grog in a separate crate. The denuder was 66 inches long, with a main body i.d. of 14.5 inches. It contained 57 diffusion channels (each 1 inch in outer diameter), spaced approximately 1 inch apart (Figure 14, Appendix B). To deal with the weight, the denuder body was mounted on brackets with wheels for placement in the EUPHORE facility (Figure 15, Appendix B).

The denuder was received at EUPHORE on May 23, 2006. Once it was assembled, it was positioned as closely as possible to the chamber injection valve, which controlled DE injection into the chamber. Because of limited vertical space and the denuder's weight, the denuder was placed on a fork lift adjacent to the chamber's instrumentation. It was secured to the ceiling beams with a stainless steel rope-and-hook system, and the DE was injected into it through 1-inch insulated copper tubing.

The NO_x denuder was regenerated between runs by heating it to 400°C with a flushing flow of oxygen and air at a preset ratio for 3 to 4 hours. It was cooled overnight (12 to 14 hours) to 80°C to help ensure efficient NO_x removal during the next DE injection. We did not observe degradation of the denuder's performance even after repeated regenerations. Evaluation of the saturation capacity of the denuder was not possible under these experimental conditions because of the long injection times (up to 35 minutes). However, even 35 minutes worth of DE passing through the denuder resulted in only trace amounts of NO_x (in the 25–30 ppb range) being found in the chamber (see Results and Appendix B).

EUPHORE CHAMBER EXPOSURES

Exposure Matrix

Using the experimental setup described above, we examined the effects of aging DE in the dark or in daylight, with and without NO_3 radicals, OH radicals, or O_3, on the resulting composition of DE. DE is a complicated mixture of NO_x species, gas-phase organic compounds, and PM. The aging of DE in daylight can produce O_3 and OH radicals. However, because modern diesel engines like ours, equipped with an oxidation catalyst, produce only very small amounts of VOCs, the production of photo-oxidants (especially O_3) would not have been sufficient to achieve the objectives of our study under the diluted atmospheric conditions of the EUPHORE chamber. VOCs that exist normally in ambient air were therefore added to the chamber for certain experiments to enhance selected reactions, such as the reaction of gas-phase PAHs with OH radicals.

The goals of the exposures in the dark were to evaluate (1) the natural aging of DE in order to provide a baseline for other experiments and (2) the aging of DE in the presence of added NO_3 radicals. These exposures were conducted chiefly in winter 2005 without the NO_x denuder (because it wasn't available yet) and then in the summers of 2005 and 2006 with and without the denuder, for comparison with the winter exposures and to help assess the denuder's effectiveness.

The NO_3 radicals originated from N_2O_5 that originated in the first place from the reaction of NO_2 with O_3 in the chamber. The NO_3 radicals and NO_2 formed the N_2O_5 and were in thermal equilibrium with it (M denotes a third body that facilitates a reaction and remains intact):

$$NO_2 + O_3 \rightarrow NO_3 + O_2 \quad (1)$$

$$NO_2 + NO_3 \overset{M}{\rightleftharpoons} N_2O_5 \quad (2)$$

NO_3 radicals are very reactive and hence are observed mostly during the late evening and night time hours; during the day, they are removed rapidly by photolysis and reaction with NO.

An additional attempt was made in summer 2005 to study O_3 reactions with DE in the dark. However, despite NO_x removal (using the first version of the denuder), NO_x was still found in the chamber with the DE. This led to the production of N_2O_5 and NO_3-radical reactions along with the O_3 reactions.

The goal of the exposures in daylight was to examine the effects of photolysis reactions on the composition of DE. As mentioned above, because modern diesel engine exhaust contains low concentrations of VOCs, VOCs were added to the chamber atmosphere to enhance the reactivity of the final mixture. In most urban ambient atmospheres, an abundance of VOCs emitted by various sources, such as gasoline powered vehicles, is available for chemical reactions. Thus, for several exposures we added formaldehyde, which forms OH radicals by photolysis; toluene (as a representative VOC); or a mixture of naphthalene and several other aromatic compounds. These exposures are described in detail below.

Table 2. Naming Convention for the EUPHORE Chamber Experiments

Experiment Type	Denuder Use During DE Injections	Year and Season	Reactants Added to Chamber	Experimental Replicate Designation
L = light, chamber open to daylight	d = denuder in use	05 = 2005 campaign	T = toluene	_1 = 1st sample
D = dark, chamber cover kept closed	No character = denuder not in use	s = summer	F = OH (from formaldehyde)	_2 = 1st replicate
		w = winter	V = VOCs	_3 = 2nd replicate
		06 = 2006 campaign	N = NO_3	_4 = 3rd replicate
		s = summer	No character = no additions	_b = blank

Our naming convention for the EUPHORE chamber experiments is explained in Table 2. Because the NO_x denuder (and hence, in effect, the experimental setup) and methods of toxicity testing were different in the 2005 and 2006 campaigns, the naming convention was designed to help keep readers aware of these differences throughout the report. "Ld06sF_2," for example, means "Light exposure with NO_x denuder in 2006, summer, OH (from formaldehyde) added, first replication of this experiment." Table 3 gives the names, dates, and descriptions of all the chamber experiments.

Protocol for EUPHORE Chamber Exposures

Before the start of each experiment, the chamber was flushed for a few hours with clean air until NO_x, particles, and O_3 (after exposures in daylight) were no longer detected. The diesel engine was operated for approximately 30 minutes to warm it up and reach a steady state of exhaust production and was then operated at approximately 2000 rpm under a load of approximately 60 Nm, representing approximately 50% of its total power. When the engine's water and oil temperatures reached approximately 88°C and 90°C, respectively, DE from the engine was injected into the chamber for several minutes (i.e., long enough to obtain sufficient material for chemical reactions, analysis, and toxicity testing). Appendix A lists the engine conditions for all experiments. During the injection of DE, the mixing fans were switched on to ensure rapid mixing of constituents. After 5 minutes, the fans were switched off to avoid excessive loss of particles to the chamber wall caused by impaction from continued turbulence. If additional reactants were going to be injected into the chamber, the fans were then switched on again briefly to ensure rapid mixing of the reactants. The emission-gas analyzer and other continuous instruments recorded data during all phases of experiments. The exposures performed are described below.

Chamber Blanks Before the summer 2005 and 2006 exposures were performed, the chamber was flushed for several hours with clean air, and chamber blanks (samples of clean chamber air for baseline analysis and testing) were collected in the dark and during the day. The dark blank (D05s_b) was collected overnight for chemical analysis. For the daylight blanks (L05s_b, L06s_1b, and L06s_2b), the chamber's protective cover was opened, the chamber was exposed to daylight for 3 to 4 hours until the cover was closed again, and the samples were collected overnight for chemical analysis and toxicity testing.

Diesel Exhaust Aged in the Dark For exposures of DE in the dark, which provided the baseline control data for the other experiments, the chamber's protective cover was closed, and DE was injected into the chamber with and without the NO_x denuder. After the DE had aged for 3 to 5 hours, the samplers were switched on, and samples (D05w_1, D05w_2, D05w_3, Dd05s_1, Dd05s_2, D06s_1, D06s_3, Dd06s_1, and Dd06s_2) were collected overnight for chemical analysis and toxicity testing, as described below in Sample Collection at EUPHORE.

Diesel Exhaust Aged in the Dark with Added NO_3 Radicals Our experiments with added NO_3 radicals were conducted with the chamber's protective cover closed. First, O_3 was injected into the chamber in concentrations sufficient to oxidize all NO from the diesel engine to NO_2 and to react with the NO_2 to form N_2O_5 and NO_3 radicals (see equations [1] and [2] above). DE was then injected into the chamber with and without the NO_x denuder. N_2O_5 and the other compounds were monitored continuously by Fourier transform infrared spectrometry. After 4 to 5 hours of exposure, samples (D05wN_2 through 5, Dd05sN_1 and 2, D06sN, and Dd06sNV) were typically collected overnight.

Diesel Exhaust Aged in the Dark with Added O_3 We undertook two exposures in summer 2005 and one in

Table 3. Samples for Chemical Analysis and Toxicity Testing from the Three EUPHORE Campaigns

Name	Date	Description
Winter 2005		
D05w_1 D05w_2 D05w_3	1/12/05 1/13/05 1/14/05	DE aged in dark (no NO_x denuder) to determine baseline conditions. Samples collected for chemical analysis only and combined for analysis
D05w_4	1/15/05 and 1/17/05	DE aged in dark (no NO_x denuder) to determine baseline conditions. Samples collected for toxicity testing only and combined for analysis
D05wN_5 D05wN_6	1/19/05 and 1/20/05 1/21/05	DE + NO_3 in dark (no NO_x denuder). Samples collected for toxicity testing only and combined for analysis
D05wN_2 D05wN_3	1/24/05 1/25/05	DE + NO_3 in dark (no NO_x denuder). Samples collected for chemical analysis only and combined for analysis
D05wN_4	1/26/05	DE + NO_3 in dark (no NO_x denuder). Samples collected for chemical analysis only
Summer 2005		
D05s_b	5/5/05	Chamber blank, dark, sampling for chemical analysis only
L05s_b	5/9/05	Chamber blank, in daylight, sampling for chemical analysis and toxicity testing
Dd05s_1 Dd05s_2	5/10/05 5/25/05	DE in dark (with NO_x denuder). Sampling for chemical analysis and toxicity testing. Toxicity samples were combined
Ld05s_1 Ld05s_2	5/11/05 5/12/05	DE + sun (with NO_x denuder). Sampling for chemical analysis and toxicity testing. Toxicity samples were combined
Ld05sF_1 Ld05sF_2 Ld05sF_3 Ld05sF_4	5/13/05 5/18/05 5/23/05 5/24/05	DE + sun + OH (from formaldehyde decomposition) (with NO_x denuder). Sampling for chemical analysis and toxicity testing. Toxicity samples were combined
Dd05sN_1 Dd05sN_2	5/16/05 5/17/05	DE + NO_3 in dark, low NO_x (with NO_x denuder). Sampling for chemical analysis and toxicity testing. Toxicity samples were combined

(*Table continues next column*)

Table 3 (*Continued*). Samples for Chemical Analysis and Toxicity Testing from the Three EUPHORE Campaigns

Name	Date	Description
Summer 2005 (*continued*)		
Ld05sT_1 Ld05sT_2	5/19/05 5/20/05	DE + sun + toluene (with NO_x denuder). Sampling for chemical analysis and toxicity testing. Toxicity samples were combined
L05s_1	5/26/05	DE + sun (no NO_x denuder). Sampling for chemical analysis and toxicity testing
Summer 2006		
L06s_1b L06s_2b	5/23/06 5/24/06	Chamber blank, in daylight, sampling for chemical analysis and toxicity testing. Toxicity samples were combined
D06s_1 D06s_2 D06s_3	5/25/06 5/26/06 6/13/06	DE in dark (no NO_x denuder). Sampling for chemical analysis and toxicity testing. Samples 1 and 3 were combined for toxicity testing and chemical analysis. Sample 2 not valid
Dd06s_1 Dd06s_2	5/30/06 5/31/06	DE in dark (with NO_x denuder). Sampling for chemical analysis and toxicity testing. Toxicity samples were combined
Dd06sNV	6/1/06	DE + NO_3 + VOCs in dark, low NO_x (with NO_x denuder). Sampling for chemical analysis and toxicity testing
D06sN	6/12/06	DE + NO_3 in dark (no NO_x denuder). Sampling for chemical analysis and toxicity testing
Ld06sV_1	6/2/06	DE + sun + VOCs (with NO_x denuder). Sampling for chemical analysis and toxicity testing
Ld06s_1	6/8/06	DE + sun (with NO_x denuder). Sampling for chemical analysis and toxicity testing
Ld06sF_1	6/5/06	DE + sun + OH (with NO_x denuder). Sampling for chemical analysis and toxicity testing
Ld06sFV_1	6/7/06	DE + sun + OH + VOCs (with NO_x denuder). Sampling for chemical analysis and toxicity testing
Ld06sT_1 Ld06sT_2	6/6/06 6/9/06	DE + sun + toluene (with NO_x denuder). Sampling for chemical analysis and toxicity testing

summer 2006 to examine the effects of O_3 on DE in the dark. The O_3 was injected into the chamber in concentrations of 0.5 to 1 ppm, as described above. However, because NO_x was still present in low concentrations (~30–50 ppb; see Table 1 in Appendix C [available on the HEI Web site]), N_2O_5 was formed (~17–18 ppb), with the result that NO_3-radical reactions occurred. For this reason, we designated these three exposures as NO_3-radical reactions (and called them Dd05sN_1, Dd05sN_2, and Dd06sNV, respectively). Samples collected for toxicity testing in summer 2005 were combined and designated as one sample (Dd05sN_1 + 2). However, N_2O_5 concentrations were much lower in these three exposures than in all winter 2005 exposures, where N_2O_5 concentrations were in the range of 1 ppm.

Diesel Exhaust Aged in Daylight Our experiments with DE aged in daylight were performed in summer 2005 and 2006 with the NO_x denuder to remove excess NO_x that would otherwise have shut down photochemical transformations in the chamber. The DE was injected into the chamber for 3 to 5 minutes in summer 2005 and for 25 to 30 minutes in summer 2006. The shorter injection times in summer 2005 were dictated by the lower efficiency of the denuder at that time in removing NO_x; when NO_x was detected in the chamber by the measuring instruments, DE injection was terminated. With the 2006 denuder, which was much more efficient, longer injection times were possible. However, because the engine was overheating as a result of the longer run times under load (as described in the Diesel Engine section above), we performed two or three separate partial injections to obtain complete injections for most of the runs. The chamber cover was then opened, and exposure to daylight continued for 4 to 5 hours. Once aging was completed, the chamber cover was closed, and samples (Ld05s_1, Ld05s_2, Ld06s_1, and Ld06sV_1) for chemical analysis and toxicity testing were collected overnight.

Diesel Exhaust Aged in Daylight with Added OH Radicals To examine the effects of OH-radical reactions on DE, formaldehyde was added to the chamber as a precursor source of OH radicals in a number of experiments. DE was first injected into the chamber with the NO_x denuder, and then approximately 30 mg paraformaldehyde was placed in a glass tube and injected into the chamber by evaporative heating through a specially designed port. After a few minutes of mixing, the fans were switched off, and the chamber's protective cover was opened to allow 4 to 5 hours of exposure to daylight. The cover was then closed, and samples (Ld05sF_1, Ld05sF_2, Ld05sF_3, Ld05sF_4, Ld06sF_1, and Ld06sFV_ 1) for chemical analysis and toxicity testing were collected overnight.

Diesel Exhaust Aged in Daylight with Added Toluene For the experiments with added toluene, approximately 500 ppb of toluene was added to the DE in the chamber to simulate the VOCs in real atmosphere and enhance the reactivity of the DE. The exposures were carried out, and samples (Ld05sT_1, Ld05sT_2, Ld06sT_1, and Ld06sT_2) were collected as described above.

Diesel Exhaust Aged in Daylight with Added VOCs When we noticed from in situ GC–MS measurements that the second version of the NO_x denuder (the one used in summer 2006) appeared to be partially removing aromatic compounds from the DE, two different VOC mixtures (Table 4) were added to the chamber to supplement the atmospheres for three exposures. Mixture #1, added only to exposure Dd06sNV (see Table 3), consisted of a 10-µL

Table 4. Composition of VOC Mixtures Added to the EUPHORE Chamber for Three Exposures

Compound	Density (g/mL)	Mixture #1[a]	Amounts Added to Chamber	Concentrations in Chamber (µg/m^3)	Mixture #2[b]	Amounts Added to Chamber	Concentrations in Chamber (µg/m^3)
Benzene	0.88	None	None	None	75 µL	5.94 µL	0.026
o-Xylene	0.87	None	None	None	175 µL	13.86 µL	0.060
p-Cymene	0.86	50 µL	2.63 µL	0.011	250 µL	19.80 µL	0.085
1,2-Diethylbenzene	0.86	50 µL	2.63 µL	0.011	250 µL	19.80 µL	0.085
1,2,4-Trimethylbenzene	0.88	40 µL	2.11 µL	0.009	200 µL	15.84 µL	0.070
Isobutylbenzene	0.85	50 µL	2.63 µL	0.011	250 µL	19.80 µL	0.084
Naphthalene	Solid	1.9 mg	1.9 mg	9.5	37.3 mg	2.95 mg	14.7
1,2,4,5-Tetramethylbenzene	Solid	1.6 mg	1.6 mg	8.0	25.2 mg	2.0 mg	9.98

[a] Mixture #1 was added only to exposure Dd06sNV (DE + NO_3 + VOCs).

[b] Mixture #2 was added to exposures Ld06sV_1 (DE + sun + VOCs) and Ld06sFV_1 (DE + sun + OH + VOCs).

aliquot of a liquid and two compounds in solid form. Mixture #2, added to exposures Ld06sV_1 and Ld06sFV_1 (see Table 3), consisted of a 100-µL aliquot of a liquid and the same two compounds in solid form. The compositions of both mixtures and the resulting initial concentrations in the chamber are shown in Table 4.

SAMPLE COLLECTION AND ANALYTIC METHODS

Sample Collection at EUPHORE

After several hours of exposure, samples for SVOC analysis were collected using an XAD-coated annular denuder (Gundel et al. 1995) followed by a 90-mm Teflon-impregnated glass-fiber filter and an XAD cartridge (Zielinska et al. 2004a). The XAD denuder strips the gas-phase species out of the laminar flow stream by molecular diffusion before collection of the particles on the second-stage filter and cartridge (Peters et al. 2000). A flow rate of 100 L/min was used. Samples for toxicity testing were collected overnight, using 8-by-10-inch Teflon-impregnated glass-fiber filters followed by two XAD cartridges, with a flow rate of approximately 200 L/min. (For the winter campaign, samples for chemical analysis and toxicity testing were collected sequentially, unlike the simultaneous sample collecting of the summer campaigns.) During the summer campaigns, a higher-flow pump was used to collect the samples for toxicity testing, allowing us to increase the flow rate to approximately 250 L/min. Because the chamber atmosphere was being replenished with clean air during sampling, the gradual dilution of the reactants in it was monitored by adding sulfur hexafluoride (SF_6) to the chamber at the beginning of each experiment and measuring its dilution. Figure 5 shows the calculated sampling times at three different sampling rates needed to recover a desired mass of reactants from the chamber, assuming that mass was neither gained nor destroyed during sampling.

The figure shows that if the initial mass of reactants in the chamber was 20 mg, for example, we needed to sample for 77 hours at 100 L/min, 38 hours at 200 L/min, or 19 hour at 400 L/min in order to remove 90% of this mass from the chamber. Because our sampling times were generally in the range of 16 to 19 hours, we did not collect much mass when sampling for chemical analysis and toxicity testing was done sequentially. The decision was therefore made to sample simultaneously during the summer campaigns, allowing more experiments to be conducted.

In addition to the SVOC samples, canister samples for VOC analysis were collected for several experiments in 2005, and diesel particles were collected on quartz-fiber filters for analysis of OC, EC, sulfate, and nitrate. Filters and XAD cartridges were stored in a freezer at the EUPHORE facility. Denuder samples were extracted on-site, and the extracts were stored in the freezer; at the conclusion of the campaigns, they were shipped to the Desert Research Institute in coolers with reusable frozen "blue ice" packs using an overnight delivery service (resulting in 2- to 4-day transfer times). Canister samples were stored at EUPHORE and later shipped to the Desert Research Institute at room temperature.

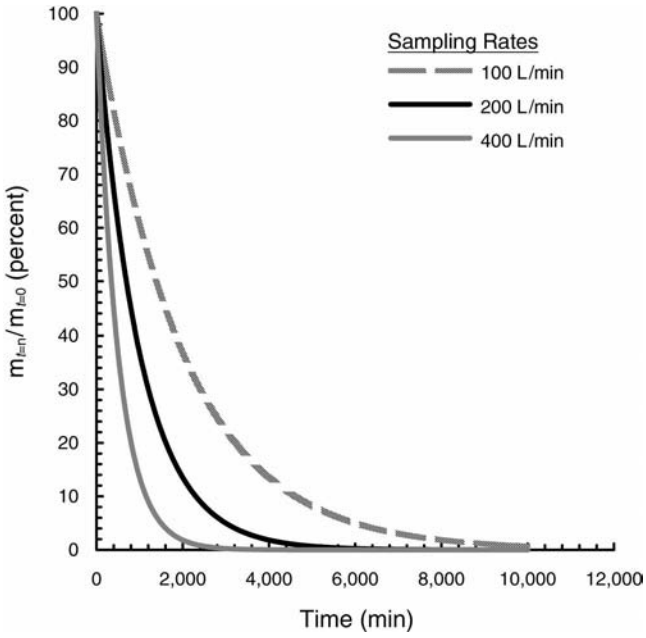

Figure 5. Sampling times needed to recover a desired mass of reactants from the chamber. The *y*-axis shows the percentages of the mass remaining in the chamber at any given time *n* for the three hypothetical sampling rates. The percentages were calculated as $m_{t=n}/m_{t=0}$, where $m_{t=n}$ is the mass at *t* (time) *n* and $m_{t=0}$ is the initial mass at $t = 0$. For a hypothetical initial mass of 20 mg reactants, it would take 77 hours of sampling at 100 L/min, 38 hours at 200 L/min, and 19 hours at 400 L/min to recover 90% of the mass.

Analysis of Organic Compounds

Extraction of XAD Denuder, Filters, and XAD Cartridges for Chemical Analysis Before each campaign, the 90-mm Teflon-impregnated glass-fiber filters were cleaned twice by sonication for 10 minutes in dichloromethane that was replaced between cleanings and then were cleaned two more times by sonication for 10 minutes in methanol that was also replaced between cleanings. The XAD resin (Amberlite XAD4, Aldrich Chemical Company, Milwaukee, WI) was washed with Liqui-Nox soap and rinsed in hot water, followed by deionized water and technical-grade methanol (three to four times). It was extracted using an accelerated solvent extractor (Dionex Corporation, Sunnyvale, CA) for 15 minutes per cell with dichloromethane at 1500 psi

and 80°C followed by acetone and then dried in a vacuum oven at 50°C. The SVOCs collected on each denuder–filter–XAD sampling train were extracted separately with high-purity, high-performance-liquid-chromatography–grade solvents. The chemistry filters and XAD were extracted at the Desert Research Institute with approximately 170 mL of dichloromethane, hexane, and methanol (1:1:1) by accelerated solvent extraction. In accelerated solvent extraction, the media are pressurized and heated for 15 minutes per cell at 1500 psi and 80°C. All media were extracted twice under the same conditions and then combined for each sample to assure complete extraction of analytes.

The following deuterated internal standards were added to the XAD and filters before extraction: naphthalene-d_8, acenaphthylene-d_8, phenanthrene-d_{10}, anthracene-d_{10}, chrysene-d_{12}, pyrene-d_{10}, benz[*a*]anthracene-d_{12}, benzo[*a*]pyrene-d_{12}, benzo[*e*]pyrene-d_{12}, benzo[*k*]fluoranthene-d_{12}, benzo[*g,h,i*]perylene-d_{12}, coronene-d_{12}, cholestane-d_{50}, hexanoic-d_{11} acid, benzoic-d_5 acid, succinic-d_4 acid, adipic-d_{10} acid, suberic-d_{12} acid, homovanillic-2,2 acid-d_2, myristic-d_{27} acid, oleic-9,10-d_2 acid, tetradecanedioic-d_{24} acid, eicosanoic-d_{39} acid, cholesterol-d_6, 1-nitronaphthalene-d_7, 2-nitrobiphenyl-d_9, 1-nitrofluorene-d_9, 9-nitroanthracene-d_9, 3-nitrofluoranthene-d_9, 1-nitropyrene-d_9, 9-nitrochrysene-d_{11}, 6-nitrobenzo[*a*]pyrene-d_{11}, dodecane-d_{26}, hexadecane-d_{34}, eicosane-d_{42}, octacosane-d_{58}, triacontane-d_{62}, hexatriacontane-d_{74}, and tetracosane-d_{50}. The extracts were concentrated to approximately 1 mL by rotary evaporation at 35°C to 45°C under gentle vacuum and filtered through a 0.2-µm Teflon disposable filter (Puradisc 25TF, Whatman International Ltd., Kent, United Kingdom). The filtrate was collected in a 4-mL amber glass vial, for a total volume of approximately 4 mL (including flask rinse with solvent). The extracts were reduced in volume under a gentle stream of ultra-high-purity nitrogen with a Chrompack Gas Clean Moisture Filter (CP17971, Analytical Columns, New Addington, UK) to 500 µL and split into two fractions for nonpolar and polar analysis. The first fraction, consisting of 50% of the extract (approximately 250 µL), was suspended in toluene (evaporated to approximately 200 µL in final volume) and analyzed for nonpolar analytes without further alteration.

The second fraction, consisting of the other 50% of the extract (approximately 250 µL), was evaporated to dryness under moisture-filtered ultra-high-purity nitrogen and resuspended in acetonitrile. The extract underwent a trimethylsilyl derivatization (Nolte et al. 2001, 2002; Rinehart et al. 2006), using a mixture of bis(trimethylsilyl)trifluoroacetamide and 1% (by weight) trimethylchlorosilane with pyridine (silylation grade) to enhance detection sensitivity. Selected derivatized samples were analyzed by GC–MS at the Desert Research Institute.

The XAD-coated annular denuder was extracted at the EUPHORE facility immediately after sampling, using the solvent ratio described above. The denuder section was capped at one end, and approximately 200 mL of solvent was poured into it. Then the other end was capped, the denuder was manually inverted about 30 times, and the solvent was drained. The procedure was repeated two more times. Extractions of chamber blanks were performed on-site, and all extracts were concentrated to approximately 3 mL by rotary evaporation. The extracts were refrigerated during each campaign and later shipped (with the filter and XAD cartridges) to the Desert Research Institute for analysis by GC–MS.

Extraction of Filters and XAD Cartridges for Toxicity Testing XAD cartridges for toxicity testing were extracted at the Desert Research Institute with dichloromethane followed by acetone, using accelerated solvent extraction. Extracts were concentrated by rotary evaporation at 35°C to 45°C and reduced in volume to 1 mL under a gentle stream of ultra-high-purity nitrogen, and 50-µL aliquots of extract were then evaporated on preweighed aluminum-foil weighing boats (Cahn Instruments, Madison, WI). Once post-evaporation weights were recorded, a total suspended mass weight was calculated for the entire extract. The extracts and filters were shipped to the Lovelace Respiratory Research Institute for toxicity testing. PM fractions were then extracted from the Teflon filters by sonication in a mixture of 90% acetone and 10% dichloromethane and concentrated by evaporation at room temperature under nitrogen. The concentrated samples were stored at −20°C in amber glass vials. The mass for each fraction was estimated by weighing the residual mass after evaporation of an aliquot of the sample on preweighed aluminum-foil weighing boats.

Analysis of SVOCs The filter and XAD (denuder and cartridge) extracts for chemical analysis were analyzed separately for PAHs, polar compounds, and alkanes using an electron-impact GC–MS system (model 4000 GC–MS, Varian, Palo Alto, CA) equipped with an autosampler (model CP-8400, Varian). One microliter of extract was injected onto a 30-m (5% phenyl methyl silicone) fused-silica capillary column (model DB-5MS + DG, J&W Scientific, Folsom, CA) using a 1:20 injector split ratio. The compounds and corresponding deuterated internal standards were quantified by selective ion monitoring. Additional analyses for hopanes, steranes, and nitro-PAHs were performed on a gas chromatograph (model CP-3800, Varian) interfaced with a tandem mass spectrometer (model 1200L, Varian). For the hopanes and steranes, the capillary column described above was used; for the nitro-PAHs, a 30-m column (model DB-17MS, J&W Scientific) was used.

The chamber sample extracts were extremely complex and needed extensive clean-up before nitro-PAH analysis in order to remove interferences that would have reduced peak resolution and increased baseline noise. The nitro-PAH-rich fraction was isolated with the use of an aminopropyl cartridge (Sep-Pak PSA Solid-Phase Extraction Sorbent, Waters Corporation, Milford, MA) followed by fractionation by normal-phase high-performance liquid chromatography (with a semi-preparative amino-cyano phase column [Chromegabond, ES Industries, West Berlin, NJ]). Negative-ion chemical ionization with methane as a reagent gas was used to enhance detection sensitivity (Zielinska and Samy 2006).

A 3- to 6-level calibration was performed for each compound of interest, and a midlevel check standard was run at least once every 10 chamber samples. If the relative accuracy of measurement (defined as the percentage difference from a standard value) was greater than 20%, then the instrument underwent routine injector, column, and detector clean-up or replacement followed by recalibration. Nitro-PAH analysis is particularly sensitive to column age because of the chemical affinity of the target compounds for active sites. Tables 5 through 9 list the organic compounds for which the chamber samples were analyzed.

Analysis of Inorganic Compounds

Gravimetric Analysis Filter weighing was performed on an electro-microbalance (Cahn model 31, Thermo Fisher Scientific, Waltham, MA) with a sensitivity of ±0.001 mg. Exposed and unexposed Teflon filters were equilibrated at a temperature of 20 ± 5°C and a relative humidity of 30 ± 5% for a minimum of 24 hours before weighing. The charge on each filter was neutralized by exposing the filter to a polonium source for 30 seconds before placing it on the balance pan.

Ion Chromatography The quartz filters were analyzed for nitrate (NO_3^-) and sulfate (SO_4^{2-}) ions using an ion chromatograph (Model 2020i, Dionex Corporation, Sunnyvale, CA) containing a guard column (part AG4a, catalog number 37042, Dionex Corporation) and an anion-separator column (part AS4a, catalog number 37041, Dionex Corporation) with a strong basic anion-exchange resin as well as an anion micro-membrane suppressor column (250 ft × 6 mm i.d.) with a strong acid ion-exchange resin. The anion eluent consisted of sodium carbonate and sodium bicarbonate prepared in distilled deionized water.

Carbon Analysis EC and OC were measured by thermal optical reflectance using the Interagency Monitoring of Protected Visual Environments (IMPROVE) temperature-oxygen

Table 5. Alkanes Analyzed for This Study[a]

Code	Full Name
NORFARN	Norfarnesane
HPYCYHX	Heptylcyclohexane
FARNES	Farnesane
TDEC	Tetradecane
OCYCYHX	Octylcyclohexane
PENTAD	Pentadecane
NOYCYHX	Nonylcyclohexane
HEXAD	Hexadecane
NORPRST	Norpristane
HEPD	Heptadecane
DECYHX	Decylcyclohexane
HEPTDPRIS	Heptadecane & pristane
DEC1YHX	Undecylcyclohexane
OCTAD	Octadecane
PHYTAN	Phytane
DEC2YHX	Dodecylcyclohexane
NONAD	Nonadecane
DEC3YHX	Tridecylcyclohexane
EICOSA	Eicosane
DEC4YHX	Tetradecylcyclohexane
HENEIC	Heneicosane
DEC5YHX	Pentadecylcyclohexane
DOCOSA	Docosane
DEC6YHX	Hexadecylcyclohexane
TRICOSA	Tricosane
DEC7YHX	Heptadecylcyclohexane
DEC8YHX	Octadecylcyclohexane
TETCOS	Tetracosane
PENCOS	Pentacosane
DEC9YHX	Nonadecylcyclohexane
HEXCOS	Hexacosane
CYHXEIC	Eicosylcyclohexane
HEPCOS	Heptacosane
CYHXHEN	Heneicosylcyclohexane
OCTCOS	Octacosane
NONCOS	Nonacosane
TRICONT	Triacontane
HTRICONT	Hentriacontane
DTRICONT	Dotriacontane
TTRICONT	Tritriacontane
TETRICONT	Tetratriacontane
PTRICONT	Pentatriacontane
HXTRICONT	Hexatriacontane
HPTRICONT	Heptatriacontane
OTRICONT	Octatriacontane
NTRICONT	Nonatriacontane
TECONT	Tetracontane

[a] Entries are listed in retention-time order.

Table 6. PAHs Analyzed for This Study[a]

Code	Full Name
NAPHTH	Naphthalene
MNAPH2	2-Methylnaphthalene
MNAPH1	1-Methylnaphthalene
BIPHEN	Biphenyl
ENAP12	1+2-Ethylnaphthalene
DMN267	2,6+2,7-Dimethylnaphthalene
DM1367	1,3+1,6+1,7-Dimethylnaphthalene
D14523	1,4+1,5+2,3-Dimethylnaphthalene
DMN12	1,2-Dimethylnaphthalene
M_2BPH	2-Methylbiphenyl
M_3BPH	3-Methylbiphenyl
M_4BPH	4-Methylbiphenyl
DBZFUR	Dibenzofuran
BIBENZ	Bibenzyl
ATMNAP	A-Trimethylnaphthalene
EM_12N	1-Ethyl-2-methylnaphthalene
BTMNAP	B-Trimethylnaphthalene
CTMNAP	C-Trimethylnaphthalene
EM_21N	2-Ethyl-1-methylnaphthalene
ETMNAP	E-Trimethylnaphthalene
FTMNAP	F-Trimethylnaphthalene
TMI235N	2,3,5+I-Trimethylnaphthalene
TM245N	2,4,5-Trimethylnaphthalene
JTMNAP	J-Trimethylnaphthalene
TM145N	1,4,5-Trimethylnaphthalene
ACNAPY	Acenaphthylene
ACNAPE	Acenaphthene
FLUORE	Fluorene
DBTH	Dibenzothiophene
PHENAN	Phenanthrene
ANTHRA	Anthracene
FL9ONE	9-Fluorenone
XANONE	Xanthone
ACQUONE	Acenaphthenequinone
PNAPONE	Perinaphthenone
M_2ANTH	2-Methylanthracene
M_3PHEN	3-Methylphenanthrene
M_2PHEN	2-Methylphenanthrene
M_9PHEN	9-Methylphenanthrene
M_45PHEN	4,5-Methylenephenanthrene
MPHT_1	1-Methylphenanthrene
ANTHONE	Anthrone
ANRQUONE	Anthraquinone
DM36PH	3,6-Dimethylphenanthrene
A_DMPH	A-Dimethylphenanthrene

(*Table continues next column*)

[a] Entries are listed in retention-time order.

Table 6 (*Continued*). PAHs Analyzed for This Study[a]

Code	Full Name
B_DMPH	B-Dimethylphenanthrene
C_DMPH	C-Dimethylphenanthrene
D_DMPH	D-Dimethylphenanthrene
DM17PH	1,7-Dimethylphenanthrene
E_DMPH	E-Dimethylphenanthrene
M_9ANT	9-Methylanthracene
FLUORA	Fluoranthene
PYRENE	Pyrene
ANTAL9	9-Anthraaldehyde
RETENE	Retene
BNTIOP	Benzonaphthothiophene
M_13FL	1+3-Methylfluoranthene
C1MFLPY	C-Methylfluoranthene or methylpyrene
BMPYFL	B-Methylpyrene or methylfluoranthene
CMPYFL	C-Methylpyrene or methylfluoranthene
DMPYFL	D-Methylpyrene or methylfluoranthene
M_4PYR	4-Methylpyrene
M_1PYR	1-Methylpyrene
BZCPHEN	Benzo[*c*]phenanthrene
BGHIFL	Benzo[*g*,*h*,*i*]fluoranthene
CP_CDPYR	Cyclopenta[*c*,*d*]pyrene
BAANTH	Benz[*a*]anthracene
CHR_TR	Chrysene-triphenylene
BZANTHR	Benzanthrone
M_7BAA	7-Methylbenz[*a*]anthracene
M_3CHR	3-Methylchrysene
BAA7_12	Benz[*a*]anthracene-7,12-dione
CHRY56M	5+6-Methylchrysene
BBJKFL	Benzo[*b*+*j*+*k*]fluoranthene
BAFL	Benzo[*a*]fluoranthene
BEPYRN	Benzo[*e*]pyrene
BAPYRN	Benzo[*a*]pyrene
PERYLE	Perylene
M_7BPY	7-Methylbenzo[*a*]pyrene
BPY910DIH	9,10-Dihydrobenzo[*a*]pyrene-7(8*H*)-one
DBAJAN	Dibenzo[*a*,*j*]anthracene
IN123PYR	Indeno[1,2,3-*cd*]pyrene
DBAHACAN	Dibenzo[*ah*+*ac*]anthracene
BBCHR	Benzo[*b*]chrysene
PIC	Picene
BGHIPE	Benzo[*g*,*h*,*i*]perylene
ANTHAN	Anthanthrene
DBBKFL	Dibenzo[*b*,*k*]fluoranthene
DBAEPYR	Dibenzo[*a*,*e*]pyrene
CORONE	Coronene
DBAHPYR	Dibenzo[*a*,*h*]pyrene

[a] Entries are listed in retention-time order.

Table 7. Nitro-PAHs Analyzed for This Study[a]

Code	Full Name
1NN	1-Nitronaphthalene
1Me5NN	1-Methyl-5-nitronaphthalene
2NN	2-Nitronaphthalene
2NBip	2-Nitrobiphenyl
2Me4NN	2-Methyl-4-nitronaphthalene
1Me4NN	1-Methyl-4-nitronaphthalene
1Me6NN	1-Methyl-6-nitronaphthalene
3NBip	3-Nitrobiphenyl
4NBip	4-Nitrobiphenyl
2NFluore	2-Nitrofluorene
5NAce	5-Nitroacenaphthene
9NAnt	9-Nitroanthracene
4NPhe	4-Nitrophenanthrene
9NPhe	9-Nitrophenanthrene
3NPhe	3-Nitrophenanthrene
3NFl	3-Nitrofluoranthene
2NFl	2-Nitrofluoranthene
4NPyr	4-Nitropyrene
1NPyr	1-Nitropyrene
2NPyr	2-Nitropyrene
2,7dNFluone	2,7-Dinitrofluorene
2,7dNFlu9one	2,7-Dinitrofluoren-9-one
7NB[a]A	7-Nitrobenz[*a*]anthracene
6NChr	6-Nitrochrysene
1,3dNPyr	1,3-Dinitropyrene
1,6dNPyr	1,6-Dinitropyrene
1,8dNPyr	1,8-Dinitropyrene
6NB[a]P	6-Nitrobenz[*a*]pyrene

[a] Entries are listed in retention-time order.

Table 8. Polar Organic Compounds Analyzed for This Study[a]

Code	Full Name
oxalic	Oxalic acid
heptac	Heptanoic acid
malon	Malonic acid
memalon	Methylmalonic acid
octanac	Octanoic acid
phenaa	Phenylacetic acid
maleac	Maleic acid
sucac	Succinic acid
otoluic	*o*-Toluic acid
mesucac	Methylsuccinic acid

(*Table continues next column*)

[a] Entries are listed in retention-time order.

Table 8 (*Continued*). Polar Organic Compounds Analyzed for This Study[a]

Code	Full Name
mtoluic	*m*-Toluic acid
nonac	Nonanoic acid
ptoluic	*p*-Toluic acid
guac	Glutaric acid
meglu2	2-Methylglutaric acid
dimeb25	2,5-Dimethylbenzoic acid
meglu3	3-Methylglutaric acid
dimeb24	2,4-Dimethylbenzoic acid
decac	Decanoic acid
mesyr4	4-Methylsyringol
dimeb34	3,4-Dimethylbenzoic acid
hexdac	Hexanedioic (adipic) acid
meadip3	3-Methyladipic acid
undec	Undecanoic acid
hepdac	Heptanedioic (pimelic) acid
phthac	Phthalic acid
suber	Suberic acid
levg	Levoglucosan
dimeo34	3,4-Dimethoxybenzoic acid
dimeo24	2,4-Dimethoxybenzoic acid
isphac	Isophthalic acid
myrol	Myristoleic acid
myrac	Myristic acid
sebac	Sebacic acid
pdecac	Pentadecanoic acid
undecdi	Undecanedioic acid
palac	Palmitic acid
isster	Isostearic acid
dodecd	Dodecanedioic acid
traum	Traumatic acid
olac	Oleic acid
steac	Stearic acid
ndecac	Nonadecanoic acid
dhydpim	Dihydroisopimaric acid
dhabac	Dehydroabietic acid
abie814	8,14-Abietenic acid
abac	Abietic acid
ecosac	Eicosanoic acid
oxodeh7	7-Oxodehydroabietic acid
docosa	Docosanoic acid
tricosa	Tricosanoic acid
tetraco	Tetracosanoic acid

[a] Entries are listed in retention-time order.

Table 9. Hopanes and Steranes Analyzed for This Study

Code	Full Name
hop13	18α(H)-22,29,30-Trisnorneohopane (T)
hop15	17α(H)-22,29,30-Trisnorhopane (T)
hop17	17α(H),21β(H)-29-Norhopane[a]
hop18	18α(H)-29-Norneohopane[b]
hop19	17α(H),21β(H)-Hopane
hop21	22(*S*)-17α(H),21β(H)-30-Homohopane[c]
hop22	22(*R*)-17α(H),21β(H)-30-Homohopane[c]
hop23	17β(H),21β(H)-Hopane
hop24	22(*S*)-17α(H),21β(H)-30,31-Bishomohopane
hop25	22(*R*)-17α(H),21β(H)-30,31-Bishomohopane
hop26	22(*S*)-17α(H),21β(H)-30,31,32-Trishomohopane
hop27	22(*R*)-17α(H),21β(H)-30,31,32-Trishomohopane
ster42	20(*S*)-5α(H),14α(H),17α(H)-Cholestane
ster43	20(*R*)-5α(H),14β(H),17β(H)-Cholestane
ster44	20(*S*)-5α(H),14β(H),17β(H)-Cholestane
ster45_40	20(*R*)-5α(H),14α(H),17α(H)-Cholestane and 20(*S*)-13β(H),17α(H)-Diastigmastane[d]
ster46	20(*S*)-5α(H),14α(H),17α(H)-Ergostane[e]
ster47	20(*R*)-5α(H),14β(H),17β(H)-Ergostane
ster48_41	20(*S*)-5α(H),14β(H),17β(H)-Ergostane and 20(*R*)-13α(H),17β(H)-Diastigmastane[f]
ster49	20(*R*)-5α(H),14α(H),17α(H)-Ergostane
ster50	20(*S*)-5α(H),14α(H),17α(H)-Stigmastane[g]
ster51	20(*R*)-5α(H),14β(H),17β(H)-Stigmastane
ster52	20(*S*)-5α(H),14β(H),17β(H)-Stigmastane
ster53	20(*R*)-5α(H),14α(H),17α(H)-Stigmastane

[a] Also called 17α(H),21β(H)-30-norhopane (Chiron, Trondheim, Norway).
[b] Also called 18α(H),21β(H)-30-norneohopane.
[c] Also called 17α(H),21β(H)-22S (or 22R)-homohopane (Chiron, Trondheim, Norway).
[d] Also called C_{29} 20S-13β(H),17α(H)-diasterane.
[e] Ergostane indicates 24-methylcholestane.
[f] Also called C_{29} 20R-13α(H),17β(H)-diasterane.
[g] Stigmastane indicates 24-ethylcholestane.

cycle (Chow et al. 1993, 2001). The quartz filters were first heated under oxygen-free helium purge gas. The resulting volatilized or pyrolyzed carbonaceous gases were carried by the purge gas to an oxidizer catalyst, where all carbon compounds were converted to CO_2. The CO_2 was then reduced to methane, which was quantified by a flame ionization detector. The carbon evolved during the oxygen-free heating stage was defined as OC. The sample was then heated in the presence of helium gas containing 2% oxygen; the carbon evolved during this stage was defined as EC (Peterson and Richards 2002). Some organic compounds became pyrolyzed (charred) when heated during the oxygen-free stage and produced additional EC, which was classified as POC. The formation of POC was monitored during the analysis by sample reflectance or transmittance. EC and OC were distinguished by measuring the refractory properties of the EC using a thermal-evolution carbon analyzer with optical (reflectance or transmittance) correction to compensate for the pyrolysis of OC. Carbon fractions in the IMPROVE method correspond to temperature stages of 120°C, 250°C, 450°C, and 550°C in a nonoxidizing helium atmosphere and of 550°C, 700°C, and 850°C in an oxidizing atmosphere (Chow et al. 2004). The IMPROVE method uses variable hold times of 150 to 580 seconds to allow carbon responses to return to their baseline values.

Continuous and Semicontinuous Analyses at EUPHORE

A number of continuous measurements were made during the chamber experiments. These included measurements of the following:

- NO, NO_2, and NO_x (in ppb), using a combined chemiluminescence NO detector (model CLD 770, Tecan Group, Männedorf, Switzerland) and photolytic converter (model PLC 760, Tecan Group Ltd.)
- NO, NO_2, and NO_x (in ppb), using a NO_x detector (model 200AU, Advanced Pollution Instrumentation, San Diego, CA)
- NO_y (in ppb), using a gas-phase chemiluminescence NO_x detector (model ML9841A, Teledyne Monitor Labs, Englewood, CO) and a catalytic converter (Molycon, Teledyne Monitor Labs)
- Sulfur dioxide (SO_2) (in ppb), using a SO_2 monitor (model 4108, Dasibi Environmental Corp., Glendale, CA)
- O_3 (in ppb), using an ultraviolet photometer (model ML 9810, Casella Measurement, Bedfordshire, United Kingdom)
- Various gas-phase compounds, using Fourier transform infrared spectroscopy
- Particle mass, using a tapered-element oscillating microbalance (Rupprecht & Patashnick Co., East Greenbush, NY)
- Aerosol size, number concentrations, and volume, using a scanning mobility particle sizer
- Peroxyacetyl nitrate, using GC and a semicontinuous electron-capture detector
- HONO, using the long-path-absorption-photometer wet method (2005 campaigns only)
- Formaldehyde, using a wet method (summer campaigns only) described below (with monitor model AL4021, Aero-Laser, Garmisch-Partenkirchen, Germany)
- VOCs, using semicontinuous GC–MS
- Chamber temperature, pressure, relative humidity, and J(NO_2) (the NO_2 photolysis rate).

More detailed information about these instruments is available in the EUPHORE reports and can be obtained upon request. Additional information about the instruments used for measuring peroxyacetyl nitrate, HONO, and formaldehyde is presented below; data from these instruments will be discussed in more detail later in this report.

Detection of Peroxyacetyl Nitrate Peroxyacetyl nitrate was detected at EUPHORE using a GC equipped with a semicontinuous electron-capture detector. The GC was also equipped with a 7.5-m DB-5 (5% phenyl polysiloxane) fused-silica capillary analytic column with a 0.53-mm i.d. and a 5-µm film. The column was mounted in a thermostatically controlled oven cooled by Peltier elements. A 4.5-m DB-1 (100% dimethyl polysiloxane) back-flush precolumn with a 0.53-mm i.d. and a 5-µm film prevented contamination of the analytic column and cut down analysis run times by preventing compounds with long retention times from entering it. The temperature of the analytic column was held isothermally at 14°C, and ultra-high-purity nitrogen acted as the carrier gas. Column switching, sample loading, and injection were handled using a pneumatically actuated 10-port valve (model EC10W, Valco Instruments Co., Houston, TX). The electron-capture detector (model 80, Fisons Instruments, Milan, Italy) was equipped with a control module (model ECD 800, Fisons Instruments). Calibration was based on the synthesis of peroxyacetyl nitrate by ultraviolet photolysis of acetone in the presence of NO (20 ppm standard) in a flow reactor, with subsequent dynamic dilution in purified air to concentrations of 200 ppt to 2 ppb.

Detection of HONO In the summer 2005 campaign, a long-path absorption photometer was used to detect HONO (Heland et al. 2001; Kleffman et al. 2002). This technique is based on the spectrophotometric detection of an azo dye formed during the liquid reaction of HONO in a mixture of sulfanilamide (0.06 M), hydrochloric acid (1 M), and *N*-(1-naphthyl)ethylenediamine dihydrochloride (0.8 mM). A 10-cm glass stripping coil was used to strip the gas-phase HONO from the sampling stream. A long (0.95 m) Teflon liquid-core waveguide tube (type AF 2400, Biogeneral, San Diego, CA) acted as an absorption cell; a halogen lamp (model HL-2000-LL, Ocean Optics, Dunedin, FL) was used as the main light source. The sampling unit used a double-stripping-coil differencing technique to account for possible interferences, and good agreement with other sensitive measurement techniques has been established (Kleffman et al. 2006). The HONO monitor was operated under standard conditions and switched on at least 30 minutes before the DE was injected into the chamber to ensure stable operation. Calibrations were performed using diluted standards freshly prepared from a liquid-nitrite stock solution. The reagent system tended to undergo baseline drift in the absence of HONO because of deposition of the azo dye in the absorption cell. To correct for this, the zero level was measured routinely throughout the sampling times.

Detection of Formaldehyde The detection of formaldehyde was based on the Hantzsch reaction (a liquid-phase reaction of formaldehyde with acetylacetone and an amine). The reaction produces α,α′-dimethyl-β,β′-diacetylpyridine, which is excited at 400 nm (using a mercury lamp) and fluoresces at 510 nm. The technique is sensitive to formaldehyde in aqueous solution. Transfer of gaseous formaldehyde into solution was achieved in a stripping coil, where air and stripping solution were brought into contact at defined flow rates and contact surfaces. The air and liquid streams were afterward separated, and the solution was analyzed for formaldehyde. The formaldehyde mixing ratio in air was then calculated from the concentration in solution and the ratio of the air- and stripping-flow rates. The formaldehyde detector at EUPHORE (model AL4021, Aero-Laser GmbH, Garmisch-Partenkirchen, Germany) consisted of a chemistry module, an electronics module, and a fluorimeter. The detector had a 0.08-ppb detection limit and a delay time of 500 seconds (the time needed for gas and liquid formaldehyde to reach equilibrium). The range of gas-phase measurements (typically 0 to 250 ppb), provided by liquid-formaldehyde standardization, could be set by the user.

In Situ Versus Dilution-Corrected Concentration Values To maintain consistent pressure and compensate for volume loss (caused by sampling and minor leaks), clean air was continuously injected into the chamber throughout each experiment (Becker 1996). To correct for the resulting dilution of the atmosphere's gaseous and particle constituents by the clean air, SF_6 was injected into the chamber at the beginning of each experiment. Monitoring the SF_6 by Fourier transform infrared spectroscopy allowed us to calculate a chamber dilution rate that could be used to correct for the declining constituent concentrations. Unlike in situ concentration values, corrected values represented the "true production" resulting from photochemical processes (e.g., O_3; see Results). Because our study was focused on toxicity, the in situ values were more appropriate indicators of the character of the collected samples (i.e., true real-time mixing ratios before and during sampling). Yet in certain scenarios (e.g., the production of peroxyacetyl nitrate), dilution correction gave a more accurate representation of the chamber system's potential for producing secondary compounds.

TOXICITY TESTING

Preparation of Samples for Instillation

The targeted masses of PM and SVOC fractions were removed from the storage vials and transferred to separate polypropylene tubes. To keep the final acetone concentration at < 2%, the samples were further concentrated under nitrogen, if necessary. A volume of 10% of the intended final volume of 0.1% polysorbate 80 (Tween 80, ICI Americas, Wilmington, DE) in 0.9% sterile saline solution was added, and the suspension was sonicated for 1 minute in a cup-style sonicator as previously described (Seagrave et al. 2002). The volume was then corrected to the target final volume with the saline solution, resulting in a final suspension in < 2% acetone and 0.01% Tween 80 in saline solution. The samples were kept as dark as feasible throughout the processing. For rats, the target masses for delivery were 0.25 mg, 0.50 mg, and 0.75 mg of combined PM and SVOC fractions. The final samples were approximately 10% PM and 90% SVOCs for all samples. For mice, the masses were 25 µg, 50 µg, and 75 µg (except for samples for which adequate mass was not available, in which case only the highest dose was prepared and tested). For logistic reasons (processing of more than 55 animals a day turned out to be impractical), the experiments were grouped into blocks (four blocks jointly for the winter and summer 2005 campaigns and four for the summer 2006 campaign), each of which included a negative control, a positive control, and three doses each of two or three samples (or three doses of two samples and one dose of a sample for which the supply of mass was limited). The negative control consisted of the sample vehicle (2% acetone and 0.01% Tween 80 in 0.9% saline solution) and was included for testing in each experiment. In the summer 2006 campaign, a blank consisting of extracts from unexposed filters was also included. The positive control consisted of a suspension of diesel soot (DS) (National Institute of Standards and Technology Standard Reference Material 2975, collected from an industrial fork lift; 1 mg for rats, 0.1 mg for mice) prepared in the same manner as the other samples. In all three campaigns, an additional blank was included, consisting of the material collected from a comparable volume of atmosphere passing through the chamber. A single dose of this material, with the same relative volume as the highest dose of the DE samples, was tested.

Animal Husbandry

Male F344 rats were used to investigate the toxicity of the samples collected in winter and summer 2005. In summer 2006, male BALB/c mice were used because of the limited mass for some samples (after test instillations in both species confirmed the similarity of the relative toxicity of the two samples for which the most mass was available). The rodents, approximately six weeks old at receipt, were obtained from Charles River Laboratories (Wilmington, MA) and were quarantined for two weeks before use. Food (Teklad Lab blocks) and municipal tap water were provided ad libitum. The rodents were housed in "shoebox" cages, two per cage, on a 12-hour-light, 12-hour-dark cycle in an environment maintained at 20°C to 22°C and 20% to 50% relative humidity. This protocol was approved by the Animal Use Committee at the Lovelace Respiratory Research Institute.

Intratracheal Instillation

The rodents were anesthetized with isoflurane in an induction chamber and placed on a slanted board to facilitate visualization of the vocal cords. A soft plastic cannula (16-gauge for rats, 22-gauge for mice) was inserted into the trachea with the aid of a rigid stylet. Insertion was confirmed using a glass syringe to inflate the lungs. The intended volume of the suspension (0.5 mL for rats, 0.1 mL for mice) was injected through the cannula followed by two small puffs of air delivered with the glass syringe. The cannula was removed, and the animal was returned to its cage for recovery.

Killing and Processing

Twenty-four hours after instillation, the rodents were killed with an overdose of a pentobarbital-based euthanasia solution (Euthasol, Virbac AH, Fort Worth, TX), and the body weight was recorded. The animals were killed and necropsied in the same order as they had been instilled. The instillations and necropsies of each set of animals were completed within 4 hours of each other (to reduce the likelihood of diurnal variations or differences in the time between instillation and death contributing to differences in results). From mice only, blood was collected into tubes containing ethylene-diamine-tetra-acetic acid (EDTA) for an estimated final concentration of 10 mM EDTA. Plasma was removed and transferred to a separate tube containing butylated hydroxytoluene (BHT) for an estimated final concentration of 0.1 mM BHT. The lungs were carefully dissected free, and a microvascular clamp was placed on the left bronchus. A cannula was ligated into the trachea, and the right lung was lavaged with three volumes (3 mL for rats, 0.5 mL for mice) of phosphate-buffered saline. The three volumes of lavage fluids were combined and held on ice until being processed for indicators of toxicity and inflammation. The clamp was then removed from the left lung, the right bronchus was tied off, the right lung was removed, and its lobes were frozen separately. The left lung was inflated with neutral buffered formalin and immersed in the same fixative for at least 48 hours. The

specimens were then embedded in paraffin, cut into 3-μm sections, stained with hematoxylin and eosin, and evaluated by a board-certified veterinary pathologist.

The following indicators were scored on a scale of 0 ("not observed") to 5 ("extreme") for each animal: inflammation, as suggested by the presence of focal alveolar neutrophils, suppurative bronchiolitis, focal suppurative bronchiolitis, focal eosinophilic or mixed peribronchiolitis or vasculitis, increased alveolar macrophages, intra-alveolar neutrophil infiltration, focal intra-alveolar neutrophil infiltration, microgranuloma, mononuclear cell infiltration in alveolar walls, mononuclear perivascular cuffing, or neutrophilic perivascular cuffing; cytotoxicity, as suggested by the presence of focal bronchiolar epithelial erosion, intra-alveolar hemorrhaging, focal intra-alveolar hemorrhaging, or pulmonary edema; and parenchymal changes, as suggested by the presence of focal alveolar-wall thickening, congestion, emphysema, focal fibrosis, increased bronchial goblet cells, perivascular edema, or pneumocyte hypertrophy or hyperplasia. The scores in each category for each animal were then added, averaged for the animals in each dose-and-sample group, and reported along with the standard error of the mean.

The total number of nucleated cells in the lavage fluid was evaluated with a hemocytometer. A cytocentrifuge was used to prepare slides of the cells, which were then stained with Diff-Quick, and the fractions of each type of cell (macrophages, neutrophils, lymphocytes, and eosinophils) were evaluated under a microscope at 20× power. For mice only, the remaining lavage fluid was centrifuged, and the cells were resuspended in HEPES (4-[2-hydroxyethyl]-1-piperazineethanesulfonic acid)-buffered Earle salts containing fluorescent microspheres (Fluoresbrite YG Microspheres 0.5 μm, Polysciences, Warrington, PA), incubated for 30 minutes at 37°C, and fixed with an equal volume of 4% paraformaldehyde. For each dose of each sample, a single pooled sample was processed similarly but without the addition of the microspheres, as a control for autofluorescence. Phagocytosis of the microspheres was evaluated by flow cytometry, gating for neutrophils separately from macrophages. Data from the neutrophil populations were collected but not reported, because of the small populations in many of the samples. Lymphocyte and eosinophil populations were extremely small and were not further evaluated.

The cell-free lavage fluid was analyzed for lactate dehydrogenase as an indicator of cytotoxicity (Gay et al. 1968), total protein as an indicator of loss of epithelial integrity (Watanabe et al. 1986), and alkaline phosphatase as a possible indicator of the activation of type II cells or profibrotic responses. These analyses were carried out on a Hitachi 911 chemistry analyzer (Roche Diagnostics, Basel, Switzerland) using commercially available clinical kits, except for the alkaline phosphatase in mice, which (because of its very low concentrations in the mouse lavage fluid) was analyzed in a 96-well plate format using *para*-nitrophenyl phosphate as the substrate in diethanolamine buffer (catalog number 172-1063, AP Substrate Kit, Bio-Rad Laboratories, Carlsbad, CA) and incubated for 2 hours at 37°C.

One lobe of the frozen right lungs from the mice was homogenized in a buffer containing proteinase inhibitors, EDTA (10 mM), and BHT (0.1 mM). The supernatant was analyzed for heme oxygenase-1 by Western blotting on 10% polyacrylamide gels blotted to nitrocellulose and blocked with nonfat dry milk. Each blot included a standard of authentic heme oxygenase-1, and the target was detected using a Stressgen primary antibody (Assay Designs, Ann Arbor, MI) and a secondary horseradish-peroxidase–conjugated antibody (Sigma Chemical Co., St. Louis, MO). Quantification was accomplished using Amersham enhanced chemiluminescence reagent (GE Healthcare Bio-Sciences AB, Uppsala, Sweden) captured on X-ray film and analyzed by densitometry on a Bio-Rad Laboratories imaging system. Although the number of samples made it impractical to include a standard curve on each gel, multiple exposures were taken to avoid issues of film saturation. The supernatant was also assayed for thiobarbituric-acid–reactive substances (TBARS) as a measure of lipid peroxidation. In addition, plasma collected from the mice was assayed for TBARS as a measure of lipid peroxidation (Rhoden et al. 2004).

A separate lobe of the frozen right lungs from the mice was homogenized in 5% sulfosalicylic acid. The supernatant was analyzed for total glutathione and oxidized glutathione, as measures of oxidative stress, using a Bioxytech assay kit (Oxis International, Beverly Hills, CA) based on the Tietze reaction (Tietze 1969) as modified by Anderson (Anderson 1985).

STATISTICAL METHODS AND DATA ANALYSIS

Data Analysis for Chemical Compositions

Software programs have been developed at the Desert Research Institute to automate analytic data processing and reporting. All analytic results were evaluated in terms of their associated measurement errors according to the following equation:

$$\text{analyte uncertainty} = \sqrt{(\text{precision} \times \text{concentration})^2 + (\text{MDL})^2}, \quad (3)$$

where MDL is the method detection limit. The equation incorporates the analyte detection limit for each compound,

such that when concentrations approach zero the error is reported as the analyte detection limit.

Data analysis included level-1 and level-2 validations of all analytic data, flagging of outliers, and removal of invalid values. All suspected values were examined and, where applicable, corrected. Graphs showing the chemical composition of samples were prepared using Microsoft Excel, version 2002 (Microsoft Corporation, Redmond, WA).

Statistical Analysis for Toxicity Testing

The data were inspected, and a small number of points meeting the criterion for statistical outliers at $P < 0.01$ were omitted from our analyses. These were generally on the order of 10 times the mean of the other samples for that endpoint and sample dose and were most likely the result of inhomogeneous instillation or instrument errors. After omitting these data points, the dose–response for each sample and each endpoint was analyzed by linear regression. Because no significant differences were observed in responses to the sample vehicle (i.e., the negative control) among the various blocks of experiments, the average value of this control was used as the *y*-intercept for each endpoint. Similarly, responses to the suspended DS (i.e., the positive control) were averaged for all blocks and reported as a single point along with its standard error. No weighting was applied. The slope of this line, along with its standard error, was reported as the potency score. The exception to this procedure was that, because of a strongly biphasic response for TBARS in plasma in mice, the linear regression was performed only for the negative control and the low and medium exhaust-sample doses. For all samples (including the positive control and chamber blanks) for which only one dose was tested, the slope was simply the net difference between the response to the sample and the negative control divided by the dose. Slopes significantly different from zero were reported. Graphs for all endpoints were produced using GraphPad Prism software, version 4.3 for the data generated for the 2005 samples and version 5.0 for the 2006 samples (GraphPad Software, San Diego, CA). Statistical analyses were performed using version 5.0 for all samples. One-way analysis of variance (ANOVA; a procedure for determining whether significant differences exist between two or more sample means) was used to compare all samples for each endpoint (including the chamber blanks but not the positive control), using Newman–Keuls post-tests. In addition, selected samples from the 2006 campaign were compared with the sample aged in the dark with the denuder present, using the Dunnett post-test. Pairwise differences between selected potency scores in rats and mice, respectively, were evaluated using unequal-variance *t* tests, based on degrees of freedom calculated with the Welch–Satterthwaite correction.

RESULTS

This study created a large amount of new information on the atmospheric chemistry and toxicity of DE. Because of the exploratory nature of several of the atmospheres used and the need to evaluate the effect of the denuder on toxicity, a range of experimental variables are reported (see Table 3) and described here. An even more comprehensive guide to our analysis is presented in Appendix C for atmospheric chemistry and Appendix D for toxicity testing. To facilitate explicit evaluation of the role of exhaust aging on chemistry and toxicity, the main body of this section of the report distills the data on our final atmospheres and test conditions (see Effect of Atmospheric Transformations on Composition of Diesel Exhaust, below) and finally integrates the data on chemistry and toxicity (see Effect of Atmospheric Transformations on Toxicity of Diesel Exhaust, below).

As mentioned earlier, the diesel engine was new during the first campaign, in winter 2005, and had been in operation for only a few hours before starting the exposures. This was probably a reason why some of the data obtained during this campaign, most notably on diesel-particle size distribution and chemical composition, were somewhat different than those from the two subsequent campaigns. In addition, the experiments in winter 2005 were performed without a NO_x denuder (because the problem of excess NO_x only became apparent during the campaign). Because of these differences, we have presented detailed data for winter 2005 only in Appendices C and D (as text) and G (as an electronic database).

EFFECTS OF ATMOSPHERIC TRANSFORMATION ON THE COMPOSITION OF DIESEL EXHAUST

The main objective of this study was to investigate changes in the chemical composition and toxicity of DE resulting from its exposure and aging over time in the atmosphere. As a consequence, the establishment of realistic atmospheric conditions for these experiments was very important. We ensured that the chamber used for the study was of sufficient volume to permit the establishment of realistic concentrations of DE (our diesel PM concentrations, for example, were usually lower in the chamber than the U.S. EPA's 24-hour standard for ambient particulate matter < 2.5 μm in aerodynamic diameter [$PM_{2.5}$], which had until recently been 65 $\mu g/m^3$). We also made every effort to ensure that the concentrations of gaseous species were comparable to those of real-world atmospheres. This was especially important for NO_x concentrations, which in urban air are in the range of 50 to 200 ppb but seldom actually reach 200 ppb, even on a busy freeway (Fujita et al.

2003). This was also why we put so much effort into developing an efficient NO_x denuder after the winter 2005 campaign and used it for all subsequent experiments.

In addition, real ambient atmospheres contain higher concentrations of VOCs than our chamber atmospheres did, originating from sources other than diesel engines (which are usually quite low in VOCs, especially modern engines). The lower VOC concentrations in the DE in the chamber would have limited photochemical reactions (by limiting the formation of OH radicals and O_3) more than is the case in the real troposphere. For several experiments, therefore, we added toluene (as a representative of aromatic VOCs in air) or a mixture of aromatic compounds, including naphthalene.

As mentioned in the previous section, we eliminated the samples collected during the winter 2005 campaign because the diesel engine was brand new and the DE proved to be chemically and physically different from that of the subsequent campaigns.

For the final comparison of chemical compositions and toxicity testing, then, we selected only the types of samples that were relevant to realistic atmospheres:

1. DE injected into the chamber with the NO_x denuder and exposed in the dark ("DE"). This category included samples Dd05s_1 and Dd05s_2 (from summer 2005) and Dd06s_1 and Dd06s_2 (from summer 2006). The equivalent samples for toxicity testing were the combined 1 and 2 (i.e., Dd05s_1 + 2 and Dd06s_1 + 2).
2. DE injected into the chamber with the NO_x denuder and exposed in the dark with added O_3 to produce NO_3 radicals in low-NO_x conditions ("DE + NO_3"). This category included samples Dd05sN_1 and Dd05sN_2 (from summer 2005). The equivalent sample for toxicity testing was Dd05sN_1 + 2.
3. DE injected into the chamber with the NO_x denuder and exposed in the dark with added O_3 to produce NO_3 radicals in low-NO_x conditions and with added VOCs ("DE + NO_3 + VOCs"). This category included the one sample Dd06sNV (from summer 2006) for chemistry and toxicity testing.
4. DE injected into the chamber with the NO_x denuder and exposed in daylight ("DE + sun"). This category included samples Ld05s_1 and Ld05s_2 (from summer 2005) and Ld06s_1 (from summer 2006). The equivalent samples for toxicity testing were Ld05s_1 + 2 and Ld06s_1.
5. DE injected into the chamber with the NO_x denuder and exposed in daylight with added VOCs ("DE + sun + VOCs"). This category included the one sample Ld06sV_1 (from summer 2006) for chemistry and toxicity testing.
6. DE injected into the chamber with the NO_x denuder and exposed in daylight with added formaldehyde to produce OH radicals ("DE + sun + OH"). This category included samples Ld05sF_1 and Ld05sF_2 + 3 (from summer 2005) and Ld06sF_1 (from summer 2006). The equivalent samples for toxicity testing were Ld05sF_1–4 and Ld06sF_1.
7. DE injected into the chamber with the NO_x denuder and exposed in daylight with added formaldehyde and VOCs ("DE + sun + OH + VOCs"). This category included the one sample Ld06sFV_1 (from summer 2006) for chemistry and toxicity testing.
8. DE injected into the chamber with the NO_x denuder and exposed in daylight with added toluene ("DE + sun + toluene"). This category included samples Ld05sT_1 and Ld05sT_2 (from summer 2005) and Ld06sT_1 and Ld06sT_2 (from summer 2006). The equivalent samples for toxicity testing were Ld05sT_1 + 2 and Ld06sT_1.

Detailed chemical data for the samples collected from these atmospheres were tabulated in electronic form (see Appendix F, available on the HEI Web site). Please note that all organic-compound concentrations were expressed in relation to EC (i.e., micrograms or nanograms of species per milligram of EC). The assumption in this normalization procedure was that the total EC mass in the chamber would remain unchanged while atmospheric transformations of the organic compounds took place. (In other words, individual organic compounds would either be produced as secondary organic aerosols or be consumed in transformation reactions.) These processes can change the total PM mass while leaving the EC mass unchanged. An additional assumption was that the wall losses for organic compounds and EC were approximately the same. In cases where more than one run was performed for a given type of atmosphere, the data were averaged and standard deviations between runs are provided. The figures presented below show only the most abundant species in each type of atmosphere.

In Figure 6, the top panel compares the OC, POC, and EC fractions of the total PM mass as measured in the sample types described earlier. If more than one sample was included in a given sample type, the percentages were averaged (see Appendix F for mean concentrations and standard deviations). The middle panel compares the ratios of OC to EC for each sample type, and the bottom panel compares the total carbon (TC; i.e., OC [including POC] plus EC), nitrate, and sulfate fractions for each sample type. As can be seen in the top panel, the percent contribution of OC fractions to TC was higher for all DE exposures in daylight compared with DE aged in the dark,

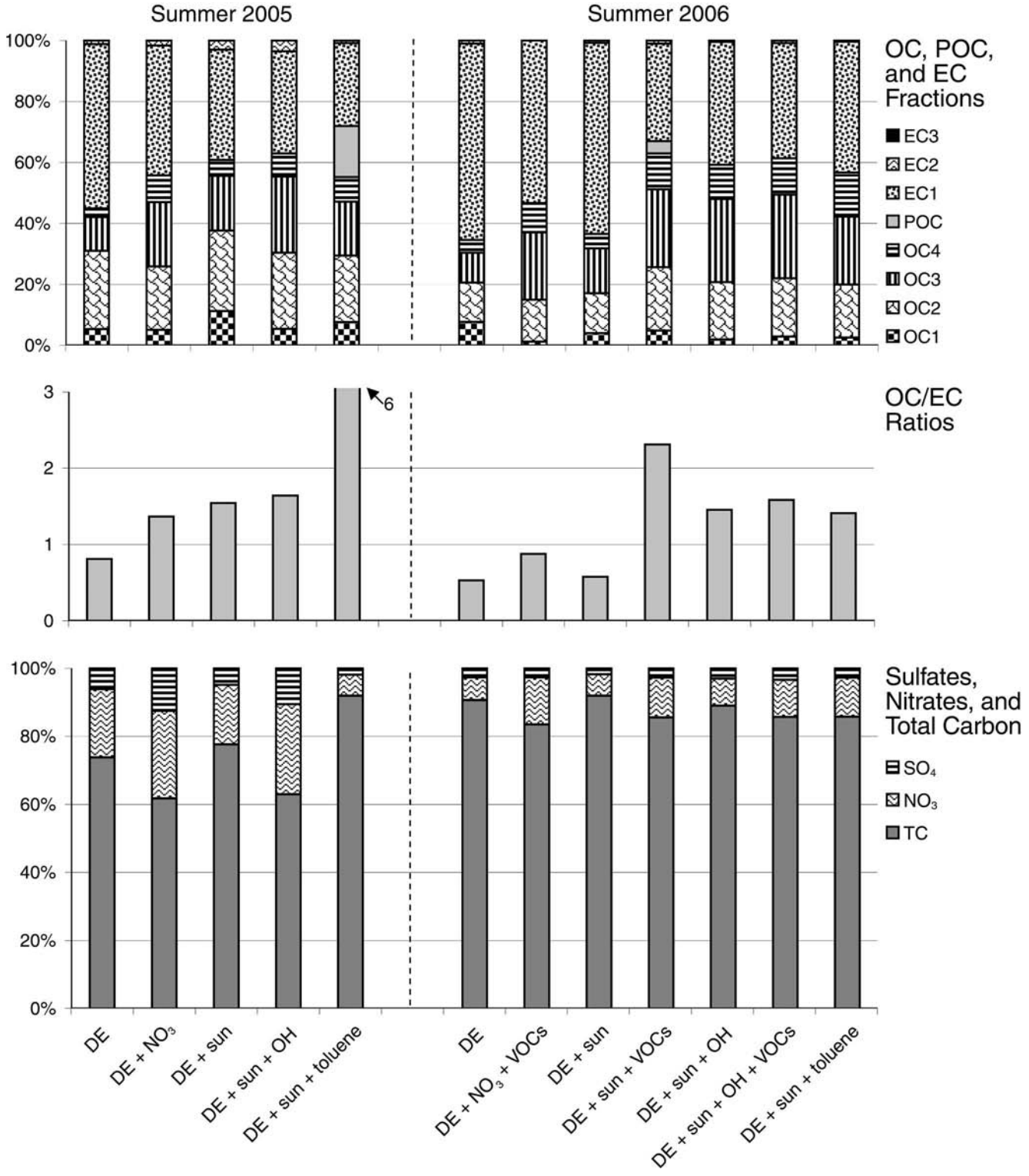

Figure 6. Comparison of carbon fractions in samples collected from chamber exposures with the NO_x denuder in summer 2005 and 2006. (Top panel) OC, POC, and EC fractions as percentages of the total PM mass in each sample type, corresponding to temperature steps of 120°C (OC1), 250°C (OC2), 450°C (OC3), and 550°C (OC4) in a nonoxidizing helium atmosphere and of 550°C (EC1), 700°C (EC2), and 850°C (EC3) in an oxidizing atmosphere. (Middle panel) Ratios of OC to EC in each sample type. (At 6 to 1, the ratio for DE aged in daylight with added toluene in 2005 was off the top of the *y*-axis scale.) (Bottom panel) Nitrates, sulfates, and TC (includes OC, POC, and EC) as percentages of each sample type.

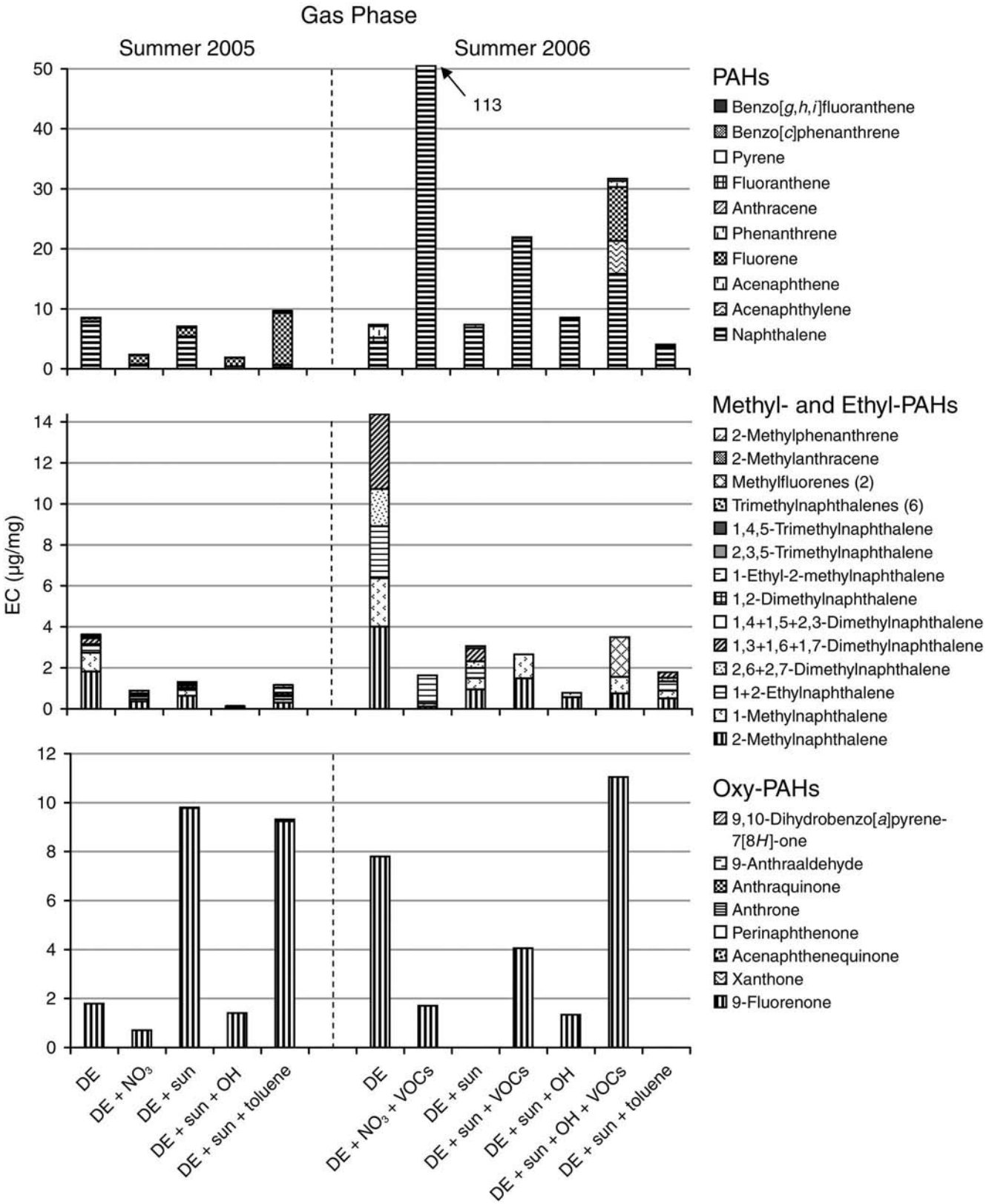

Figure 7. Comparison of gas- and particle-phase nonsubstituted PAHs, methyl- and ethyl-substituted PAHs, and oxy-substituted PAHs in samples collected from chamber exposures with the NO_x denuder in summer 2005 and 2006. Note that the *y*-axis scales differ from panel to panel. (Numbers with arrows are concentration measures, in micrograms PAH per milligram EC, that ran off the top of some of the *y*-axis scales.)

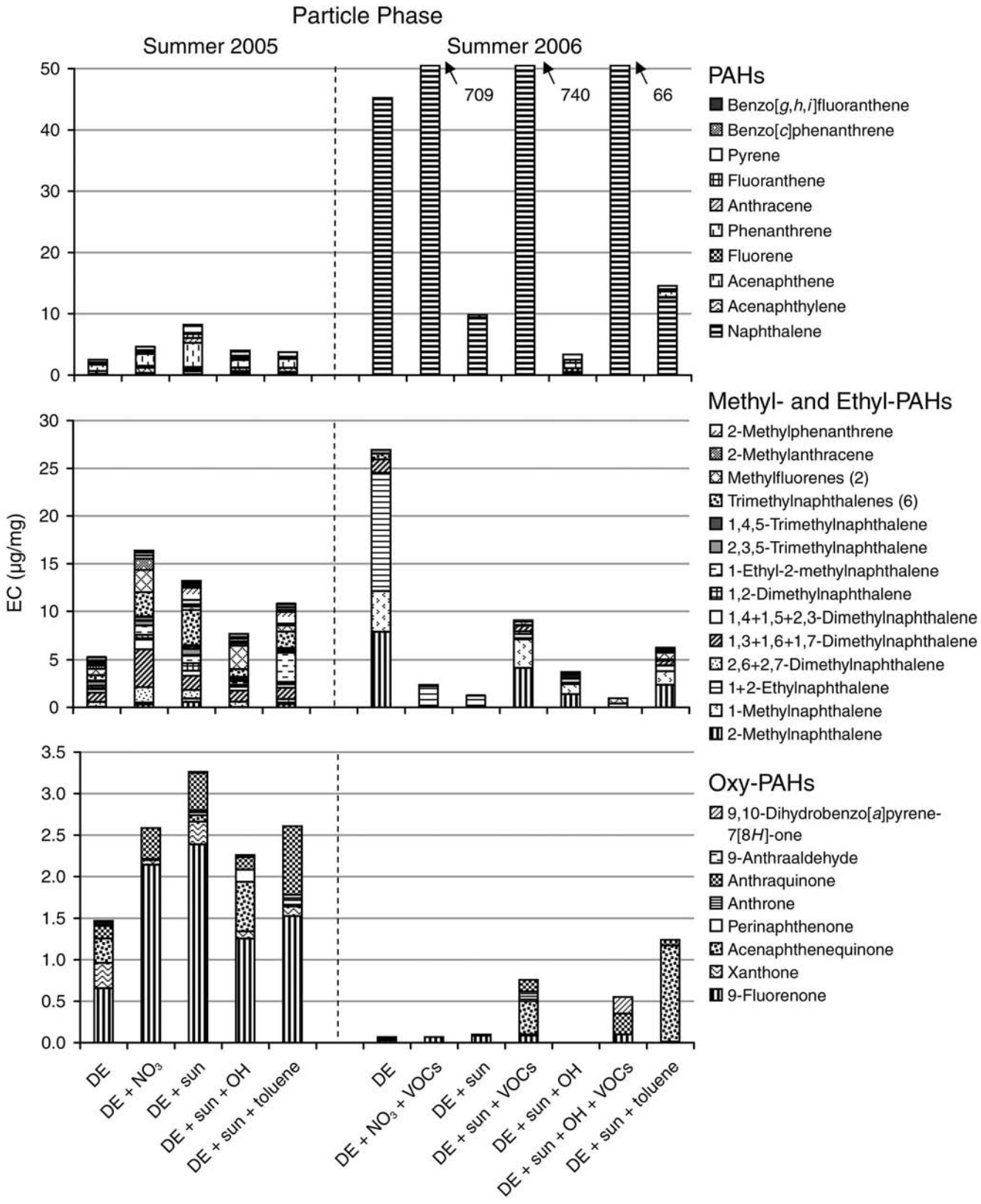

Figure 7 (*Continued*).

except for DE aged in daylight in 2006, an atmosphere that was not photochemically active because of its very low concentrations of VOCs. The addition of NO_3 radicals, OH radicals, VOCs, or toluene greatly enhanced the reactivity of the system, leading to the production of secondary organic aerosols and the higher-percent contributions of OC fractions seen among the other sample types. The greatest increase was observed for DE aged in daylight with added toluene in 2005. As discussed in Appendix C, the difference in results between the toluene exposures in summer 2005 and summer 2006 was probably caused by the higher toluene-to-NO_x ratios in summer 2006. DE aged in daylight with added toluene (in both summer 2005 and summer 2006) and DE aged in daylight with added VOCs showed significant contributions of POC, indicating the presence of highly polar or oligomeric organic compounds formed as secondary organic aerosols. The contribution of nitrates and sulfates was higher in summer 2005, before the more efficient NO_x denuder was put into use.

Figure 7 compares gas- and solid-phase PAHs—including non-substituted PAHs, methyl- and ethyl-substituted PAHs, and oxygen-substituted PAHs—as measured in the sample types described earlier. As the figure shows, in the summer 2005 campaign, gas-phase naphthalene concentrations decreased noticeably for samples of DE aged with added NO_3 radicals and OH radicals (as compared with baseline DE). In the summer 2006 campaign, naphthalene was added in rather high concentrations (approximately 10–15 $\mu g/m^3$; see Table 4) to DE aged in the dark with added NO_3 radicals and VOCs and to DE aged in daylight with added VOCs or with added OH radicals and VOCs, with the result that it was unclear if naphthalene concentrations had decreased for the exposures in daylight. The figure also shows a decrease in gas-phase 1- and 2-methylnaphthalene for all exposures in 2005 and 2006. The greatest decreases occurred for DE aged in daylight with added OH radicals, VOCs, or toluene. This indicated the reactions of these PAHs and presumably the formation of secondary organic aerosols. It was also consistent with the methylnaphthalenes having much shorter lifetimes (because of the reaction with OH radicals) than the naphthalene (approximately 3 hours compared with 7 hours). Gas-phase 9-fluorenone was the most abundant oxy-PAH; its concentrations seemed to increase in exposures in daylight, especially for DE aged in daylight with added OH radicals and VOCs. Particle-phase oxy-PAH concentrations were generally much lower but also seemed to increase in exposures in daylight, most noticeably in 2005.

There were differences in PAH composition between the samples from 2005 and 2006, most notably in the concentrations of naphthalene and 1- and 2-methylnaphthalene, which were higher in 2006. This might have been an indication of changes in the composition of the DE caused by further use of the diesel engine as its components (e.g., valves, seals, and internal surfaces) accrued wear. More likely, however, the differences were caused by the much longer times for which the engine was run in 2006 than in 2005. In 2005, because of the low efficiency of the first NO_x denuder, DE was injected into the chamber for just 4 to 6 minutes at a time to avoid NO_x breakthrough. In summer 2006, the much higher efficiency of the improved denuder allowed us to inject DE for an average of 20 to 30 minutes at a time. However, as noted earlier, the engine was overheating during these longer runs, which might have re-sulted in a higher proportion of unburned diesel fuel in the exhaust.

Figure 8 compares gas- and particle-phase nitro-PAHs as measured in the sample types described earlier. Again, there were differences in composition between the samples from 2005 and 2006. High concentrations of 1-nitronaphthalene and lesser concentrations of 2-nitronaphthalene distributed between the gas and particle phases were found in the 2006 samples, especially for DE aged in the dark with added NO_3 radicals and VOCs and for DE aged in daylight with added VOCs or with added OH radicals and VOCs, the samples in which naphthalene was added to the exposure atmospheres. (This was expected, because nitronaphthalene isomers are formed from the reaction of naphthalene with NO_3 radicals and OH radicals.) Although the concentrations of nitro-PAHs were lower in the remaining samples, a variety of nitro-PAHs distributed between the gas and particle phases were present in samples from all exposures.

Figure 9 compares particle-phase nitropyrene and nitrofluoranthene isomers as measured in the sample types described earlier. The isomers 1-nitropyrene and 3-nitrofluoranthene are thought to be directly emitted from motor vehicle engines; 2-nitrofluoranthene and 2- and 4-nitropyrene are formed from the gas-phase reactions of fluoranthane and pyrene with NO_3 radicals or OH radicals (Arey et al. 1986; Zielinska et al. 1986). As can be seen from the figure, 1-nitropyrene was the most abundant isomer in all samples; 2-nitrofluoranthene, 4-nitropyrene, and to a lesser extent 2-nitropyrene were also present in the exposures with added NO_3 radicals and OH radicals (especially in DE aged in the dark with added NO_3 radicals and VOCs and in DE aged in daylight with added OH radicals).

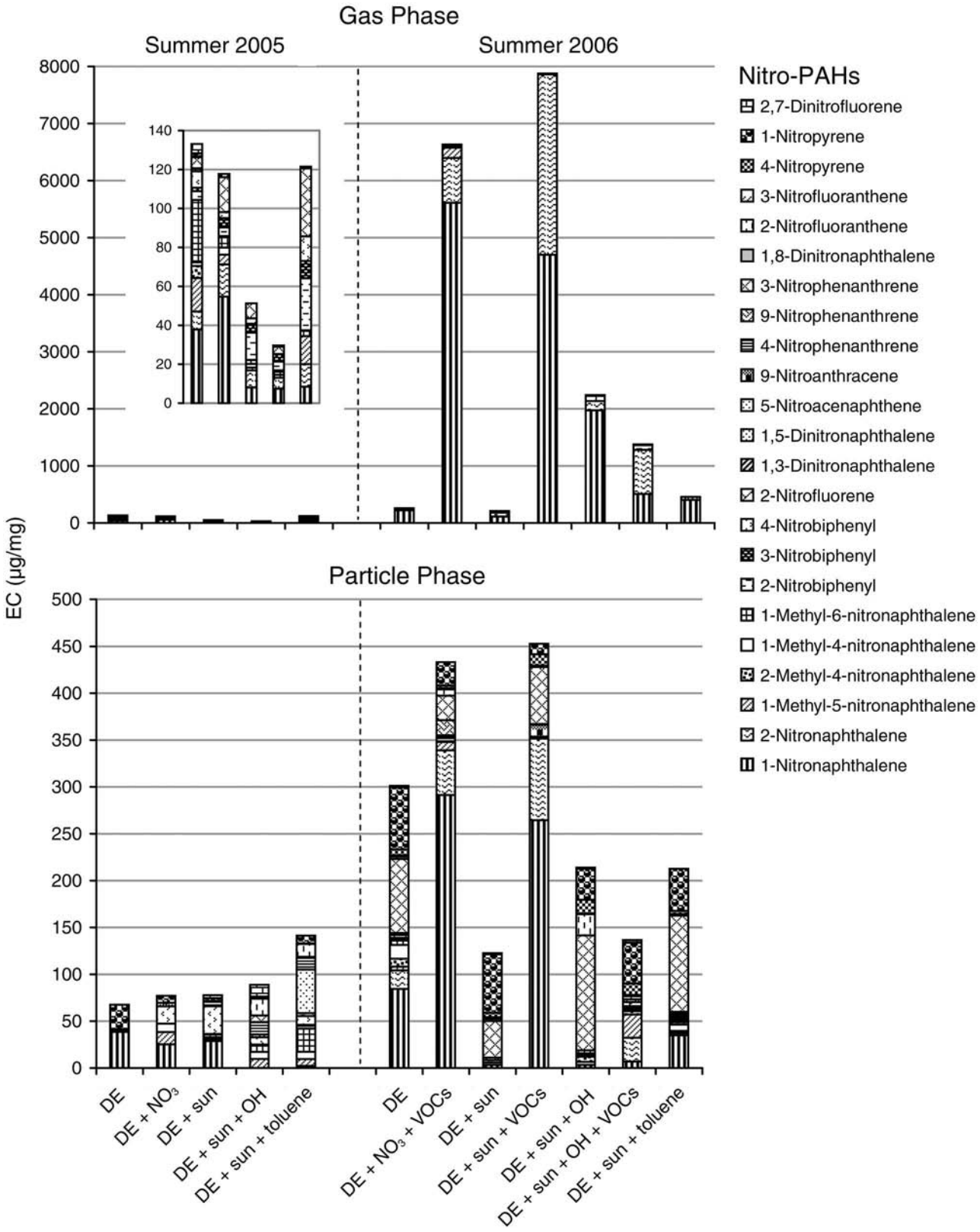

Figure 8. Comparison of gas- and particle-phase nitro-PAHs in samples collected from chamber exposures with the NO_x denuder in summer 2005 and 2006. Concentrations are shown in nanograms of nitro-PAH per milligram of EC. The inset box shows 2005 gas-phase concentrations at a finer scale. Note that the *y*-axis scales differ from panel to panel.

Figure 10 compares alkanes — including gas- and particle-phase *n*-alkanes, gas- and particle-phase *n*-alkylcyclohexanes, and gas-phase iso-alkanes — as measured in the sample types described earlier. Concentrations were much higher in the 2006 samples than in the 2005 samples. As mentioned before, this might have been caused by the much longer running times (and overheating) of the diesel engine in 2006, resulting in higher contributions of unburned diesel fuel to the exhaust. The figure shows that, in the summer 2006 campaign, concentrations of *n*-alkanes were relatively high in all samples; in most cases they decreased in exposures in daylight (especially in gas-phase DE aged in daylight with added OH radicals and VOCs). As can be seen, *n*-alkylcyclohexanes were much more abundant in the gas phase than in the particle phase and their concentrations decreased in exposures in daylight. The figure also shows that the light iso-alkanes C13 to C20 were present only in the gas phase and that their concentrations decreased significantly in all exposures in daylight or with added NO_3 radicals. The decrease in alkane concentrations in general indicated that atmospheric reactions of these compounds were in fact taking place in our experiments.

Figure 11 compares selected gas- and particle-phase polar compounds — including alkanoic acids, alkanedioic acids, and aromatic acids — as measured in selected samples collected from exposures in all three campaigns (i.e., winter and summer 2005 and summer 2006), including samples from winter 2005 of DE and of DE aged in the dark with added NO_3 radicals without the NO_x denuder. (Samples of DE aged in the dark with the denuder were not analyzed.) The concentrations of these compounds are shown in Appendix F. As might have been expected, significant increases in all concentrations occurred in exposures in daylight, especially for those with added VOCs. It is particularly interesting to note that concentrations of the alkanedioic acids, which are considered to be tracers of atmospheric transformations, increased in all exposures in daylight. (However, the highly polar, multifunctional, and oligomeric compounds that are likely to have been formed in such exposures were not measured by our analytic method.)

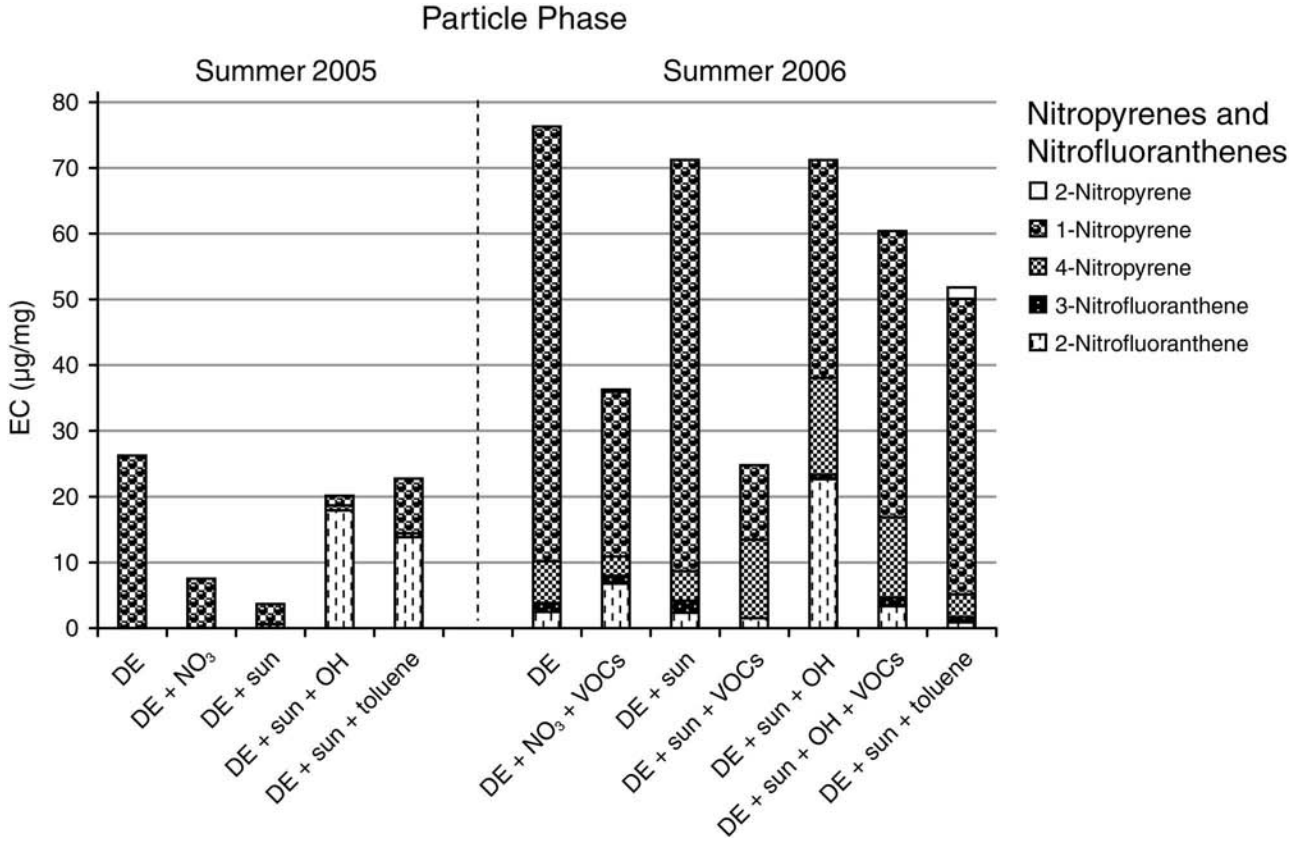

Figure 9. Comparison of particle-phase nitropyrene and nitrofluoranthene isomers in samples collected from chamber exposures with the NO_x denuder in summer 2005 and 2006. Concentrations are shown in nanograms of isomer per milligram of EC.

Figure 12 compares particle-phase hopanes and steranes as measured in samples collected from exposures in summer 2006. (Summer 2005 samples were not analyzed for these compounds.) Hopanes and steranes originating from engine lubrication oil are found mostly in the particle phase and, as might have been expected because of the newness of the diesel engine, were present in our samples only in very low concentrations. Nevertheless, these concentrations decreased even further in some exposures, especially for those with added VOCs.

EFFECTS OF ATMOSPHERIC TRANSFORMATION ON THE TOXICITY OF DIESEL EXHAUST

Figure 13 shows estimated potency scores for selected toxicologic indicators resulting from samples collected from chamber exposures in the summer 2005 and 2006 campaigns (i.e., again, those for which a NO_x denuder was in place). To facilitate comparisons of these data with those from the chemical analyses, the exposure samples used for both had been intended to be quite similar. However, several factors nevertheless affected the comparability of results from the two campaigns, including differences in the engine's baseline DE output and composition, differences in the NO_x denuders, and, perhaps most important, differences in the animal species tested. The masses of the samples collected in 2006 were relatively small, and they were not combined (as they had been in the previous campaigns), which precluded testing in rats. Testing in mice, because of their smaller body size and lung-surface area, had been estimated to require only approximately 10% as much sample mass to attain a ratio of mass to lung-surface area comparable to that attained in the rats, such that most sample types could be tested at the three intended doses. However, the mice's smaller body size also resulted in less uniform deposition of the samples when delivered by intratracheal instillation, leading to larger error estimates for the dose–response curves and the potency scores derived from them.

The figure shows that, compared with the DE control sample in the summer 2005 campaign, neither DE aged in the dark with added NO_3 radicals nor DE aged in daylight had much effect on potency scores for either lactate dehydrogenase (LDH) expression in lavage fluid, an indicator of cytotoxicity, or polymorphonuclear neutrophil (PMN) response in lavage fluid, an indicator of inflammation. However, DE aged in daylight with added OH radicals or toluene significantly increased cytotoxicity. Interestingly, the DE aged in daylight with added toluene did not increase the inflammatory response.

In the summer 2006 campaign, similarly, DE aged in daylight with added OH radicals caused a small increase in potency scores for PMNs (but not LDH) compared with DE aged in daylight, and DE aged in daylight with added toluene caused an increase in potency scores for LDH (but not PMNs). However, unlike the results from summer 2005, none of the results from summer 2006 were significantly different from that of the DE control sample. In addition, although inter-species comparisons are difficult, it should be noted that the DE control sample in summer 2005 (Dd05s_1 + 2), tested in rats, had a potency score similar to that of the diesel soot sample used as the LDH positive control and a lower score than (i.e., approximately 40% as high as) that of the diesel soot sample used as the PMN positive control. In contrast, the DE control sample in summer 2006 (Dd06s_1 + 3), tested in mice, had a much higher potency score than the DS control for LDH and, again, a lower score than (i.e., approximately 40% as high as) that of the diesel soot control for PMNs. This difference suggests that perhaps LDH expression for the DE control sample in 2006 was artificially high for some unknown reason. If that were the case, then the "real" score for LDH and DE aged in daylight with added toluene in summer 2006 could well have been more like that for LDH and DE aged in daylight with added toluene in summer 2005.

Figure 14 shows estimated potency scores for oxidative-stress and functional (i.e., macrophage phagocytosis) responses resulting from samples collected from exposures in summer 2006. Taken as a whole, these data suggest that DE aged in daylight with added OH radicals, VOCs, or both increased oxidative stress on the lungs. Specifically, compared with results for the DE control sample, there were significant increases in the potency score for heme oxygenase-1 for DE aged in daylight with added VOCs; in the potency scores for oxidized glutathione for DE aged in daylight and for DE aged in daylight with added OH radicals, VOCs, or both; and in the potency score for lung tissue TBARS for DE aged in daylight with added OH radicals; as well as a significant decrease in the potency score for total glutathione for DE aged in daylight with added OH radicals and VOCs. As the figure shows, results that were similar but did not reach statistical significance were often observed in the other tests of these samples. In contrast, the results for DE aged in daylight with added toluene were generally not significant, with the exception of the result for heme oxygenase-1, which had a potency score significantly *lower* than that of the DE control sample (but not significantly different from zero). The results for TBARS in plasma were puzzling: oxidative stress would have been expected to increase these indicators of lipid peroxidation rather than decrease them as observed. A possible explanation is that the more highly

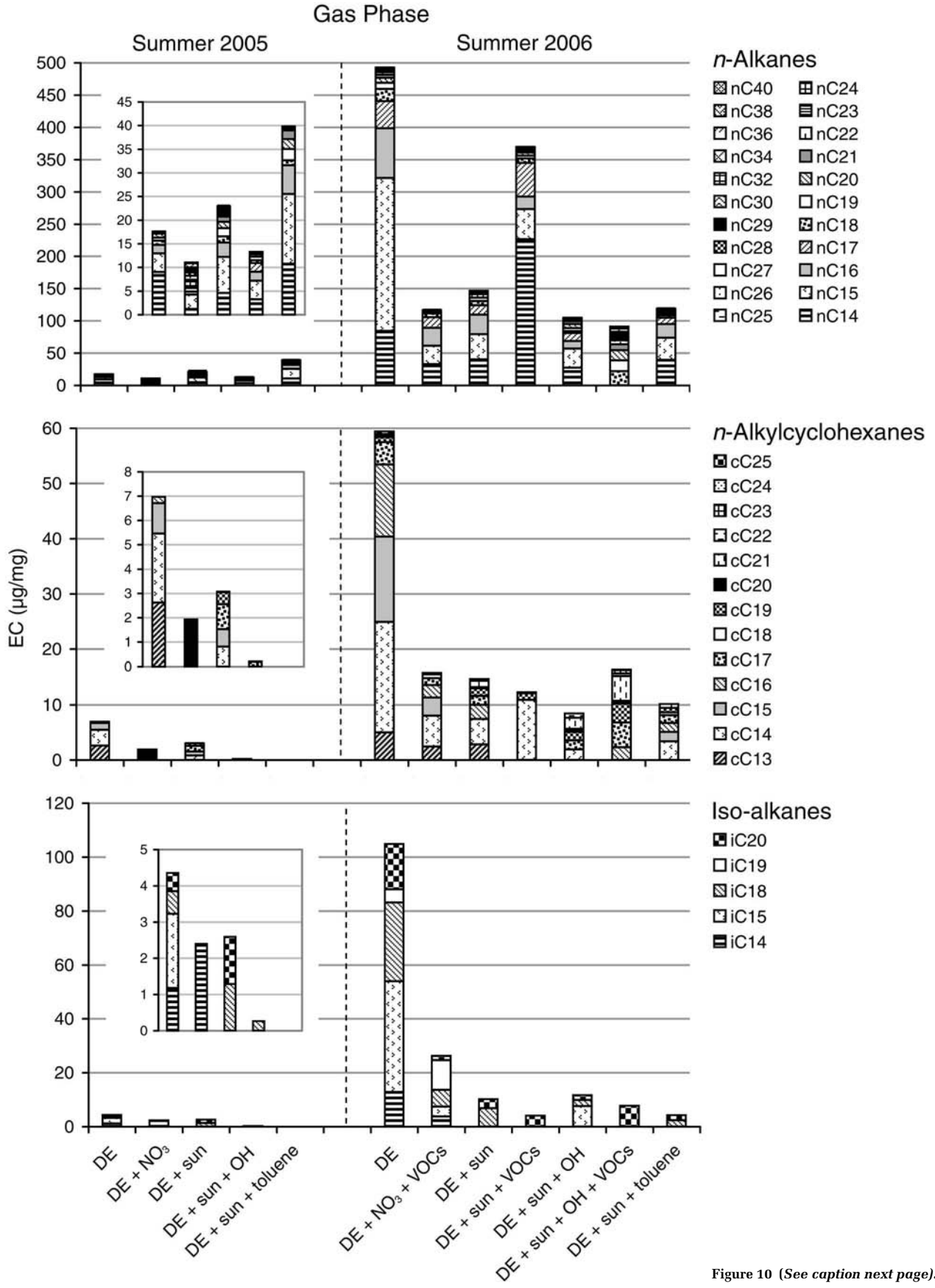

Figure 10 (*See caption next page).*

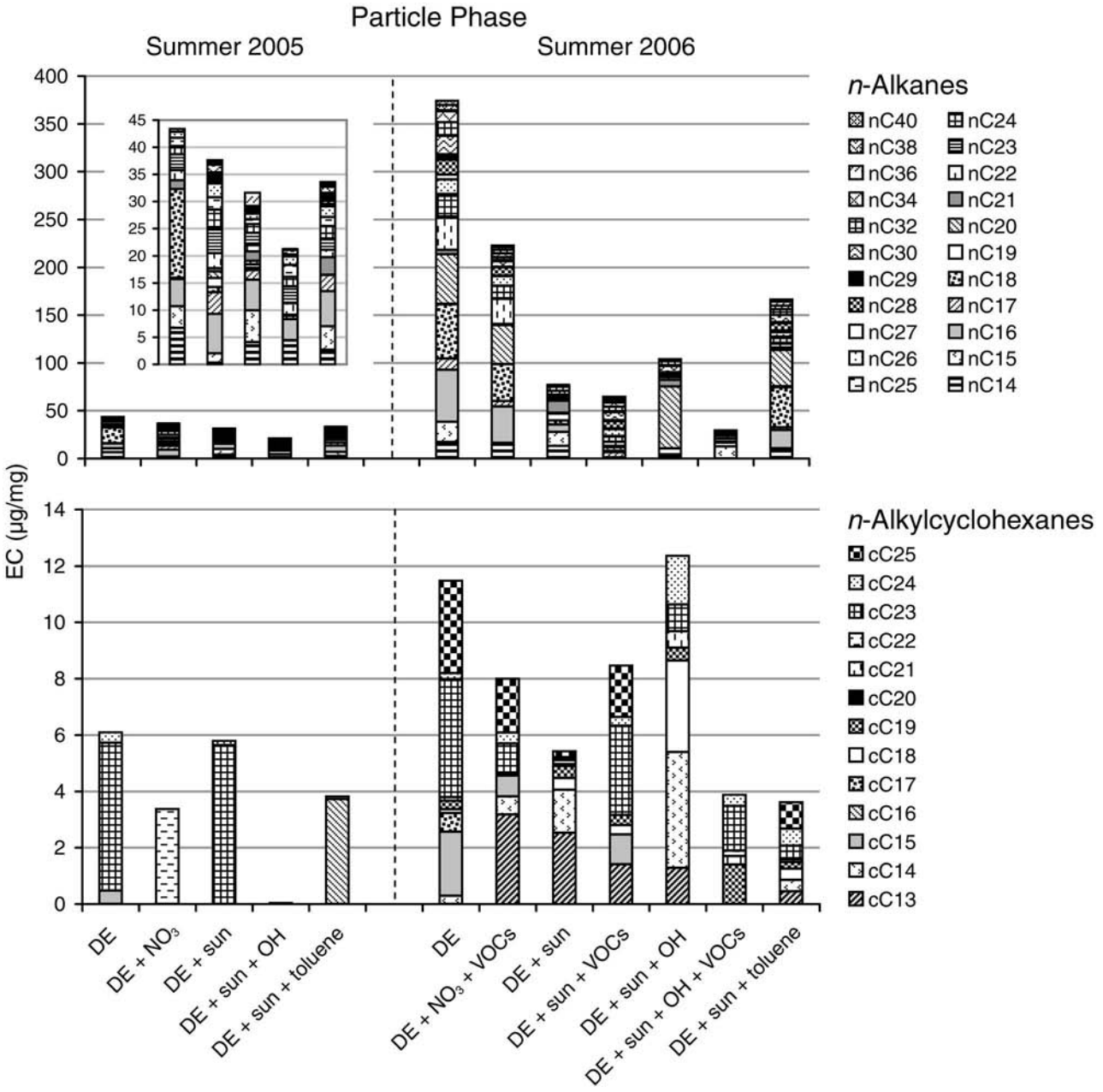

Figure 10. Comparison of gas- and particle-phase *n*-alkanes, gas- and particle-phase *n*-alkylcyclohexanes, and gas-phase iso-alkanes in samples collected from chamber exposures with the NO_x denuder in summer 2005 and 2006. Concentrations are shown in nanograms of alkane per milligram of EC. The inset boxes show selected 2005 concentrations at finer scales. nCx indicates an *n*-alkane with *x* carbon atoms. cCx indicates a cyclohexane with a (c–x) alkyl substitution. iCx indicates an iso-alkane with *x* carbon atoms. Note that the *y*-axis scales differ from panel to panel.

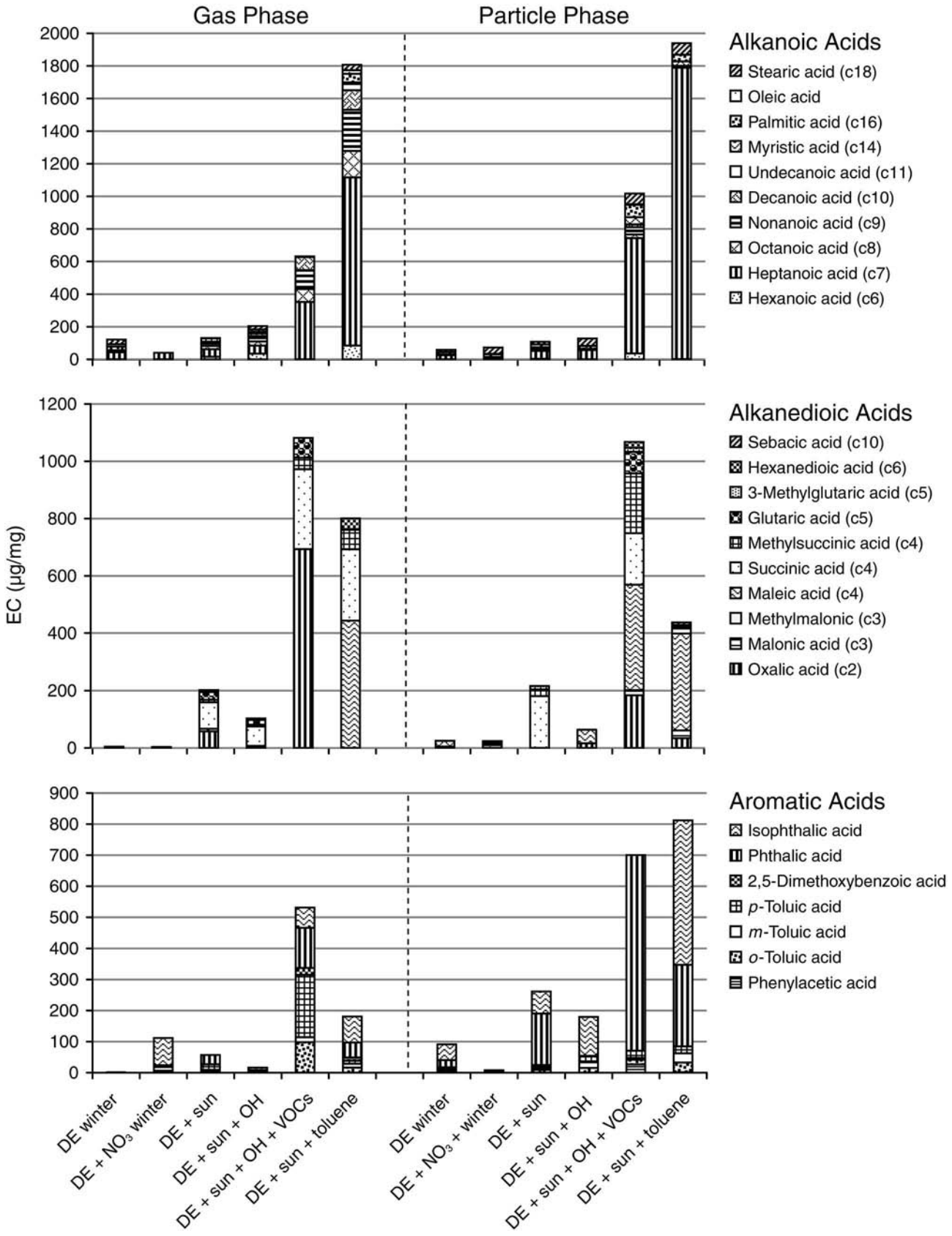

Figure 11. Comparison of selected polar compounds in samples collected from chamber exposures without the NO_x denuder in winter 2005 and with the denuder in summer 2005 and 2006. Shown are *n*-alkanoic acids, *n*-alkanedioic acids, and aromatic acids. Concentrations are shown in micrograms of compound per milligram of EC. Note that the *y*-axis scales differ from panel to panel.

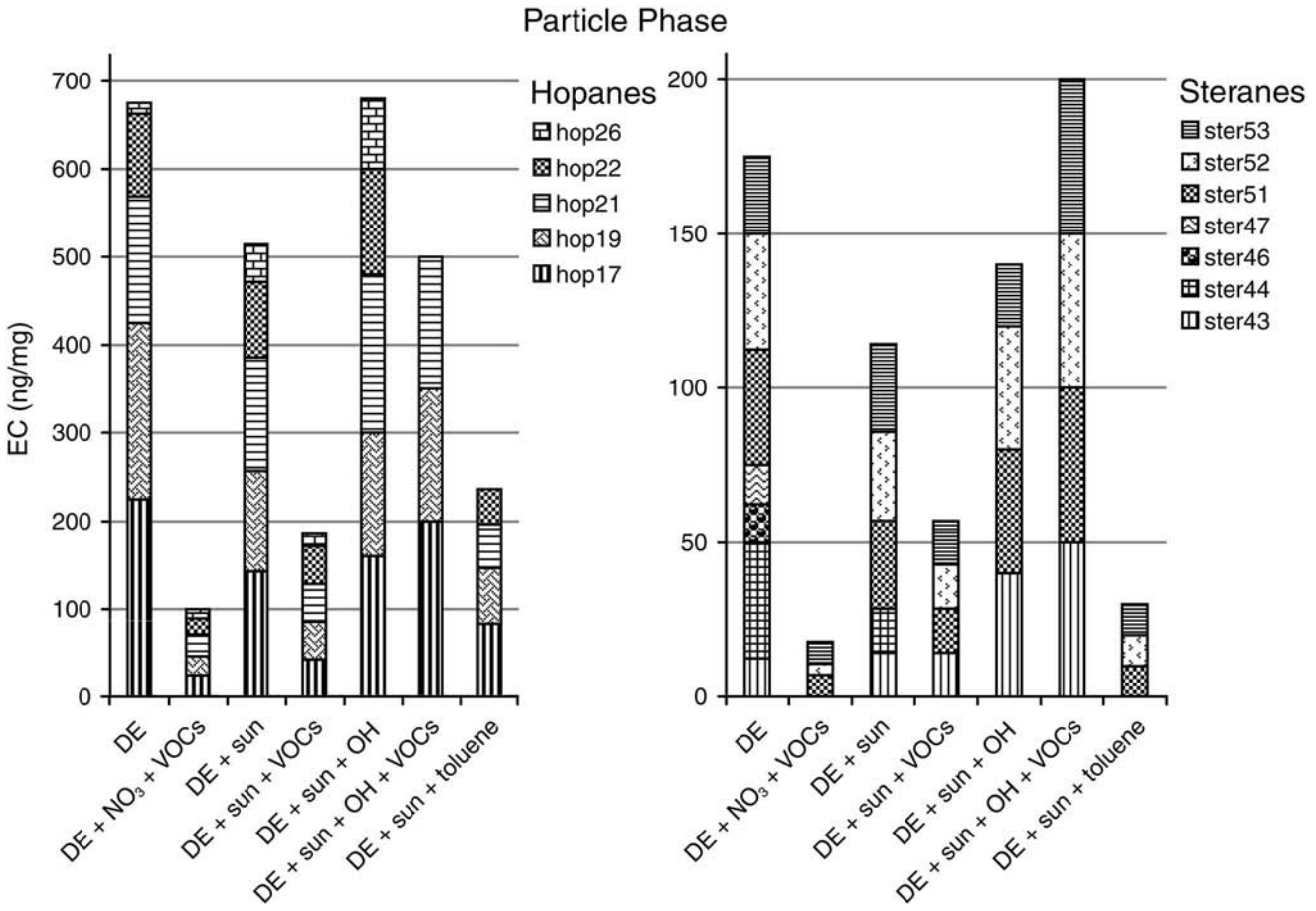

Figure 12. Comparison of particle-phase hopanes and steranes in samples collected from chamber exposures with the NO_x denuder in summer 2006. Concentrations are shown in nanograms of compound per milligram of EC. Note that the *y*-axis scales differ from panel to panel. See Table 9 for compounds' full names.

oxidized lipids, particularly those associated with lipoproteins (especially low-density lipoproteins [LDLs]), were removed from circulation by scavenger receptors. The fact that these results were notably biphasic (i.e., increased responses at lower doses and decreased responses at higher doses for several samples) is consistent with some form of a dose-dependent clearance, or protective, response. Macrophage phagocytosis decreased for all samples to a degree similar to that of the DE and diesel soot controls, except for DE aged in the dark with added NO_3 radicals and VOCs, which did not decrease phagocytosis and had significantly lower potency scores than the controls.

The relatively large number of samples tested in 2006 provided an opportunity to investigate the hypothesis that inflammatory responses and oxidative stress are correlated. Figure 15 shows a high correlation between the various samples' potency scores for PMN response, considered a highly sensitive indicator of inflammation, and for heme oxygenase-1 response, considered the most sensitive indicator of oxidative stress. Causality, however, cannot be inferred from data about a single time point unless there was an intervention that affected one of the variables (by, for example, preventing the inflammatory response or the oxidative stress) to see if it affected the other variable. Until then, inflammation caused by oxidative stress, oxidative stress caused by inflammation, or indeed an unknown third variable causing both of the other two responses all remain as hypotheses consistent with the correlation data shown in the figure. Similar, though slightly less striking, correlations were observed between PMNs and other indicators of oxidative stress (i.e., oxidized glutathione, TBARS in lung tissue, and total glutathione; data not shown).

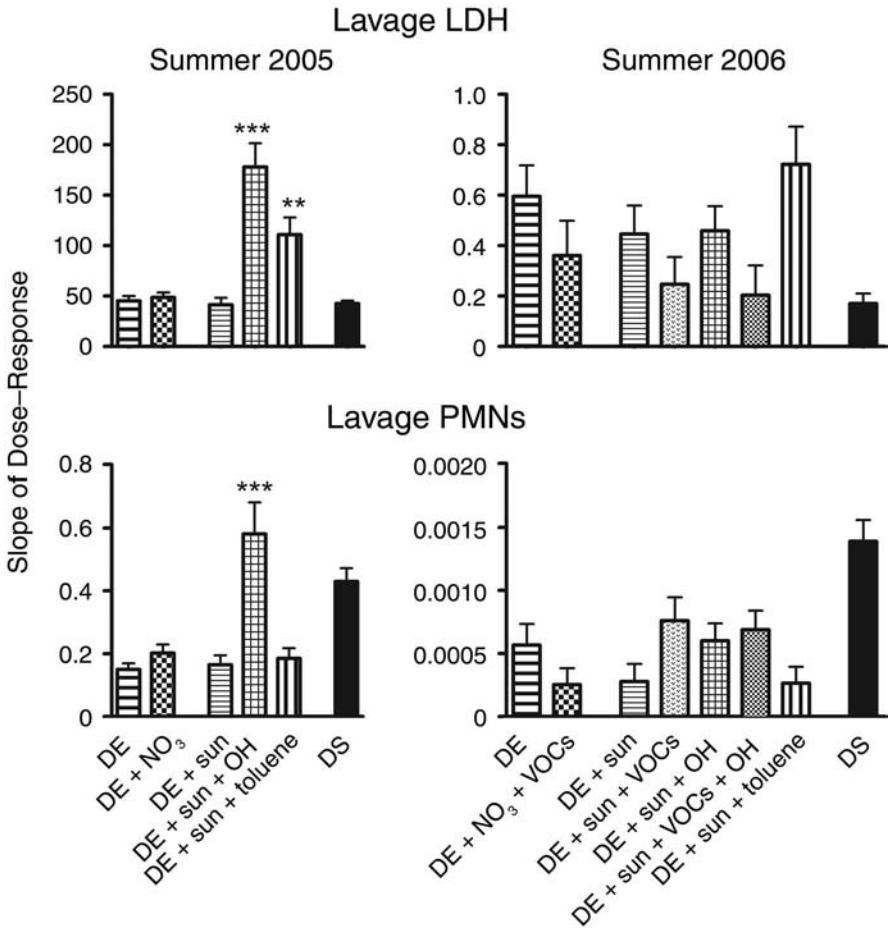

Figure 13. Comparison of estimated potency scores for cytotoxic and inflammatory responses to samples collected from chamber exposures with the NO_x denuder in summer 2005 and 2006. Shown are LDH expression in lavage fluid, an indicator of cytotoxicity, and PMN response in lavage fluid, an indicator of inflammation. Samples from 2005 for PMN response were tested in rats; 2006 samples were tested in mice. Asterisks (** and ***) indicate scores that were significantly different (at $P < 0.01$ or 0.005, respectively) from that of the DE control sample (DE). Diesel soot (DS) was the positive control. Note that the *y*-axis scales differ from panel to panel.

Figure 15. Correlation between estimated potency scores for heme oxygenase-1 (HO-1) response and for PMN response in lavage fluid for samples collected from chamber exposures in summer 2006. Error bars indicate the standard error of the mean for the potency scores. The dotted gray line indicates the linear regression of the relationship.

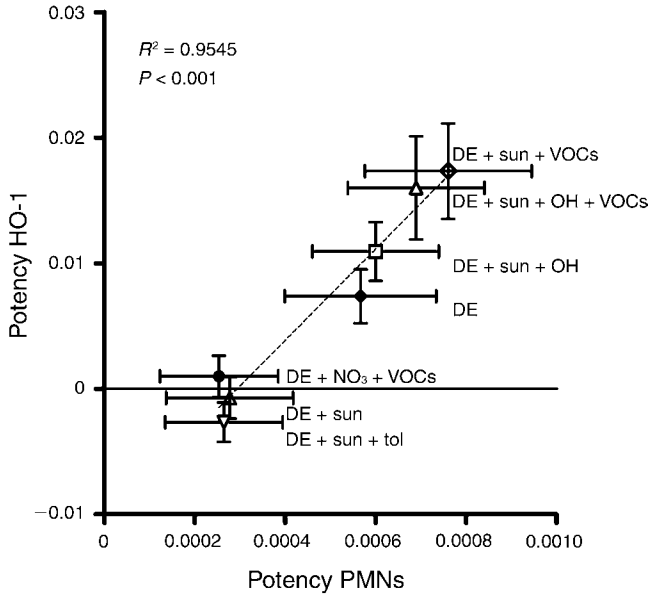

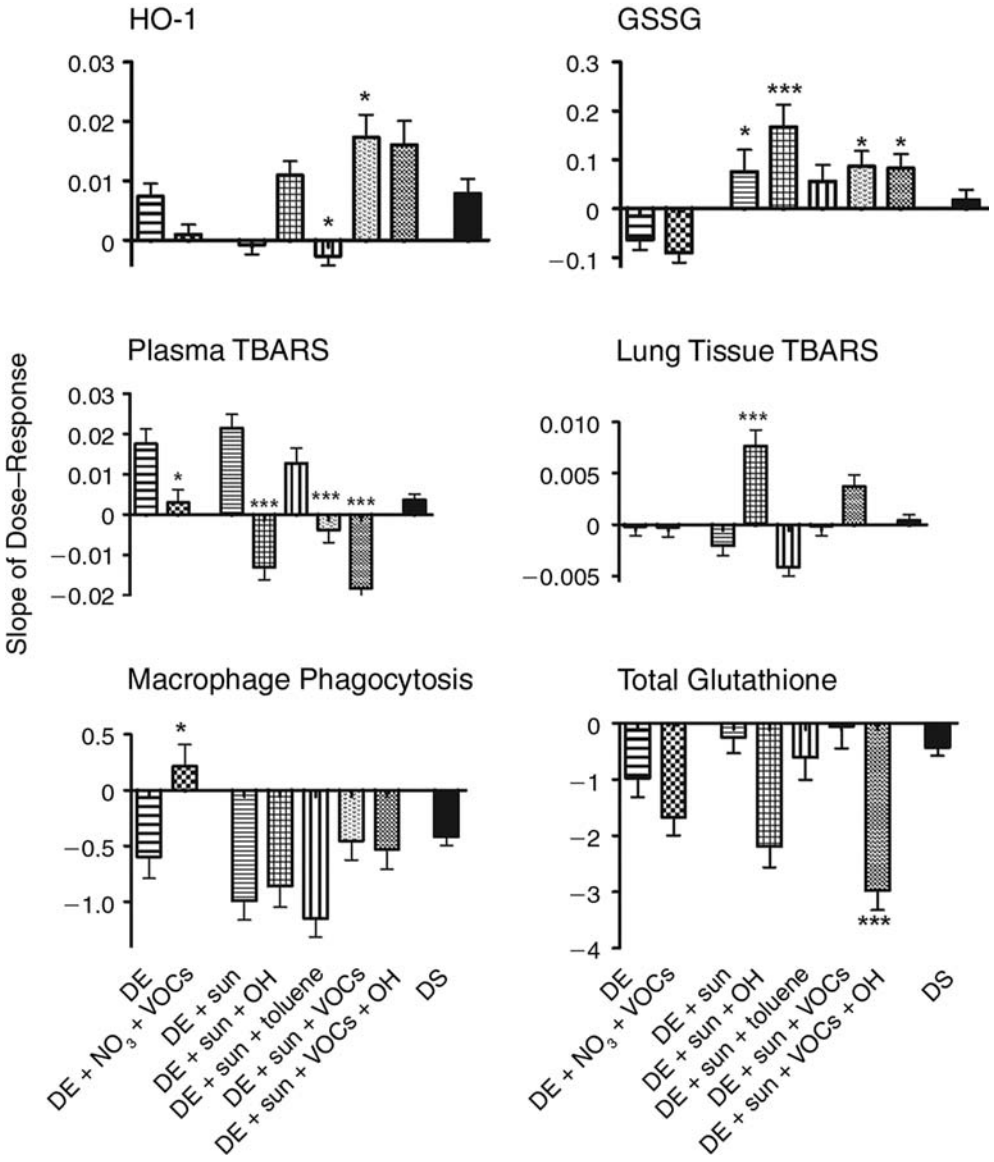

Figure 14. Comparison of estimated potency scores for oxidative-stress and functional (i.e., macrophage phagocytosis) responses to samples collected from chamber exposures in summer 2006. All samples were tested in mice. HO-1 indicates heme oxygenase-1. GSSG indicates oxidized glutathione. Asterisks (* and ***) indicate scores that were significantly different (at $P < 0.05$ or 0.005, respectively) from that of the DE control sample (DE). Diesel soot (DS) was the positive control. Note that the y-axis scales differ from panel to panel.

SUPPLEMENTAL STATISTICAL ANALYSES

The estimated potency scores for the samples from summer 2005 and 2006 were further analyzed. Tables 10 and 11 show the results of evaluating pairwise differences between selected potency scores in rats and mice, respectively, using unequal-variance *t* tests, based on degrees of freedom calculated with the Welch–Satterthwaite correction.

Despite the relatively small number of samples from summer 2005 tested in rats, it is obvious from Table 10 that DE aged in the dark with added NO_3 radicals had effects in all three classes of responses (cytotoxicity, inflammatory responses, and parenchymal changes), if not on every indicator in every class. It caused significant increases in histopathologic indicators of cytotoxicity, protein in lavage fluid, and total cells in lavage fluid as well as significant decreases in histopathologic indicators of parenchymal changes and in alkaline phosphatase in lavage fluid. Macrophages and PMNs in lavage fluid increased, too, although the effects did not reach statistical significance. DE aged in daylight caused similar effects, including increases in histopathologic indicators of cytotoxicity, protein, and lymphocytes in lavage fluid as well as, again, significant decreases in histopathologic indicators of parenchymal changes and in alkaline phosphatase. More dramatic effects were observed for DE aged in daylight with added OH radicals or toluene, both of which significantly increased LDH expression, protein, inflammatory histopathology, macrophages, and total cells. Both also affected histopathologic indicators of cytotoxicity (in opposite directions) and increased alkaline phosphatase (although the effects of the sample with toluene on cytotoxicity indicators and of the sample with OH radicals on alkaline phosphatase did not reach statistical significance). Interestingly, however, only the sample with added OH radicals increased PMNs.

Pairwise comparisons of the effects in mice were more complex, because of the larger numbers of samples and responses. Table 11 shows that there were few statistically significant effects on indicators of cytotoxicity: DE aged in daylight with added OH radicals and VOCs caused minor increases in histopathologic indicators of cytotoxicity. DE aged in the dark with added NO_3 radicals and VOCs as well as DE aged in daylight both caused significant decreases in protein. DE aged in daylight with added toluene significantly increased histopathologic indicators of cytotoxicity and marginally increased protein but did not affect LDH expression.

Inflammatory responses were similarly diverse. DE aged in daylight significantly decreased macrophages and total cells but did not significantly affect histopathologic indicators of inflammation or PMNs. In contrast, DE aged in daylight with added OH radicals and VOCs increased inflammatory histopathology and PMNs but decreased macrophages. It is possible that this was caused by increased expression of adhesion molecules, resulting in increased retention of macrophages in tissue or vasculature. The effect appears to have been driven in the first place by the addition of the OH radicals, because it was also observed in the comparisons of (1) DE aged in daylight with added VOCs and (2) DE aged in daylight with added OH radicals and VOCs but not in the comparisons of (3) DE aged in daylight with added OH radicals and (4) DE aged in daylight with added OH radicals and VOCs. VOCs, however, were not without effects of their own; it was observed that DE aged in daylight with added VOCs significantly increased macrophages, PMNs, and therefore total cells, without affecting inflammatory histopathology. These effects were not mimicked by toluene: DE aged in daylight with added toluene significantly increased inflammatory histopathology without affecting any of the lavage-cell responses.

The changes we classed as parenchymal included a variety of responses that might not be mechanistically related. Compared with DE aged in daylight with added OH radicals, DE aged in daylight with added OH radicals and VOCs significantly decreased parenchymal histopathology. Compared with DE aged in the dark, DE aged in daylight significantly decreased alkaline phosphatase; DE aged in daylight with added toluene restored alkaline phosphatase to a level similar to that observed for DE aged in the dark. All but one of the samples strongly decreased macrophage phagocytosis; DE aged in the dark with added NO_3 radicals and VOCs or aged in daylight with added VOCs both decreased macrophage phagocytosis significantly.

Among the oxidative-stress responses, most of the samples increased heme oxygenase-1 expression, decreased glutathione, and increased oxidized glutathione. DE aged in daylight significantly decreased heme oxygenase-1 (a result consistent with the nonsignificant decrease in glutathione) but significantly increased oxidized glutathione. There were mixed responses for TBARS in lung tissue. DE aged in daylight with added OH radicals, VOCs, or both increased heme oxygenase-1 (again, a result consistent with the decrease in glutathione). DE aged in daylight with added OH radicals or with added OH radicals and VOCs (but not with VOCs alone) significantly increased TBARS in lung tissue.

Effects on TBARS in plasma did not correlate well with the other oxidative-stress responses. DE aged in the dark or in daylight both increased TBARS in plasma, but DE aged in daylight with added NO_3 radicals and VOCs significantly decreased them. DE aged in daylight with added OH

Table 10. Pairwise Comparisons of Potency Scores for Selected Toxicity Tests in Rats

Response	Sample 1	Sample 2	Sample 1 Potency ± SE	Sample 2 Potency ± SE	*P* Value[a]
Cytotoxicity					
Cytotoxic histopathology	DE	DE + NO_3	0.000 ± 0.000	0.286 ± 0.105	0.010↑
	DE	DE + sun	0.000 ± 0.000	0.267 ± 0.109	0.022↑
	DE + sun	DE + sun + OH	0.267 ± 0.109	0.000 ± 0.000	0.022↓
	DE + sun	DE + sun + toluene	0.267 ± 0.109	0.686 ± 0.182	0.054(↑)
LDH	DE	DE + NO_3	45.257 ± 4.867	48.800 ± 4.753	0.604
	DE	DE + sun	45.257 ± 4.867	41.333 ± 7.047	0.649
	DE + sun	DE + sun + OH	41.333 ± 7.047	178.05 ± 23.551	< 0.001↑
	DE + sun	DE + sun + toluene	41.333 ± 7.047	110.86 ± 17.092	< 0.001↑
Protein	DE	DE + NO_3	25.086 ± 3.696	48.457 ± 5.935	0.001↑
	DE	DE + sun	25.086 ± 3.696	42.400 ± 5.756	0.015↑
	DE + sun	DE + sun + OH	42.400 ± 5.756	164.20 ± 24.988	< 0.001↑
	DE + sun	DE + sun + toluene	42.400 ± 5.756	136.11 ± 21.165	< 0.001↑
Inflammation					
Inflammatory histopathology	DE	DE + NO_3	6.029 ± 0.651	6.600 ± 0.506	0.491
	DE	DE + sun	6.029 ± 0.651	4.467 ± 0.889	0.163
	DE + sun	DE + sun + OH	4.467 ± 0.889	9.688 ± 1.207	< 0.001↑
	DE + sun	DE + sun + toluene	4.467 ± 0.889	9.171 ± 0.718	< 0.001↑
Lymphocytes	DE	DE + NO_3	0.002 ± 0.001	0.003 ± 0.001	0.396
	DE	DE + sun	0.002 ± 0.001	0.009 ± 0.002	< 0.001↑
	DE + sun	DE + sun + OH	0.009 ± 0.002	0.016 ± 0.005	0.171
	DE + sun	DE + sun + toluene	0.009 ± 0.002	0.007 ± 0.002	0.390
Macrophages	DE	DE + NO_3	0.026 ± 0.051	0.201 ± 0.067	0.042
	DE	DE + sun	0.026 ± 0.051	0.060 ± 0.064	0.682
	DE + sun	DE + sun + OH	0.060 ± 0.064	0.548 ± 0.104	< 0.001↑
	DE + sun	DE + sun + toluene	0.060 ± 0.064	0.420 ± 0.081	< 0.001↑
PMNs	DE	DE + NO_3	0.149 ± 0.020	0.203 ± 0.027	0.119
	DE	DE + sun	0.149 ± 0.020	0.165 ± 0.030	0.668
	DE + sun	DE + sun + OH	0.165 ± 0.030	0.582 ± 0.100	< 0.001↑
	DE + sun	DE + sun + toluene	0.165 ± 0.030	0.185 ± 0.033	0.656
Total cells	DE	DE + NO_3	0.236 ± 0.060	0.464 ± 0.073	0.019↑
	DE	DE + sun	0.236 ± 0.060	0.279 ± 0.081	0.675
	DE + sun	DE + sun + OH	0.279 ± 0.081	1.257 ± 0.170	< 0.001↑
	DE + sun	DE + sun + toluene	0.279 ± 0.081	0.804 ± 0.114	< 0.001↑
Parenchymal Changes					
Parenchymal histopathology	DE	DE + NO_3	0.248 ± 0.088	0.000 ± 0.000	0.008↓
	DE	DE + sun	0.248 ± 0.088	0.000 ± 0.000	0.008↓
	DE + sun	DE + sun + OH	0.000 ± 0.000	0.000 ± 0.000	—
	DE + sun	DE + sun + toluene	0.000 ± 0.000	0.000 ± 0.000	—
Alkaline phosphatase	DE	DE + NO_3	18.571 ± 3.073	−0.057 ± 2.944	< 0.001↓
	DE	DE + sun	18.571 ± 3.073	−5.067 ± 3.598	< 0.001↓
	DE + sun	DE + sun + OH	−5.067 ± 3.598	6.009 ± 4.990	0.077(↑)
	DE + sun	DE + sun + toluene	−5.067 ± 3.598	6.343 ± 3.248	0.022↑

[a] Statistically significant ($P \leq 0.05$) effects are marked with an arrow to indicate the direction of the effect (i.e., increase or decrease). Effects with *P* values between 0.1 and 0.05 are marked with arrows in parentheses.

Table 11. Pairwise Comparisons of Potency Scores for Selected Toxicity Tests in Mice

Response	Sample 1	Sample 2	Sample 1 Potency ± SE	Sample 2 Potency ± SE	*P* Value[a]
Cytotoxicity					
Cytotoxic histopathology	DE	DE + sun	0.0034 ± 0.0017	0.0023 ± 0.0028	0.725
	DE	DE + NO_3 + VOCs	0.0034 ± 0.0017	0.0069 ± 0.0027	0.278
	DE + sun	DE + sun + OH + VOCs	0.0023 ± 0.0028	0.0040 ± 0.0018	0.609
	DE + sun + OH	DE + sun + OH + VOCs	0.0051 ± 0.0025	0.0040 ± 0.0018	0.713
	DE + sun + VOCs	DE + sun + OH + VOCs	0.0000 ± 0.0000	0.0040 ± 0.0018	0.037↑
	DE + sun	DE + sun + OH	0.0023 ± 0.0028	0.0051 ± 0.0025	0.446
	DE + sun	DE + sun + VOCs	0.0023 ± 0.0028	0.0000 ± 0.0000	0.416
	DE + sun	DE + sun + toluene	0.0023 ± 0.0028	0.0137 ± 0.0045	0.035↑
LDH	DE	DE + sun	0.5954 ± 0.1230	0.4463 ± 0.1122	0.373
	DE	DE + NO_3 + VOCs	0.5954 ± 0.1230	0.3600 ± 0.1385	0.208
	DE + sun	DE + sun + OH + VOCs	0.4463 ± 0.1122	0.2035 ± 0.1185	0.141
	DE + sun + OH	DE + sun + OH + VOCs	0.4589 ± 0.0971	0.2035 ± 0.1185	0.100
	DE + sun + VOCs	DE + sun + OH + VOCs	0.2469 ± 0.1087	0.2035 ± 0.1185	0.788
	DE + sun	DE + sun + OH	0.4463 ± 0.1122	0.4589 ± 0.0971	0.933
	DE + sun	DE + sun + VOCs	0.4463 ± 0.1122	0.2469 ± 0.1087	0.206
	DE + sun	DE + sun + toluene	0.4463 ± 0.1122	0.7223 ± 0.1502	0.146
Protein	DE	DE + sun	0.5469 ± 0.0620	0.3126 ± 0.0814	0.025↓
	DE	DE + NO_3 + VOCs	0.5469 ± 0.0620	0.2769 ± 0.0816	0.011↓
	DE + sun	DE + sun + OH + VOCs	0.3126 ± 0.0814	0.1832 ± 0.0496	0.180
	DE + sun + OH	DE + sun + OH + VOCs	0.2080 ± 0.0420	0.1832 ± 0.0496	0.704
	DE + sun + VOCs	DE + sun + OH + VOCs	0.2389 ± 0.0694	0.1832 ± 0.0496	0.517
	DE + sun	DE + sun + OH	0.3126 ± 0.0814	0.2080 ± 0.0420	0.259
	DE + sun	DE + sun + VOCs	0.3126 ± 0.0814	0.2389 ± 0.0694	0.493
	DE + sun	DE + sun + toluene	0.3126 ± 0.0814	0.5434 ± 0.0923	0.065(↑)
Inflammation					
Inflammatory histopathology	DE	DE + sun	0.0394 ± 0.0094	0.0234 ± 0.0109	0.271
	DE	DE + NO_3 + VOCs	0.0394 ± 0.0094	0.1080 ± 0.0120	< 0.001↑
	DE + sun	DE + sun + OH + VOCs	0.0234 ± 0.0109	0.0869 ± 0.0153	0.001↑
	DE + sun + OH	DE + sun + OH + VOCs	0.0754 ± 0.0128	0.0869 ± 0.0153	0.569
	DE + sun + VOCs	DE + sun + OH + VOCs	0.0394 ± 0.0131	0.0869 ± 0.0153	0.022↑
	DE + sun	DE + sun + OH	0.0234 ± 0.0109	0.0754 ± 0.0128	0.003↑
	DE + sun	DE + sun + VOCs	0.0234 ± 0.0109	0.0394 ± 0.0131	0.353
	DE + sun	DE + sun + toluene	0.0234 ± 0.0109	0.0920 ± 0.0123	< 0.001↑
Macrophages	DE	DE + sun	0.0021 ± 0.0004	0.0010 ± 0.0003	0.028↓
	DE	DE + NO_3 + VOCs	0.0021 ± 0.0004	0.0019 ± 0.0003	0.643
	DE + sun	DE + sun + OH + VOCs	0.0010 ± 0.0003	0.0000 ± 0.0003	0.048↓
	DE + sun + OH	DE + sun + OH + VOCs	−0.0004 ± 0.0003	0.0000 ± 0.0003	0.342
	DE + sun + VOCs	DE + sun + OH + VOCs	0.0026 ± 0.0003	0.0000 ± 0.0003	< 0.001↓
	DE + sun	DE + sun + OH	0.0010 ± 0.0003	−0.0004 ± 0.0003	0.004↓
	DE + sun	DE + sun + VOCs	0.0010 ± 0.0003	0.0026 ± 0.0003	< 0.001↑
	DE + sun	DE + sun + toluene	0.0010 ± 0.0003	0.0012 ± 0.0003	0.580

(*Table continues next page*)

[a] Statistically significant ($P \leq 0.05$) effects are marked with an arrow to indicate the direction of the effect (i.e., increase or decrease). Effects with *P* values between 0.1 and 0.05 are marked with arrows in parentheses.

[b] Decreases in macrophage phagocytosis and in glutathione are considered increases in toxicity.

Table 11 (*Continued*). Pairwise Comparisons of Potency Scores for Selected Toxicity Tests in Mice

Response	Sample 1	Sample 2	Sample 1 Potency ± SE	Sample 2 Potency ± SE	*P* Value[a]
Inflammation (*continued*)					
PMNs	DE	DE + sun	0.0006 ± 0.0002	0.0003 ± 0.0001	0.190
	DE	DE + NO_3 + VOCs	0.0006 ± 0.0002	0.0003 ± 0.0001	0.146
	DE + sun	DE + sun + OH + VOCs	0.0003 ± 0.0001	0.0007 ± 0.0002	0.050↑
	DE + sun + OH	DE + sun + OH + VOCs	0.0006 ± 0.0001	0.0007 ± 0.0002	0.665
	DE + sun + VOCs	DE + sun + OH + VOCs	0.0008 ± 0.0002	0.0007 ± 0.0002	0.766
	DE + sun	DE + sun + OH	0.0003 ± 0.0001	0.0006 ± 0.0001	0.108
	DE + sun	DE + sun + VOCs	0.0003 ± 0.0001	0.0008 ± 0.0002	0.041↑
	DE + sun	DE + sun + toluene	0.0003 ± 0.0001	0.0003 ± 0.0001	0.948
Total cells	DE	DE + sun	0.0027 ± 0.0003	0.0012 ± 0.0003	0.002↓
	DE	DE + NO_3 + VOCs	0.0027 ± 0.0003	0.0021 ± 0.0003	0.240
	DE + sun	DE + sun + OH + VOCs	0.0012 ± 0.0003	0.0008 ± 0.0003	0.280
	DE + sun + OH	DE + sun + OH + VOCs	0.0003 ± 0.0003	0.0008 ± 0.0003	0.215
	DE + sun + VOCs	DE + sun + OH + VOCs	0.0033 ± 0.0003	0.0008 ± 0.0003	< 0.001↓
	DE + sun	DE + sun + OH	0.0012 ± 0.0003	0.0003 ± 0.0003	0.023↓
	DE + sun	DE + sun + VOCs	0.0012 ± 0.0003	0.0033 ± 0.0003	< 0.001↑
	DE + sun	DE + sun + toluene	0.0012 ± 0.0003	0.0015 ± 0.0003	0.563
Parenchymal/Functional Changes					
Parenchymal histopathology	DE	DE + sun	0.0000 ± 0.0000	0.0023 ± 0.0028	0.416
	DE	DE + NO_3 + VOCs	0.0000 ± 0.0000	0.0069 ± 0.0027	0.014↑
	DE + sun	DE + sun + OH + VOCs	0.0023 ± 0.0028	0.0000 ± 0.0000	0.416
	DE + sun + OH	DE + sun + OH + VOCs	0.0051 ± 0.0025	0.0000 ± 0.0000	0.046↓
	DE + sun + VOCs	DE + sun + OH + VOCs	0.0000 ± 0.0000	0.0000 ± 0.0000	—
	DE + sun	DE + sun + OH	0.0023 ± 0.0028	0.0051 ± 0.0025	0.446
	DE + sun	DE + sun + VOCs	0.0023 ± 0.0028	0.0000 ± 0.0000	0.416
	DE + sun	DE + sun + toluene	0.0023 ± 0.0028	0.0000 ± 0.0000	0.416
Alkaline phosphatase	DE	DE + sun	0.0043 ± 0.0005	0.0017 ± 0.0004	< 0.001↓
	DE	DE + NO_3 + VOCs	0.0043 ± 0.0005	0.0017 ± 0.0005	< 0.001↓
	DE + sun	DE + sun + OH + VOCs	0.0017 ± 0.0004	0.0013 ± 0.0003	0.502
	DE + sun + OH	DE + sun + OH + VOCs	0.0016 ± 0.0003	0.0013 ± 0.0003	0.510
	DE + sun + VOCs	DE + sun + OH + VOCs	0.0024 ± 0.0007	0.0013 ± 0.0003	0.150
	DE + sun	DE + sun + OH	0.0017 ± 0.0004	0.0016 ± 0.0003	0.901
	DE + sun	DE + sun + VOCs	0.0017 ± 0.0004	0.0024 ± 0.0007	0.372
	DE + sun	DE + sun + toluene	0.0017 ± 0.0004	0.0045 ± 0.0006	< 0.001↑
Macrophage phagocytosis[b]	DE	DE + sun	−0.5950 ± 0.1946	−0.9888 ± 0.1744	0.136
	DE	DE + NO_3 + VOCs	−0.5950 ± 0.1946	0.2162 ± 0.1951	0.004↓
	DE + sun	DE + sun + OH + VOCs	−0.9888 ± 0.1744	−0.5250 ± 0.1858	0.073(↓)
	DE + sun + OH	DE + sun + OH + VOCs	−0.8594 ± 0.1884	−0.5250 ± 0.1858	0.211
	DE + sun + VOCs	DE + sun + OH + VOCs	−0.4529 ± 0.1692	−0.5250 ± 0.1858	0.775
	DE + sun	DE + sun + OH	−0.9888 ± 0.1744	−0.8594 ± 0.1884	0.616
	DE + sun	DE + sun + VOCs	−0.9888 ± 0.1744	−0.4529 ± 0.1692	0.031↓
	DE + sun	DE + sun + toluene	−0.9888 ± 0.1744	−1.1468 ± 0.1712	0.520

(*Table continues next page*)

[a] Statistically significant ($P \leq 0.05$) effects are marked with an arrow to indicate the direction of the effect (i.e., increase or decrease). Effects with *P* values between 0.1 and 0.05 are marked with arrows in parentheses.

[b] Decreases in macrophage phagocytosis and in glutathione are considered increases in toxicity.

Table 11 (*Continued*). Pairwise Comparisons of Potency Scores for Selected Toxicity Tests in Mice

Response	Sample 1	Sample 2	Sample 1 Potency ± SE	Sample 2 Potency ± SE	*P* Value[a]
Oxidative Stress					
Heme oxygenase-1	DE	DE + sun	0.0074 ± 0.0021	−0.0007 ± 0.0016	0.004↓
	DE	DE + NO_3 + VOCs	0.0074 ± 0.0021	0.0010 ± 0.0017	0.022↓
	DE + sun	DE + sun + OH + VOCs	−0.0007 ± 0.0016	0.0160 ± 0.0041	< 0.001↑
	DE + sun + OH	DE + sun + OH + VOCs	0.0109 ± 0.0024	0.0160 ± 0.0041	0.289
	DE + sun + VOCs	DE + sun + OH + VOCs	0.0173 ± 0.0038	0.0160 ± 0.0041	0.813
	DE + sun	DE + sun + OH	−0.0007 ± 0.0016	0.0109 ± 0.0024	< 0.001↑
	DE + sun	DE + sun + VOCs	−0.0007 ± 0.0016	0.0173 ± 0.0038	< 0.001↑
	DE + sun	DE + sun + toluene	−0.0007 ± 0.0016	−0.0027 ± 0.0016	0.399
Glutathione[b]	DE	DE + sun	−0.9796 ± 0.3346	−0.2510 ± 0.2840	0.102
	DE	DE + NO_3 + VOCs	−0.9796 ± 0.3346	−1.6678 ± 0.3264	0.146
	DE + sun	DE + sun + OH + VOCs	−0.2510 ± 0.2840	−2.9799 ± 0.3436	< 0.001↑
	DE + sun + OH	DE + sun + OH + VOCs	−2.1874 ± 0.3779	−2.9799 ± 0.3436	0.125
	DE + sun + VOCs	DE + sun + OH + VOCs	−0.0534 ± 0.3953	−2.9799 ± 0.3436	< 0.001↑
	DE + sun	DE + sun + OH	−0.2510 ± 0.2840	−2.1874 ± 0.3779	< 0.001↑
	DE + sun	DE + sun + VOCs	−0.2510 ± 0.2840	−0.0534 ± 0.3953	0.686
	DE + sun	DE + sun + toluene	−0.2510 ± 0.2840	−0.6086 ± 0.3965	0.466
Oxidized glutathione	DE	DE + sun	−0.0637 ± 0.0204	0.0752 ± 0.0455	0.008↑
	DE	DE + NO_3 + VOCs	−0.0637 ± 0.0204	−0.0901 ± 0.0203	0.363
	DE + sun	DE + sun + OH + VOCs	0.0752 ± 0.0455	0.0828 ± 0.0292	0.889
	DE + sun + OH	DE + sun + OH + VOCs	0.1668 ± 0.0460	0.0828 ± 0.0292	0.128
	DE + sun + VOCs	DE + sun + OH + VOCs	0.0863 ± 0.0316	0.0828 ± 0.0292	0.935
	DE + sun	DE + sun + OH	0.0752 ± 0.0455	0.1668 ± 0.0460	0.162
	DE + sun	DE + sun + VOCs	0.0752 ± 0.0455	0.0863 ± 0.0316	0.842
	DE + sun	DE + sun + toluene	0.0752 ± 0.0455	0.0561 ± 0.0338	0.737
Lung tissue TBARS	DE	DE + sun	−0.0002 ± 0.0009	−0.0021 ± 0.0010	0.155
	DE	DE + NO_3 + VOCs	−0.0002 ± 0.0009	−0.0002 ± 0.0010	0.966
	DE + sun	DE + sun + OH + VOCs	−0.0021 ± 0.0010	0.0037 ± 0.0011	< 0.001↑
	DE + sun + OH	DE + sun + OH + VOCs	0.0077 ± 0.0016	0.0037 ± 0.0011	0.045↓
	DE + sun + VOCs	DE + sun + OH + VOCs	−0.0002 ± 0.0009	0.0037 ± 0.0011	0.010↑
	DE + sun	DE + sun + OH	−0.0021 ± 0.0010	0.0077 ± 0.0016	< 0.001↑
	DE + sun	DE + sun + VOCs	−0.0021 ± 0.0010	−0.0002 ± 0.0009	0.159
	DE + sun	DE + sun + toluene	−0.0021 ± 0.0010	−0.0041 ± 0.0009	0.115
Plasma TBARS	DE	DE + sun	0.0176 ± 0.0037	0.0214 ± 0.0035	0.447
	DE	DE + NO_3 + VOCs	0.0176 ± 0.0037	0.0030 ± 0.0032	0.004↓
	DE + sun	DE + sun + OH + VOCs	0.0214 ± 0.0035	−0.0183 ± 0.0032	< 0.001↓
	DE + sun + OH	DE + sun + OH + VOCs	−0.0130 ± 0.0032	−0.0183 ± 0.0032	0.248
	DE + sun + VOCs	DE + sun + OH + VOCs	−0.0038 ± 0.0031	−0.0183 ± 0.0032	0.002↓
	DE + sun	DE + sun + OH	0.0214 ± 0.0035	−0.0130 ± 0.0032	< 0.001↓
	DE + sun	DE + sun + VOCs	0.0214 ± 0.0035	−0.0038 ± 0.0031	< 0.001↓
	DE + sun	DE + sun + toluene	0.0214 ± 0.0035	0.0128 ± 0.0038	0.095(↓)

[a] Statistically significant ($P \leq 0.05$) effects are marked with an arrow to indicate the direction of the effect (i.e., increase or decrease). Effects with *P* values between 0.1 and 0.05 are marked with arrows in parentheses.

[b] Decreases in macrophage phagocytosis and in glutathione are considered increases in toxicity.

Table 12. Effect on Estimated Potency Scores of Potential Interactions Among Reactants in Samples from Summer 2006 Tested in Mice[a]

Response	DE + Sun	DE + Sun + OH	DE + Sun + VOCs	DE + Sun + OH + VOCs	*P* Values			
					OH	VOCs	OH + VOCs	Interaction
Alkaline phosphatase	0.0017 ± 0.0004	0.0016 ± 0.0003	0.0024 ± 0.0007	0.0013 ± 0.0003	0.901	0.372	0.502	0.269
Cytotoxic histopathology	0.0023 ± 0.0028	0.0051 ± 0.0025	0.0000 ± 0.0000	0.0040 ± 0.0018	0.446	0.416	0.609	0.784
Glutathione	−0.2510 ± 0.2840	−2.1874 ± 0.3779	−0.0534 ± 0.3953	−2.9799 ± 0.3436	< 0.001	0.686	< 0.001	0.163
Oxidized glutathione	0.0752 ± 0.0455	0.1668 ± 0.0460	0.0863 ± 0.0316	0.0828 ± 0.0292	0.162	0.842	0.889	0.223
Heme oxygenase-1	−0.0007 ± 0.0016	0.0109 ± 0.0024	0.0173 ± 0.0038	0.0160 ± 0.0041	< 0.001	< 0.001	< 0.001	0.040
Inflammatory histopathology	0.0234 ± 0.0109	0.0754 ± 0.0128	0.0394 ± 0.0131	0.0869 ± 0.0153	0.003	0.353	0.001	0.862
LDH	0.4463 ± 0.1122	0.4589 ± 0.0971	0.2469 ± 0.1087	0.2035 ± 0.1185	0.933	0.206	0.141	0.799
Lung tissue TBARS	−0.0021 ± 0.0010	0.0077 ± 0.0016	−0.0002 ± 0.0009	0.0037 ± 0.0011	< 0.001	0.159	< 0.001	0.014
Macrophage phagocytosis	−0.9888 ± 0.1744	−0.8594 ± 0.1884	−0.4529 ± 0.1692	−0.5250 ± 0.1858	0.616	0.031	0.073	0.576
Macrophages	0.0010 ± 0.0003	−0.0004 ± 0.0003	0.0026 ± 0.0003	0.0000 ± 0.0003	0.004	< 0.001	0.048	0.054
PMNs	0.0003 ± 0.0001	0.0006 ± 0.0001	0.0008 ± 0.0002	0.0007 ± 0.0002	0.108	0.041	0.050	0.206
Parenchymal histopathology	0.0023 ± 0.0028	0.0051 ± 0.0025	0.0000 ± 0.0000	0.0000 ± 0.0000	0.446	0.416	0.416	0.445
Plasma TBARS	0.0214 ± 0.0035	−0.0130 ± 0.0032	−0.0038 ± 0.0031	−0.0183 ± 0.0032	< 0.001	< 0.001	< 0.001	0.002
Protein	0.3126 ± 0.0814	0.2080 ± 0.0420	0.2389 ± 0.0694	0.1832 ± 0.0496	0.259	0.493	0.180	0.696
Total cells	0.0012 ± 0.0003	0.0003 ± 0.0003	0.0033 ± 0.0003	0.0008 ± 0.0003	0.023	< 0.001	0.280	0.011

[a] Data are presented as potency scores ± SE.

radicals, VOCs, or both also decreased TBARS in plasma, actually giving the dose–response curve a negative slope. Given the increases in most of the other oxidative-stress indicators, these results might indicate the activation of some type of sequestration of the TBARS from the plasma.

The study was not specifically designed (or statistically powered) to investigate potential interactions among the reactants used to modify the chamber atmospheres. However, a set of samples from summer 2006 tested in mice, consisting of DE aged in daylight and DE aged in daylight with added OH radicals, VOCs, or both, provided an opportunity to assess a number of such interactions, using the following differences in potency scores (i.e., again, the slopes of the dose–response curves):

$$\text{Diff1} = \text{slope(DE + sun + OH)} - \text{slope(DE + sun)}, \quad (4)$$

$$\text{Diff2} = \text{slope(DE + sun + VOCs)} - \text{slope(DE + sun)}, \quad (5)$$

and

$$\text{Diff3} = \text{slope(DE + sun + OH + VOCs)} - \text{slope(DE + sun)}. \quad (6)$$

If the effects of the added OH radicals and VOCs were additive, this would imply that Diff1 + Diff2 = Diff3, which is equivalent to slope(DE + sun + OH) + slope(DE + sun + VOCs) − slope(DE + sun) − slope(DE + sun + OH + VOCs) = 0.

This hypothesis was tested under the assumption that the slopes (and their linear combination) were approximately normally distributed, with the variance of the linear combination equal to the sums of squares of the estimated standard errors of the slopes. The ratio of the linear combination to its estimated standard deviation was assumed to have a *t* distribution with degrees of freedom equal to the sum of the degrees of freedom for the four slope estimates.

The results of our analysis, shown in Table 12, suggest the existence of some modest interactions between the two added reactants for some responses, including heme oxygenase-1 (increases for both added OH radicals or VOCs), TBARS in lung tissue (increases for added OH radicals), TBARS in plasma (decreases for both), and total cells (decreases for OH radicals and increases for VOCs). However, these interactions were generally less than additive.

Finally, there were a very limited number of samples taken under similar conditions from summer 2005 tested in rats and from summer 2006 tested in mice. Table 13 shows pairwise comparisons of potency scores for these sets of samples. Although it is clear that the composition of the sets differed as a function of the two campaigns, examples of concordances between the results can be seen, including increases in histopathologic indicators of cytotoxity and protein for DE aged in daylight with added toluene; increases in inflammatory histopathology for DE aged in daylight with added OH radicals or toluene; and increases in PMNs for DE aged in daylight with added OH

Table 13. Pairwise Comparisons of Similar Samples from Summer 2005 Tested in Rats and from Summer 2006 Tested in Mice

			Rats			Mice			
Endpoint	Sample 1	Sample 2	Sample 1 Potency ± SE	Sample 2 Potency ± SE	*P* Value[a]	Sample 1 Potency ± SE	Sample 2 Potency ± SE	*P* Value[a]	Cc[b]
Cytotoxicity									
Cytotoxic histopathology	DE	DE + sun	0.000 ± 0.000	0.267 ± 0.109	0.022↑	0.0034 ± 0.0017	0.0023 ± 0.0028	0.725	
	DE + sun	DE + sun + OH	0.267 ± 0.109	0.000 ± 0.000	0.022↓	0.0023 ± 0.0028	0.0051 ± 0.0025	0.446	
	DE + sun	DE + sun + toluene	0.267 ± 0.109	0.686 ± 0.182	0.054↑	0.0023 ± 0.0028	0.0137 ± 0.0045	0.035↑	+
LDH	DE	DE + sun	45.257 ± 4.867	41.333 ± 7.05	0.649	0.5954 ± 0.1230	0.4463 ± 0.1122	0.373	
	DE + sun	DE + sun + OH	41.333 ± 7.047	178.0 ± 23.55	< 0.001↑	0.4463 ± 0.1122	0.4589 ± 0.0971	0.933	
	DE + sun	DE + sun + toluene	41.333 ± 7.047	110.9 ± 17.09	< 0.001↑	0.4463 ± 0.1122	0.7223 ± 0.1502	0.146	
Protein	DE	DE + sun	25.086 ± 3.696	42.400 ± 5.75	0.015↑	0.5469 ± 0.0620	0.3126 ± 0.0814	0.025↓	−
	DE + sun	DE + sun + OH	42.400 ± 5.756	164.2 ± 24.99	< 0.001↑	0.3126 ± 0.0814	0.2080 ± 0.0420	0.259	
	DE + sun	DE + sun + toluene	42.400 ± 5.756	136.1 ± 21.16	< 0.001↑	0.3126 ± 0.0814	0.5434 ± 0.0923	0.065(↑)	+
Inflammation									
Inflammatory histopathology	DE	DE + sun	6.029 ± 0.651	4.467 ± 0.889	0.163	0.0394 ± 0.0094	0.0234 ± 0.0109	0.271	
	DE + sun	DE + sun + OH	4.467 ± 0.889	9.688 ± 1.207	< 0.001↑	0.0234 ± 0.0109	0.0754 ± 0.0128	0.003↑	+
	DE + sun	DE + sun + toluene	4.467 ± 0.889	9.171 ± 0.718	< 0.001↑	0.0234 ± 0.0109	0.0920 ± 0.0123	< 0.001↑	+
Macrophages	DE	DE + sun	0.026 ± 0.051	0.060 ± 0.064	0.682	0.0021 ± 0.0004	0.0010 ± 0.0003	0.028↓	
	DE + sun	DE + sun + OH	0.060 ± 0.064	0.548 ± 0.104	< 0.001↑	0.0010 ± 0.0003	−0.0004 ± 0.0003	0.004↓	−
	DE + sun	DE + sun + toluene	0.060 ± 0.064	0.420 ± 0.081	< 0.001↑	0.0010 ± 0.0003	0.0012 ± 0.0003	0.580	
PMNs	DE	DE + sun	0.149 ± 0.020	0.165 ± 0.030	0.668	0.0006 ± 0.0002	0.0003 ± 0.0001	0.190	
	DE + sun	DE + sun + OH	0.165 ± 0.030	0.582 ± 0.100	< 0.001↑	0.0003 ± 0.0001	0.0006 ± 0.0001	0.108(↑)	(+)
	DE + sun	DE + sun + toluene	0.165 ± 0.030	0.185 ± 0.033	0.656	0.0003 ± 0.0001	0.0003 ± 0.0001	0.948	
Total cells	DE	DE + sun	0.236 ± 0.060	0.279 ± 0.081	0.675	0.0027 ± 0.0003	0.0012 ± 0.0003	0.002↓	
	DE + sun	DE + sun + OH	0.279 ± 0.081	1.257 ± 0.170	< 0.001↑	0.0012 ± 0.0003	0.0003 ± 0.0003	0.023↓	−
	DE + sun	DE + sun + toluene	0.279 ± 0.081	0.804 ± 0.114	< 0.001↑	0.0012 ± 0.0003	0.0015 ± 0.0003	0.563	
Parenchymal Changes									
Parenchymal histopathology	DE	DE + sun	0.248 ± 0.088	0.000 ± 0.000	0.008↓	0.0000 ± 0.0000	0.0023 ± 0.0028	0.416	
	DE + sun	DE + sun + OH	0.000 ± 0.000	0.000 ± 0.000	—	0.0023 ± 0.0028	0.0051 ± 0.0025	0.446	
	DE + sun	DE + sun + toluene	0.000 ± 0.000	0.000 ± 0.000	—	0.0023 ± 0.0028	0.0000 ± 0.0000	0.416	
Alkaline phosphatase	DE	DE + sun	18.571 ± 3.073	−5.067 ± 3.598	< 0.001↓	0.0043 ± 0.0005	0.0017 ± 0.0004	< 0.001↓	+
	DE + sun	DE + sun + OH	−5.067 ± 3.598	6.009 ± 4.990	0.077(↑)	0.0017 ± 0.0004	0.0016 ± 0.0003	0.901	
	DE + sun	DE + sun + toluene	−5.067 ± 3.598	6.343 ± 3.248	0.022↑	0.0017 ± 0.0004	0.0045 ± 0.0006	< 0.001↑	+

[a] Statistically significant ($P \leq 0.05$) effects are marked with an arrow to indicate the direction of the effect (i.e., increase or decrease). Effects with *P* values between 0.1 and 0.05 are marked with arrows in parentheses.

[b] Cc indicates concordance between results for rats and mice. The plus sign (+) indicates that both sets of results changed significantly and in the same direction. The minus sign (−) indicates that both changed significantly but in opposite directions. Parentheses indicate concordances for which one set of results was not statistically significant.

radicals; as well as striking decreases in alkaline phosphatase for DE aged in daylight (compared with DE aged in the dark) and striking increases for DE aged in daylight with added toluene. There were also three instances in which the results in rats and mice were significant but opposite. The first of these was the effect of DE aged in daylight on protein in lavage fluid, which increased in rats and decreased in mice. The other two instances, the effects of DE aged in daylight with added OH radicals on macrophages and on total cells in lavage fluid, were in fact closely related, because macrophages for the most part dominated total cell counts. This might indicate a difference between effects on cell adhesion in the two species, inasmuch as both also showed statistically significant increases in inflammatory histopathology.

In summary, the concordant results in the two species give strong support to the observation that the addition of toluene or (to a slightly lesser extent) OH radicals increases the potency of DE aged in daylight. The nonconcordant results for macrophages and total cells, with concordant results for inflammatory histopathology (and concordant but not quite statistically significant results for PMNs), are consistent with possible species-specific differences in macrophage function under conditions of stress.

DISCUSSION AND CONCLUSIONS

The hypothesis of this study was that exposure of DE to the atmosphere transforms its composition and toxicity. Three experimental campaigns were conducted to test this hypothesis. As discussed earlier, in the first (winter 2005) campaign we did not have a NO_x denuder in place and our diesel engine was new, having run for only a few hours, which resulted in DE with a significantly different composition and toxicity from those of the two subsequent (summer 2005 and summer 2006) campaigns. For this reason, we limit our discussion here to the two latter campaigns. During the summer 2005 campaign, the engine was used with a prototype denuder that reduced NO_x in the chamber to acceptable concentrations. The campaign showed, however, that only small amounts of exhaust could be injected into the chamber before the denuder became saturated and lost its ability to reduce NO_x concentrations. A new denuder was developed to provide improved capacity and was used successfully in the summer 2006 campaign. The summer 2006 campaign also differed from the previous campaign in that the engine was approximately a year older, which resulted in some differences between the DE in summer 2006 and that of the summer before.

Our results showed that DE aged in the dark with added NO_3 radicals and all varieties of DE aged in daylight formed additional particles and SVOC mass by way of reactions of VOCs, SVOCs, and inorganic gases. The greatest increases in mass occurred in DE with added VOCs or toluene. The organic mass formed increased the POC fraction, whose presence suggests the formation of polar and oligomeric compounds. An increase in inorganic-ion mass was observed only in summer 2005, before the optimization of the denuder, which further decreased NO_x (and SO_2).

It is important to note that the organic species we measured accounted for only a small portion of the total organic mass in our chamber atmospheres. There are myriad unknown organic species in DE, both in its gas and particle phases and in its associated transformation products. Our measurements illustrated key attributes of some of the transformations in composition pertaining to various combustion byproducts as well as to emissions from diesel fuel and lubricating oil. Analysis of nitro-PAHs and polar organic compounds gave insight into the formation of some of the reaction products. Among the speciated organic compounds, PAHs and alkanes decreased (as a fraction of EC) in most cases as a result of photochemical reactions that presumably broke up PAHs and transformed *n*-alkanes, alkanecyclohexanes, and especially iso-alkanes into more polar products. Nitro-PAHs increased among the more volatile nitro-PAHs, such as 1- and 2-nitronaphthalenes and methyl nitronaphthalenes, as a result of NO_3-radical and OH-radical reactions with naphthalene and methylnaphthalenes. The higher-molecular-weight nitro-PAHs were much less abundant and consistent from exposure to exposure. However, proof of reactions that form additional particle-associated nitro-PAHs was given by the presence of 2-nitrofluoranthene and 4-nitropyrene, which are presumably only formed by atmospheric transformations. In addition, most nitro-PAHs are not photochemically stable, and their rate of decomposition might influence their final concentrations (Fan et al. 1995).

Hopanes and steranes, which are considered to be markers for lubricating oil, were present in low concentrations that decreased further in most reaction conditions. The largest decrease was observed in experiments involving DE aged in the dark with added NO_3 radicals and VOCs as well as DE aged in daylight with added VOCs or toluene.

An analysis of a limited number of polar compounds was conducted to assess the formation of photochemical-transformation products. These data, which we view as preliminary, showed significant increases in polar compounds in most but not all reactions that occurred in DE aged in daylight with added OH radicals. High concentrations of polar organic compounds were observed in both summer 2005 and summer 2006 for DE aged in daylight and for DE aged in daylight with added OH radicals and VOCs or with

added toluene. Most notably, the increases in concentrations of aliphatic (i.e., alkanedioic) and aromatic diacids (such as phthalic acid), which are known atmospheric transformation products, were significant. The presence of increased polar organic compounds pointed to the role of OH radicals in the chamber atmospheres. The absence of a significant increase in polar organic compounds in our other experiments on DE aged in daylight with added OH radicals might indicate the formation of highly oxidized or oligomeric products that were not measured by the analytic techniques used in this study (i.e., derivatization reactions and GC–MS). The formation of increased organic material, evidence from real-time data on the gas and particle phases, and the decrease in other organic species suggest that significant reactions were occurring that produced more polar and oxidized reaction products. Additional analysis by complementary techniques, such as liquid chromatography–mass spectrometry (LC–MS), will be needed to further elucidate the composition of the polar fraction. Such an analysis could serve both to confirm our findings and to begin investigating the hundreds of other complex (and often unknown) polar compounds formed in reactions in the atmosphere that were not targeted here. Overall, the poor understanding of the polar fraction of atmospheric transformation products is a significant gap in the knowledge of the atmospheric sciences community. Advanced instrumentation, such as LC–MS, applied to our samples (which are archived) could help to close this gap.

The composition of the DE used in summer 2006 was somewhat different from that of the previous summer, and the amounts of DE we were able to collect in separate experiments in 2006 were less than anticipated. However, we decided against combining the 2006 samples for use in toxicity testing (as had been done in winter and summer 2005) because of the differences between experiments (i.e., DE aged in daylight and DE aged in daylight with added OH radicals, VOCs, or both). Instead, we adapted our toxicity-test protocols to make use of mice instead of rats. This allowed us to administer doses to mice in summer 2006 that were comparable (relative to body mass and, in turn, to estimated lung surface area) to those that had been administered to rats in summer 2005. Overall, however, the various changes in composition, technology, and species from summer 2005 to summer 2006 somewhat limited our ability to compare relationships quantitatively across atmospheric aging conditions, chemical composition, and toxicity. For this reason, we discuss the two campaigns in detail separately and then merge our observations qualitatively. In discussing changes in toxicity in relation to the various atmospheres, all observations are benchmarked against the control sample of DE aged in the dark (i.e., the one with presumably minimal transformations).

In summer 2005 there were clear increases in toxicity for DE aged in daylight with added OH radicals or toluene. There were only minor indications of altered toxicity for DE aged either in the dark or in daylight. PMNs increased markedly only for DE aged in daylight with added OH radicals; DE aged in daylight with added toluene did not affect PMNs but did increase macrophages. There was also an apparent increase in the overall reactivity of the mixtures when OH radicals were present, as illustrated both by the formation of gas- and particle-phase reactants and by increases in secondary particles (Samy and Zielinska 2010). DE aged in daylight without added co-reactants did not show much reactivity, to judge from its relative lack of change in chemical composition and toxicity.

In summer 2006 the baseline toxicity of the DE control sample appeared to be higher (relative to the diesel soot control) than that of the DE control sample in 2005. This sample, whose composition was also different from that of the DE control sample in 2005, appeared to have a somewhat higher toxicity than several of the samples collected from the other 2006 atmospheres. (In contrast, the toxicity of the DE control sample in 2005 was similar to that of DE aged in the dark with added NO_3 radicals and of DE aged in daylight.) In 2006, the toxicity of DE aged in the dark with added NO_3 radicals and VOCs and of DE aged in daylight was slightly lower (in terms of the samples' effects on lavage protein) than that of the DE control sample. In part because, again, the toxicity of the DE control sample in 2006 appeared to be higher than that of the DS control sample, there was little statistical difference between the cytotoxicity responses to this sample and many of the cytotoxicity responses to samples from the other atmospheres in 2006. Similarly, among the inflammatory responses, there were few statistically significant differences between the DE control sample and other samples.

As mentioned earlier, oxidative-stress indicators were measured only in 2006. They were added because of the growing interest in oxidative stress as a potential mediator of health effects, the addition of these assays to our laboratory capabilities, and the desire for additional information for making comparisons among the atmospheres. As shown in the Results section, the results for the oxidative-stress indicators were in general similar to those for the inflammatory responses. Several of the oxidative-stress indicators did, however, show mostly statistically significant increases in relative toxicity for DE aged in daylight with added OH radicals and mostly no changes or decreases for DE aged in daylight and for DE aged in the dark with added NO_3 radicals.

The technical approach used here followed the general approach that has recently been used by other researchers

to evaluate engine emissions (Seagrave et al. 2002, 2004; McDonald et al. 2004a,b) and ambient air (Seagrave et al. 2006). The harvesting of materials collected from substrates and applying them to test animals has both strengths and limitations. The most important strengths are that it gives researchers the ability to compare samples directly, or within a very short time period, and to include appropriate negative and positive controls in each sample set. Although a perfect experimental design would have involved exposing the test animals to the actual aerosols right at the generation site, this was not possible in the current study because of the lack of exposure facilities at EUPHORE. There are also some limitations to the type of approach we used. First, by delivering the materials in solution we lost the ability to deliver them by inhalation, a more physiologically relevant method. Second, we lost the potentially important physical characteristics of the aerosols and the ability to assess the effects that the surface chemistry of the materials' gas- and particle-phase constituents might have had on their relative toxicity. Finally, collecting and extracting materials into solution created several challenges pertaining to extraction efficiency, which varied with the materials' polarity, and the potential for artifacts to arise during sample handling that might have altered the samples. We took steps to ensure that our samples were handled consistently, and we had an aggressive protocol for getting them into solution or suspension promptly for testing. While the approach taken was in some ways less desirable than inhalation approaches, it had significant advantages over conventional cell culture approaches, which have not shown consistent results when used to investigate the hazards of engine emissions (Seagrave et al. 2003).

Overall, data from both years are consistent with the hypothesis that the toxicity of the samples we collected was affected by changes in their composition over time. These changes were brought about both by the samples' having aged in the chamber (in the dark or in daylight) and by variations in their initial composition presumably associated with the engine's accruing wear. In both years the various samples of DE aged in daylight with added OH radicals tended to cause either no change or increases in cytotoxicity, inflammation, and oxidative stress. This was especially true for inflammation and oxidative stress when the samples were compared with samples of DE aged in the dark with added NO_3 radicals and VOCs or of DE aged in daylight. The observed changes in the magnitude of the trends from summer 2005 to summer 2006 limit our ability to draw overarching conclusions about the effects of atmospheric aging on the toxicity of DE. Still, even the changes in the composition and toxicity of the DE control samples from 2005 to 2006 point to an important yet seldom-considered lesson in evaluating engine emissions, namely that the age, condition, and operating parameters of the engine are critical to the composition and toxicity of the emissions being investigated.

IMPLICATIONS OF FINDINGS

There have been few previous studies of the effects of atmospheric aging on changes in the composition and toxicity of DE. The current study was in many ways an exploratory effort that led to the development of new methodologies for, and the discovery of new information about, the conduct of such experiments. In particular, we developed a new denuder technology to reduce NO_x to concentrations that made the experiments described here feasible. This was needed because our diesel engine was modern and emitted low volumes of hydrocarbons and particle mass and relatively high concentrations of NO_x. Without this development, the chamber atmospheres would have had unrealistic concentrations of NO_x (compared with actual ambient air) that would have made the study impossible to conduct. Our results showed clearly that aging has a marked influence on the composition, and to some extent the toxicity, of DE. In the absence of added co-reactants, DE aged in the chamber showed limited reactivity and, in most cases, few changes in its subsequent composition and toxicity. The addition of co-reactants, especially OH radicals or VOCs, caused the largest differences in the DE's composition in most cases and in its toxicity in several cases.

In conclusion, the study described here developed new techniques and gathered new data both to indicate the extent of the atmospheric transformations of DE and to better guide future studies. However, much more work will be needed to definitively characterize the role of atmospheric aging in the composition and toxicity of diesel engine emissions.

ACKNOWLEDGMENTS

We would like to acknowledge numerous individuals for their assistance during the various phases of this study. Thanks to Dr. William Stockwell of Howard University (Washington, DC) and Prof. Dr. Peter Wiesen of the University of Wuppertal (Wuppertal, Germany) for their help in the planning and start-up of the study. Thanks to Dr. Robert Sawyer, professor emeritus at the University of California–Berkeley, for his help in obtaining and setting up the diesel engine. Thanks to Ford Motor Company's Dagenham Engine Plant (Dagenham, United Kingdom) for donating the diesel engine. Thanks to the EUPHORE staff, especially Dr. Klaus Wirtz, Dr. Montserrat Martin-Reviejo, Dr. Amalia Muñoz, Monica Vazquez, and Ester Borrás, for their help in

conducting the chamber experiments. Thanks to Drs. John Sagebiel and Fred Rogers of the Desert Research Institute (Reno, NV) for their help in conducting the study and developing the NO_x denuder. Thanks to Dr. Eric Fujita of the Desert Research Institute for helpful discussions. Thanks to pathologist Dr. Andrew Gigliotti, D.V.M., and to necropsy personnel and technologists Sandy Dunaway, Brenda Pacheco, Guy Herbert, and David Palucki of the Lovelace Respiratory Research Institute (Albuquerque, NM) for their help in the toxicity testing. Finally, thanks to Anna Cunningham of the Desert Research Institute's Organic Analytical Laboratory staff for her help in sample analysis.

REFERENCES

Albrechcinski TM, Wattle BJ, Michalovic JG. 1988. Chamber Investigations of the Fate of Diesel Emissions in the Atmosphere, Volume I, Task III Final Report. Contract Number CAPA-13-76(1-84). Report to the Coordinating Research Council, Buffalo, NY.

Ammann M. 2001. Using ^{13}N as tracer in heterogeneous atmospheric chemistry experiments. Radiochim Acta 89: 831–838.

Anderson ME. 1985. Determination of glutathione and glutathione disulfide in biological samples. Methods Enzymol 113:548–555.

Arens F, Gutzwiller L, Baltensperger U, Gaggeler HW, Ammann M. 2001. Heterogeneous reaction of NO_2 on diesel soot particles. Environ Sci Technol 35:2191–2199.

Arey J. 1998. Atmospheric reactions of PAHs including formation of nitroarenes. In: The Handbook of Environmental Chemistry. Vol 3, Part I. PAHs and Related Compounds (Neilson AH, ed). Springer-Verlag, Berlin, Heidelberg, New York.

Arey J, Zielinska B, Atkinson R, Aschmann SM. 1989. Nitroarene products from the gas-phase reactions of volatile polycyclic aromatic hydrocarbons with OH radical and N_2O_5. Int J Chem Kinet 21:775–799.

Arey J, Zielinska B, Atkinson R, Winer AM, Ramdahl T, Pitts JN Jr. 1986. The formation of nitro-PAH from the gas-phase reactions of fluoranthene and pyrene with the OH radical in the presence of NO_x. Atmos Environ 20:2339–2345.

Atkinson R. 1988. Atmospheric transformations of automotive emissions. In: Air Pollution, the Automobile, and Public Health (Watson AY, Bates RR, Kennedy D, eds.) pp 99–132. National Academy Press, Washington, DC.

Atkinson R, Arey J. 1994. Atmospheric chemistry of gas-phase polycyclic aromatic hydrocarbons: Formation of atmospheric mutagens. Environ Health Perspect 102 (Suppl. 4): 117–126.

Atkinson R, Arey J, Zielinska B, Aschmann SM. 1987. Kinetics and products of the gas-phase reactions of OH radicals and N_2O_5 with naphthalene and biphenyl. Environ Sci Technol 21:1014–1022.

Atkinson R, Arey J, Zielinska B, Aschmann SM. 1990. Kinetics and nitro-products of the gas-phase OH and NO_3 radical-initiated reactions of naphthalene-d_8, fluoranthene-d_{10} and pyrene. Int J Chem Kinet 22:999–1014.

Becker K-H, Editor. 1996. The European Photoreactor EUPHORE: Design and technical development of the European photoreactor and first experimental results. Final Report of the EC [European Commission]-Project, Contract EV5V-CT92-0059, Wuppertal Institute, Wuppertal, Germany.

Behymer TD, Hites RA. 1985. Photolysis of polycyclic aromatic hydrocarbons adsorbed on simulated atmospheric particulates. Environ Sci Technol 19:1004–1006.

Behymer TD, Hites RA. 1988. Photolysis of polycyclic aromatic hydrocarbons adsorbed on fly ash. Environ Sci Technol 22:1311–1319.

Braman RS, de la Cantera MA, Han QX. 1986. Sequential, selective hollow tube preconcentration and chemiluminescence analysis system for nitrogen oxides in air. Anal Chem 58:1537–1541.

Chow JC, Watson JG, Chen LWA, Arnott WP, Moosmuller H, Fung K. 2004. Equivalence of elemental carbon by thermal/optical reflectance and transmittance with different temperature protocols. Environ Sci Technol 38:4414–4422.

Chow JC, Watson JG, Crow D, Lowenthal DH, Merrifield T. 2001. Comparison of IMPROVE and NIOSH carbon measurements. Aerosol Sci Technol 34:23–34.

Chow JC, Watson JG, Pritchett LC, Pierson WR, Frazier CA, Purcell RG. 1993. The DRI thermal/optical reflectance carbon analysis system: Description, evaluation and applications in U.S. air quality studies. Atmos Environ 27A: 1185–1201.

Claxton LD, Barnes HM. 1981. The mutagenicity of diesel-exhaust particle extracts collected under smog-chamber conditions using the Salmonella typhimurium test system. Mutat Res 88:255–272.

DeMarini DM, Brooks LR, Warren SH, Kobayashi T, Gilmour MI, Singh P. 2004. Bioassay-directed fractionation and salmonella mutagenicity of automobile and forklift diesel exhaust particles. Environ Health Perspect 112: 814–819.

Doyle M, Sexton KG, Jeffries H, Bridge K, Jaspers I. 2004. Effects of 1,3-butadiene, isoprene, and their photochemical degradation products on human lung cells. Environ Health Perspect 112:1488–1495.

Fan Z, Chen D, Birla P, Kamens RM. 1995. Modeling of nitro-polycyclic aromatic hydrocarbon formation and decay in the atmosphere. Atmos Environ 29:1171–1181.

Finlayson-Pitts BJ, Pitts JN Jr. 2000. Chemistry of the Upper and Lower Atmosphere: Theory, Experiments, and Applications. Academic Press, San Diego, CA.

Fujita EM, Campbell DE, Zielinska B, Sagebiel JC, Bowen JL, Goliff W, Stockwell WR, Lawson DR. 2003. Diurnal and weekday variations in source contributions of ozone precursors in California's South Coast Air Basin. J Air Waste Manage Assoc 53:844–863.

Gay RJ, McComb RB, Bowers GN Jr. 1968. Optimum reaction conditions for human lactate dehydrogenase isoenzymes as they affect total lactate dehydrogenase activity. Clin Chem 14:740–753.

Graber ER, Rudich Y. 2006. Atmospheric HULIS: How humic-like are they? A comprehensive and critical review. Atmos Chem Phys 6:729–753.

Grosjean D. 1992. Formic acid and acetic acid: Emissions, atmospheric formation, and dry deposition at two Southern California locations. Atmos Environ 26A:3279–3286.

Gundel LA, Lee VC, Mahanama KRR, Stevens RK, Daisey JM. 1995. Direct determination of the phase distributions of semi-volatile polycyclic aromatic hydrocarbons using annular denuders. Atmos Environ 29:1719–1733.

Heland J, Kleffmann J, Kurtenbach R, Wiesen P. 2001. A new instrument to measure gaseous nitrous acid (HONO) in the atmosphere. Environ Sci Technol 35:3207–3212.

Hendershot RJ, Rogers B, Snively CM, Ogunnaike B, Lauterbach J. 2004. Development and optimization of NO_x storage and reduction catalysts using statistically guided high-throughput experimentation. Catalysis Today 98: 375–385.

Jaspers I, Jeffries H, Sexton K. 2003. Photochemical reactions of urban air pollution mixtures enhance inflammatory responses in lung cells. Toxicologist 72:190.

Kalberer M, Paulsen D, Sax M, Steinbacher M, Dommen J, Prevot ASH, Fisseha R, Weingartner E, Frankevich V, Zenobi R, Baltensperger U. 2004. Identification of polymers as major components of atmospheric organic aerosol. Science 303:1659.

Kleffman J, Heland J, Kurtenbach R, Lörzer JC, Wiesen P. 2002. A new instrument (LOPAP) for the detection of nitrous acid HONO. Environ Sci and Pollut Res Int 9 (special issue 4):48–54.

Kleffman J, Lörzer JC, Wiesen P, Kern C, Trick S, Volkamer R, Rodenas M, Wirtz K. 2006. Intercomparison of the DOAS and LOPAP techniques for the detection of nitrous acid (HONO). Atmos Environ 40:3640–3652.

Madden MC, Richards JH, Dailey LA, Hatch GE, Ghio AJ. 2000. Effect of ozone on diesel exhaust particle toxicity in rat lung. Toxicol Appl Pharmacol 168:140–148.

Martin-Reviejo M, Wirtz K. 2005. Is benzene a precursor for secondary organic aerosol? Environ Sci Technol 39: 1045–1054.

McDonald JD, Eide I, Seagrave J, Zielinska B, Whitney K, Lawson DR, Mauderly JL. 2004a. Relationship between composition and toxicity of motor vehicle emission samples. Environ Health Perspect 112: 1527-1538.

McDonald JD, Harrod KS, Seagrave J, Seilkop SK, Mauderly JL. 2004b. Effects of low sulfur fuel and a catalyzed particle trap on the composition and toxicity of diesel emissions. Environ Health Perspect 112:1307–1312.

Nolte CG, Schauer JJ, Cass GR, Simoneit BR. 2001. Highly polar organic compounds present in wood smoke and in the ambient atmosphere. Environ Sci Technol 35:1912–1919.

Nolte CG, Schauer JJ, Cass GR, Simoneit BRT. 2002. Trimethylsilyl derivatives of organic compounds in source samples and in atmospheric fine particulate matter. Environ Sci Technol 36:4273–4281.

Peters AJ, Lane DA, Gundel LA, Northcott GL, Jones KC. 2000. A comparison of high volume and diffusion denuder samplers for measuring semivolatile organic compounds in the atmosphere. Environ Sci Technol 34:5001–5006.

Rhoden CR, Lawrence J, Godleski JJ, Gonzalez-Flecha B. 2004. N-acetylcysteine prevents lung inflammation after short-term inhalation exposure to concentrated ambient particles. Toxicol Sci 79:296–303.

Rinehart LR, Fujita EM, Chow JC, Magliano K, Zielinska B. 2006. Spatial distribution of $PM_{2.5}$ associated organic compounds in the San Joaquin Valley. Atmos Environ 40: 290–303.

Robinson AL, Donahue NM, Shrivastava MK, Weitkamp EA, Sage AM, Grieshop AP, Lane TE, Pierce JR, Pandis SN. 2007. Rethinking organic aerosols: Semivolatile emissions and photochemical aging. Science 315:1259–1262.

Saathof H, Moehler O, Schurath U, Kamm S, Dippel B, Mihelcic D. 2003. The AIDA soot aerosol characterisation campaign 1999. J Aerosol Sci 34:1277–1296.

Samy S, Zielinska B. 2010. Secondary organic aerosol production from modern diesel engine emissions. Atmos Chem Phys 10:609–625.

Seagrave J, Gigliotti A, McDonald JD, Seilkop SK, Whitney KA, Zielinska B, Mauderly JL. 2005a. Composition, toxicity, and mutagenicity of particulate and semivolatile emissions from heavy-duty compressed natural gas-powered vehicles. Toxicol Sci 87:232–241.

Seagrave JC, McDonald JD, Gigliotti AP, Nikula KJ, Seilkop SK, Gurevich M, Mauderly JL. 2002. Mutagenicity and in vivo toxicity of combined particulate and semivolatile organic fractions of gasoline and diesel engine emissions. Toxicol Sci 70:212–226.

Seagrave J, McDonald JD, Reed MD, Seilkop SK, Mauderly JL. 2005b. Responses to subchronic inhalation of low concentrations of diesel exhaust and hardwood smoke measured in rat bronchoalveolar lavage fluid. Inhal Toxicol 17: 657–670.

Seagrave JC, Seilkop SK, Mauderly JL. 2003. In vitro relative toxicity screening of combined particulate and semivolatile organic fractions of gasoline and diesel engine emissions. J Toxicol Environ Health 66:1113–1132.

Sexton KG, Jeffries HE, Jang M, Kamens RM, Doyle M, Voicu I, Jaspers I. 2004. Photochemical products in urban mixtures enhance inflammatory responses in lung cells. Inhal Toxicol 16 Suppl 1:107–114.

Singh P, DeMarini DM, Dick CA, Tabor DG, Ryan JV, Linak WP, Kobayashi T, Gilmour MI. 2004. Sample characterization of automobile and forklift diesel exhaust particles and comparative pulmonary toxicity in mice. Environ Health Perspect 112:820–825.

Stark G, Stauff J, Miltenburger HG, Stumm-Fischer I. 1985. Photodecomposition of 1-nitropyrene and other direct-acting mutagens extracted from diesel-exhaust particulates. Mutat Res 155:27–33.

Takeda N, Teranishi K, Hamada K. 1984. Mutagenicity of the sunlight-exposed sample of pyrene in Salmonella typhimurium TA98. Bull Environ Contam Toxicol 33: 410–417.

Tietze F. 1969. Enzymic method for quantitative determination of nanogram amounts of total and oxidized glutathione: Applications to mammalian blood and other tissues. Anal Biochem 27:502–522.

U.S. Congress. 1990. Clean Air Act Amendments of 1990. S.1630.ENR. 101st Congress 2nd Session, House of Representatives. U.S. Government Printing Office. Washington, DC. Available from: *http://thomas.loc.gov/cgi-bin/query/C?c101:./temp/~c101c7RBOJ.*

Vijay R, Hendershot RJ, Rivera-Jiménez SM, Rogers WB, Feist BJ, Snively CM, Lauterbach J. 2005. Noble metal free NO_x storage catalyst using cobalt discovered via high-throughput experimentation. Catal Commun 6:167.

Volkamer R, Platt U, Wirtz K. 2001. Primary and secondary glyoxal formation from aromatics: Experimental evidences for the bicycloalkyl-radical pathway from benzene, toluene, and *p*-xylene. J Phys Chem A 105:7865–7874.

Watanabe N, Kamei S, Ohkubo A, Yamanaka M, Ohsawa S, Makino K, Tokuda K. 1986. Urinary protein as measured with a pyrogallol red-molybdate complex, manually and in a Hitachi 726 automated analyzer. Clin Chem 32:1551–1554.

Winer AM, Busby WF Jr. 1995. Atmospheric transport and transformation of diesel emissions. In: Diesel Exhaust: A Critical Analysis of Emissions, Exposure, and Health Effects. Special Report. Health Effects Institute, Cambridge, MA.

Zielinska B. 2005. Atmospheric transformation of diesel emissions. Exp Toxicol Pathol 57:31–42.

Zielinska B, Arey J, Atkinson R, McElroy PA. 1988. Nitration of acephenanthrylene under simulated atmospheric conditions and in solution and in the presence of nitroacephenathrylene(s) in ambient particles. Environ Sci Technol 22:1044–1048.

Zielinska B, Arey J, Atkinson R, McElroy PA. 1989a. Formation of methylnitronaphthalenes from the gas-phase reactions of 1- and 2-methylnaphthalene with OH radicals and N_2O_5 and their occurrence in ambient air. Environ Sci Technol 23:723–729.

Zielinska B, Arey J, Atkinson R, Ramdahl T, Winer AM, Pitts JN Jr. 1986. Reaction of dinitrogen pentoxide with fluoranthene. J Am Chem Soc 108:4126–4132.

Zielinska B, Arey J, Atkinson R, Winer AM. 1989b. The nitroarenes of molecular weight 247 in ambient particulate samples collected in Southern California. Atmos Environ 23:223–229.

Zielinska B, Sagebiel J, Arnott WP, Rogers CF, Kelly KE, Wagner DA, Lighty JS, Sarofim AF, Palmer G. 2004a. Phase and size distribution of polycyclic aromatic hydrocarbons in diesel and gasoline vehicle emissions. Environ Sci Technol 38:2557–2567.

Zielinska B, Sagebiel J, MacDonald JD, Whitney K, Lawson DR. 2004b. Emission rates and comparative chemical composition from selected in-use diesel and gasoline fueled vehicles. J Air Waste Manage Assoc 54:1138–1150.

Zielinska B, Samy S. 2006. Analysis of nitrated polycyclic aromatic hydrocarbons. Anal Bioanal Chem 386:883–890.

APPENDIX A. Instrumentation and Engine Conditions

Appendix A describes the monitors used and tabulates the engine conditions recorded during the three EUPHORE campaigns discussed in this report.

MONITORS

Weinlich MP Computer

The MP computer is an instrument system made by Weinlich GmbH & Co. KG of Reilingen, Germany, that measures parameters related to running an engine — including time, speed, torque, power, work, fuel weight, specific consumption, air volume, pressure, and relative humidity as well as air, water, oil, and reference temperatures — and sends the results every 0.25 seconds to a desktop computer for recording and storage. The most interesting and useful parameters for the experiments we conducted were the following:

- **Time (sec)** The time elapsed since the counter was reset. The counter increment was 0.25 seconds.
- **Speed (rpm)** The turn rate of the engine. Speed was measured and calculated digitally. A control allowed the engine to maintain a set value.
- **Torque (Nm)** The rotational force (torsion resistance) applied to the engine. Torque was measured using an analog instrument and was calibrated with a calibrating lever.
- **Power (kW)** The energy produced by the engine per unit of time.
- **Specific fuel consumption (g/min)** The mass of the fuel consumed per minute by the engine. The fuel in the storage tank was weighed using an electronic precision balance, and the system's PC calculated the fuel consumed per minute.
- **Relative humidity (%), and air temperature, AT (°C)** as the relative humidity and air temperature of the air aspirated by the engine for fuel combustion. The transducers making these measurements were located in a measuring turbine with a silencing chamber (to reduce pulsation).
- **Water temperature (°C)** The temperature of the engine coolant.
- **Oil temperature (°C)** The temperature of the engine lubricant.

One-minute averages were plotted for these parameters and are available upon request.

Horiba MEXA-7170D Emission-Gas Analyzer

The MEXA-7170D is an instrument system made by Horiba Instruments of Irvine, California, that uses a variety of detectors to continuously and directly measure the concentration of pollutants in engine exhaust, including:

- **CO (ppm)**

  High concentrations Measured using an AIA-722 nondispersive infrared detector with an operating range of 0 vol% to 1.0 vol%. The detector converted from vol% to ppm.

  Low concentrations Measured using an AIA-721A nondispersive infrared detector with an operating range of 0 to 250 ppm.
- **NO_x (ppm)** Measured using a CLA-720MA heated chemiluminescence detector with an operating range of 0 to 1000 ppm.
- **Total hydrocarbons (parts per million carbon [ppmC])** Measured using an FIA-721HA flame ionization detector with an operating range 0 to 1000 ppmC.
- **CO_2 (ppm)** Measured using an AIA-722 nondispersive infrared detector with an operating range of 0 vol% to 10.0 vol%. The detector converted from vol% to ppm.
- **O_2 (ppm)** Measured using an MPA-720 magnetopneumatic detector with an operating range of 0 vol% to 25.0 vol%. The detector converted from vol% to ppm.

Other Monitors

Five monitors measured O_3, NO_x, NO_y, and SO_2 concentration directly from EUPHORE's chamber B:

- **Casella ML9810 (for O_3, in ppb)** A nondispersive ultraviolet photometer that alternately switched a selective O_3 scrubber in and out of the measuring stream and computed the ratio of transmitted light. A mercury vapour lamp (254 nm) was used as the light source, and a solar-blind vacuum photodiode was used as the detector.
- **Combined Tecan CLD 770 chemiluminescent NO detector and PLC 760 photolytic converter (for NO, NO_2, and NO_x, in ppb)** The detector measured the gas-phase chemiluminescent reaction of NO with O_3. The converter selectively converted NO_2 to NO through photo-dissociation with a xenon lamp.

- **Advanced Pollution Instrumentation 200AU (for NO, NO_2, and NO_x, in ppb)** A NO_y detector that measured the light intensity of the chemiluminescent gas-phase reaction of NO with O_3, sampled the gas stream, and measured the NO concentration by digitizing the signal from the detector's photomultiplier tube. A valve then routed the sample stream through a converter containing heated molybdenum to reduce any NO_x present to NO at 315°C. NO_2 concentrations were derived by subtraction.
- **Teledyne Monitor Labs ML9841A (for NO_y, in ppb)** A gas-phase chemiluminescence NO_x detector that continuously analyzed NO, NO_x, and NO_2. The chemiluminescent reaction only occurs between O_3 and NO. NO_2 was then chemically reduced to NO using a Teledyne Monitor Labs Molycon catalytic converter. NO_2 concentrations were derived by subtraction.
- **Dasibi 4108 (for SO_2, in ppb)** A detector that made use of the ultraviolet fluorescence of SO_2.

Other Measures

- **Chamber pressure (mbar)** Measured using an AIR-DB-VOC barometer connected directly to the chamber.
- **Chamber relative humidity (mbar) and temperature (K)** Measured using a Walz dew-point mirror hygrometer. (Not the same relative-humidity measure as that made of the air aspirated by the engine.)
- **Photolysis rate ($J[NO_2]$)** Measured using a filter radiometer. The photolysis rate is the rate of dissociation for the reaction $NO_2 + h{\cdot}\nu \rightarrow NO + O$. It is a function of latitude, time of year, local time, and cloud cover.

ENGINE CONDITIONS

Table A.1 details engine conditions for the winter 2005 campaign. During this campaign the engine was operated under a constant load of approximately 60 Nm and 2000 rpm. DE was injected into the chamber when the engine's water and oil temperature had reached approximately 88°C and 90°C, respectively, for periods of approximately 2 to 6 minutes.

Table A.2 details engine conditions for the summer 2005 campaign. During this campaign, the engine was operated under a variable load on a number of occasions (May 17, 18, 23, and 24), cycling from approximately 10 or 20 Nm to approximately 120 Nm over periods of several minutes as DE was injected into the chamber. In general, variable loads slightly increased the output of diesel PM (average mass concentration 7.9 µg/L [±16%]) compared with that of constant loads (average mass concentration 5.5 µg/L [±6%]).

Tables A.3 and A.4 summarize engine conditions for the summer 2006 campaign, showing the average values obtained from the MP computer and emission-gas analyzer during the injection periods. The engine was operated under a constant load. DE was injected for approximately 20 to 35 minutes in order to obtain sufficient material for chemical analysis and toxicity testing.

Table A.1. Engine Conditions During the Winter 2005 Campaign

Date	Injection Time (UTC)	Duration (mm:ss)	Engine Speed (rpm)	Torque (Nm)			TFC (g)	SFC (g/min)	RH (%)	WT (°C)	OT (°C)	AT (°C)	ECT (mm:ss)
				Average	Minimum	Maximum							
Jan. 12	12:02	03:00	2000	66.70	65.58	67.34	185.96	61.99	7.5	88.5	95.1	38.3	17:04
Jan. 13	10:26	05:00	2000	49.79	23.25	65.09	244.44	48.89	24.7	72.5	87.8	27.2	17:36
Jan. 13	10:49	03:00	2000	64.79	63.00	66.66	178.00	59.33	15.4	88.4	94.0	34.6	07:36
Jan. 14	10:27	02:00	2000	63.69	62.82	64.57	118.84	59.42	23.4	87.4	90.0	26.1	23:37
Jan. 15	12:14	06:00	2000	64.63	61.93	67.35	366.08	61.01	18.2	88.5	95.2	31.7	14:16
Jan. 17	12:10	06:00	2000	62.74	58.96	66.40	356.82	59.47	15.0	88.0	93.8	33.3	14:30
Jan. 19	13:56	06:00	2000	62.64	59.74	65.26	369.66	61.61	11.9	88.3	95.2	30.9	18:37
Jan. 20	13:35	06:00	2000	62.78	58.90	68.37	359.29	59.88	10.9	88.4	94.3	34.1	14:24
Jan. 21	14:07	06:00	2000	65.00	62.22	67.15	365.14	60.86	6.9	88.7	94.9	37.2	12:14
Jan. 24	11:37	02:00	2000	64.03	63.38	64.68	120.44	60.22	9.5	88.2	93.4	31.9	15:58
Jan. 25	11:57	02:00	2000	64.57	65.13	64.02	122.80	61.40	1.6	88.0	93.1	24.1	16:02
Jan. 26	12:49	03:00	2000	62.63	57.81	60.79	171.74	57.25	1.6	88.3	96.1	25.1	19:40
Jan. 27	10:37	02:00	2000	65.18	64.62	65.75	123.21	61.60	4.6	87.7	91.7	23.2	16:04

UTC indicates Coordinated Universal Time; TFC indicates total fuel consumption; SFC indicates specific fuel consumption; RH indicates relative humidity; WT indicates water temperature; OT indicates oil temperature; AT indicates air temperature; ECT indicates engine-conditioning time.

Table A.2. Engine Conditions During the Summer 2005 Campaign

Date	Injection Time (UTC)	Duration (mm:ss)	Engine Speed (rpm)	Torque (Nm)			TFC (g)	SFC (g/min)	RH (%)	WT (°C)	OT (°C)	AT (°C)	ECT (hh:mm:ss)
				Average	Minimum	Maximum							
May 10	9:08	03:00	2022	60.11	59.09	61.15	175.49	58.90	18.5	93.0	101.3	38.7	0:30:23
May 10	13:08	03:00	2019	61.65	60.65	62.68	180.52	60.20	8.0	93.1	100.9	41.7	0:21:25
May 10	13:30	03:00	1906	52.92	38.40	61.16	135.21	45.07	6.6	94.4	101.7	43.7	0:43:25
May 10	13:51	03:00	1838	49.87	28.88	61.34	125.63	41.88	6.3	94.8	101.8	44.2	1:04:25
May 11	9:31	03:00	2000	63.49	62.36	64.58	177.75	59.33	19.4	93.5	101.0	39.1	0:53:19
May 11	10:21	03:00	2000	64.89	64.21	66.16	181.61	60.30	17.2	92.0	98.9	40.7	1:43:19
May 12	10:07	04:00	2006	64.74	63.17	66.50	239.60	60.17	19.3	93.0	100.8	38.8	0:27:58
May 13	9:07	03:00	2012	61.27	60.12	62.34	173.07	57.97	23.4	91.6	99.7	38.0	0:25:23
May 16	9:05	04:00	2000	64.90	63.27	66.74	241.38	60.60	22.6	92.8	100.3	36.8	0:38:09
May 17	10:02	03:00	2000	69.56	10.00	118.50	190.14	62.37	16.9	90.5	96.3	31.7	0:36:58
May 18	8:58	04:00	2000	66.42	23.00	111.50	247.24	60.80	12.4	91.0	97.5	34.1	0:27:36
May 19	7:58	03:30	2000	63.38	61.79	65.15	205.41	58.75	15.6	91.0	97.4	33.9	0:25:55
May 20	8:40	04:15	2000	60.96	58.70	63.24	245.79	57.80	17.3	91.3	99.6	38.0	0:33:16
May 23	9:23	03:45	2000	67.18	50.50	118.50	244.88	63.17	20.8	89.3	93.4	33.0	0:39:19
May 24	9:01	02:44	2000	75.01	51.50	121.50	185.99	68.13	25.5	89.9	94.4	34.1	0:18:25
May 25	9:30	10:00	2000	58.24	52.50	62.57	560.64	56.06	12.7	90.3	97.2	37.5	0:14:41
May 26	8:20	10:00	2000	55.09	50.56	59.84	529.97	52.99	14.5	92.1	101.2	39.0	0:27:29

UTC indicates Coordinated Universal Time; TFC indicates total fuel consumption; SFC indicates specific fuel consumption; RH indicates relative humidity; WT indicates water temperature; OT indicates oil temperature; AT indicates air temperature; ECT indicates engine-conditioning time.

Table A.3. Engine Conditions During the Summer 2006 Campaign

Date	Injection Time (UTC)	Duration (mm:ss)	Engine Speed (rpm)	Torque (N-m)	TFC (g)	SFC (g/min)	RH (%)	WT (°C)	OT (°C)	AT (°C)	ECT (mm:ss)
May 25	10:20	06:00	2041	62.44	292.9	59.96	6.521	93.81	102.6	39.30	48:23
May 26	10:18	10:00	2084	52.74	531.1	56.36	6.818	92.14	101.9	38.62	45:21
May 30	9:56	20:00	1971	54.66	935.9	51.97	13.61	91.11	100.2	40.65	39:17
May 31	13:57	30:00	1989	64.16	1710	58.89	15.02	93.44	103.6	39.78	47:21
June 1	11:47	28:50	1987	66.64	1698	60.49	12.22	94.00	102.7	40.66	32:14
June 2	9:53	27:12	1956	66.04	1563	59.75	7.652	94.59	104.1	41.73	43:18
June 5	8:44	15:00	1992	64.27	890	58.97	10.64	90.30	97.22	36.64	31:14
June 5	9:18	12:00	1992	63.72	757	58.24	10.44	91.70	98.62	36.45	19:09
June 5	9:42	10:00	1992	62.82	565	57.81	7.895	92.28	100.2	38.60	13:07
June 6	10:00	15:00	1993	66.52	910	60.78	12.93	88.36	97.10	38.58	34:15
June 6	10:29	10:00	1992	64.71	595	59.38	10.53	91.56	99.27	41.58	13:06
June 6	10:56	10:00	1992	63.16	571	58.30	11.60	92.63	100.4	42.16	18:08
June 7	9:26	17:00	1992	65.33	1017	59.88	12.63	88.64	97.59	39.12	31:14
June 7	10:00	07:00	1993	69.33	423	61.87	15.39	92.15	98.17	37.14	14:06
June 7	10:22	06:40	1993	67.80	428	60.69	15.78	91.15	97.31	37.15	18:09
June 8	10:40	20:00	1993	63.49	1170	58.51	21.64	89.60	98.94	38.40	32:14
June 8	11:15	10:00	1990	66.31	602	60.09	19.40	91.42	99.34	40.25	14:06
June 9	9:56	20:00	1994	64.29	1181	58.98	22.15	91.10	99.61	37.94	31:14
June 9	10:31	10:00	1986	61.68	554	57.64	19.13	92.76	100.6	39.61	14:06
June 12	12:15	10:00	1987	64.23	574	59.64	15.90	88.05	95.14	38.01	33:14
June 13	11:36	10:00	1994	65.79	584	60.25	17.89	85.83	94.08	36.79	31:13

UTC indicates Coordinated Universal Time; TFC indicates total fuel consumption; SFC indicates specific fuel consumption; RH indicates relative humidity; WT indicates water temperature; OT indicates oil temperature; AT indicates air temperature; ECT indicates engine-conditioning time.

Table A.4. Average Gas Concentrations in the EUPHORE Chamber During the Summer 2006 Campaign[a]

Date	CO[b] (ppm)	NO_x (ppm)	CO_2 (ppm)	O_2 (ppm)	THCs[c] (ppmC)
May 25	60.93	401.5	48,559	139,887	79.20
May 26	59.84	371.5	46,714	143,105	80.15
May 30	61.36	331.9	43,952	149,200	74.69
May 31	61.90	410.3	52,138	133,409	61.00
June 1	61.38	434.5	53,013	134,504	56.86
June 2	61.20	418.6	51,012	136,100	56.53
June 5	61.64	403.3	50,026	138,380	62.96
June 5	61.67	404.5	48,459	140,422	61.82
June 5	61.52	423.2	50,586	137,512	62.93
June 6	61.89	411.2	50,793	137,476	64.02
June 6	61.71	380.8	48,240	140,846	60.35
June 6	61.68	393.3	49,244	140,143	63.08
June 7	62.72	403.9	50,180	138,404	66.37
June 7	62.26	426.2	54,409	132,141	66.76
June 7	61.97	419.0	54,303	132,624	66.27
June 8	62.13	384.4	51,492	136,704	67.50
June 8	62.00	395.3	54,200	132,872	66.66
June 9	62.04	396.0	52,603	135,191	70.44
June 9	61.88	373.9	51,300	137,235	67.92
June 12	62.72	400.3	52,131	135,647	79.05
June 13	62.93	398.3	52,015	136,048	76.28

[a] Measurements were obtained using a Horiba MEXA-7170D gas analyzer. Injection conditions are given in Table A.3.

[b] CO measurements were obtained using an AIA-721A nondispersive infrared detector.

[c] THCs indicate total hydrocarbons.

APPENDICES AVAILABLE ON THE WEB

The following appendices are available on the Web at *www.healtheffects.org* or from HEI upon request.

Appendix B. Detailed Results from NO_x Denuder Development and Characterization

Appendix C. Detailed Description of the Results Obtained During EUPHORE Campaigns — Chemistry of the Atmospheres

Appendix D. Detailed Description of the Results Obtained During EUPHORE Campaigns — Toxicity Testing Results

Appendix E. Toxicological Dose Response Curves and Statistical Comparisons

Appendix F. Concentration of Species Collected During Summer 2005 and 2006 Campaigns (Electronic Database)

Appendix G. Concentration of Species Collected During Winter 2005 Campaign (Electronic Database)

ABOUT THE AUTHORS

Barbara Zielinska, Ph.D., is a research professor and the director of the Organic Analytical Laboratory at the Desert Research Institute in Reno, Nevada. Her current primary areas of interest include the collection and analysis of trace atmospheric organic species in the gas and particle phases; the development of analytic methods for the speciation of primary and secondary particulate organic matter; the kinetics and products of the gas-phase reactions of organic compounds; measurement methods for volatile, semivolatile, and particle-phase compounds in ambient air; and emissions of particle-associated and volatile organic compounds from diesel and gasoline fueled vehicles, wood combustion, biomass burning, meat cooking, and other sources. Dr. Zielinska served three consecutive terms (from 2000 to 2006) as a member of the U.S. EPA's Clean Air Scientific Advisory Committee. She is an active participant in several scientific societies and is involved in the organization of conferences and the peer-reviewing of scientific publications and proposals. Dr. Zielinska has authored or coauthored more than 100 peer-reviewed papers.

Shahryar "Shar" Samy was a doctoral candidate in the atmospheric sciences program at the Desert Research Institute in Reno, Nevada, and was conducting his Ph.D. research under the direction of Dr. Zielinska at the time of the research project. He completed his Ph.D. in December 2009. Mr. Samy has several years of research experience in environmental and analytic chemistry. He completed a B.S. in Chemistry in 1998 at the University of Montana in Missoula, Montana, and after several years of professional work experience completed a Master's thesis in Geography and Environmental Studies at the University of Colorado in Colorado Springs, Colorado, on the topic of spatial and temporal variability in volatile organic compounds in the Colorado Springs airshed. He is currently focusing on the atmospheric transformations of gas- and particle-phase constituents and recently completed an independent project on water-soluble polar organic compounds at the Storm Peak Laboratory above Steamboat, Colorado.

Jacob D. McDonald, Ph.D., is a scientist at, and the program manager of, the chemistry and inhalation-exposure groups at the Lovelace Respiratory Research Institute in Albuquerque, New Mexico. Dr. McDonald graduated in 2000 from the University of Nevada in Reno, Nevada, where he conducted his graduate work in atmospheric chemistry at the Desert Research Institute. He is currently the associate director of the National Environmental Respiratory Center at Lovelace. His research focuses on understanding the relationships between atmospheric composition and

toxicity. He is currently involved in research characterizing the health effects of laboratory-generated environmental aerosols, including engine emissions, secondary organic and inorganic aerosols, road dust, and wood smoke.

JeanClare Seagrave, Ph.D., is an associate scientist in the experimental toxicology program at the Lovelace Respiratory Research Institute and a clinical associate professor of pathology at the University of New Mexico, both in Albuquerque, New Mexico. She completed her doctorate in biochemistry at the University of New Mexico and a postdoctoral fellowship at Los Alamos National Laboratory in Los Alamos, New Mexico. Currently, her primary research activities focus on the structural, functional, and biochemical responses of the lung to air pollution constituents, including mainstream and secondhand cigarette smoke. Ongoing projects in her laboratory make use of laboratory animals and cultured cells to assess the relative toxicity of air pollutants and to determine how cigarette smoke causes emphysema and cardiovascular disease. Dr. Seagrave is affiliated with numerous professional associations, including the American Society for Cell Biology, American Physiological Society, Society for Toxicology, and American Thoracic Society. She has published nearly 60 peer-reviewed papers.

OTHER PUBLICATIONS RESULTING FROM THIS RESEARCH

Samy S, Zielinska B. 2009. Secondary organic aerosol production from modern diesel engine emissions. Atmos Chem Phys Discuss 9:17665–17704.

Samy S, Zielinska B. 2010. Secondary organic aerosol production from modern diesel engine emissions. Atmos Chem Phys 10:609–625.

Zielinska B. 2005. Atmospheric transformations of diesel emissions. Exp Toxicol Pathol 57:31–42.

Zielinska B, Sagebiel J, Stockwell W, McDonald J, Seagrave JC, Wissen P, Wirtz K. 2006. Investigation of atmospheric transformations of diesel emissions in the European Photoreactor (EUPHORE). In: Environmental Simulation Chambers: Application to Atmospheric Chemical Processes (Barnes I, Rudzinski KJ, eds). Springer, Netherlands. Proceeding of the NATO Advanced Research Workshop, Zakopane, Poland, 1–4 October 2004.

ABBREVIATIONS AND OTHER TERMS

Al_2O_3	aluminum oxide
ANOVA	analysis of variance
AT	air temperature (in tables)
BHT	butylated hydroxytoluene
CH_2O	formaldehyde
CO	carbon monoxide
CO_2	carbon dioxide
Co_2O_3	cobalt(III) oxide
Co_3O_4	cobalt(II,III) oxide
CoO	cobalt(II) oxide
DE	diesel exhaust
DS	diesel soot
EC	elemental carbon
ECD	electron-capture device (in tables)
ECT	engine conditioning time (in tables)
EDTA	ethylene-diamine-tetraacetic acid
EUPHORE	European Photoreactor
FEP	fluorinated ethylene propylene
FID	flame ionization detector (in tables)
FTIR	Fourier transform infrared spectrometer (in tables)
GC	gas chromatography
GC–MS	gas chromatography–mass spectrometry
GSSG	oxidized glutathione (in figures)
HEPES	4-(2-hydroxyethyl)-1-piperazineethanesulfonic acid
HNO_3	nitric acid
HO-1	heme oxygenase-1 (in figures)
HONO	nitrous acid
i.d.	internal diameter
IMPROVE	Interagency Monitoring of Protected Visual Environments
$J(NO_2)$	NO_2 photolysis rate
LDH	lactate dehydrogenase
LDLs	low-density lipoproteins
LC–MS	liquid chromatography–mass spectrometry
MDL	method detection limit

MS	mass spectrometry
N_2O_5	dinitrogen pentoxide
Nm	Newton-meter
NO	nitric oxide
NO_2	nitrogen dioxide
NO_3	nitrate radical (in figures and tables)
NO_x	nitrogen oxides
NO_y	reactive nitrogen oxides
O_2	oxygen
O_3	ozone
OC	organic carbon
OH	hydroxyl radical (in figures and tables)
OT	oil temperature (in tables)
PAH	polycyclic aromatic hydrocarbon
PID	plasma ionization detector (in tables)
PM	particulate matter
$PM_{2.5}$	particulate matter < 2.5 μm in aerodynamic diameter
PMN	polymorphonuclear neutrophil
POC	pyrolized organic carbon
ppmC	parts per million carbon
ppt	parts per trillion
RH	relative humidity (in tables)
SF_6	sulfur hexafluoride
SFC	specific fuel consumption (in tables)
SMPS	scanning mobility particle sizer (in tables)
SO_2	sulfur dioxide
SVOC	semivolatile organic compound
TBARS	thiobarbituric-acid–reactive substances
TFC	total fuel consumption (in tables)
TC	total carbon
THC	total hydrocarbon (in tables)
U.S. EPA	U.S. Environmental Protection Agency
UTC	Coordinated Universal Time (in tables)
VOC	volatile organic compound
WT	water temperature (in tables)
XAD	adsorbent polystyrene divinylbenzene resin used in sampling cartridges

Research Report 147, *Atmospheric Transformation of Diesel Emissions*, B. Zielinska et al.

INTRODUCTION

Diesel exhaust (DE*) is an important contributor to air pollution and consists of a complex mixture of hundreds of compounds in either gas or particle form. Uncontrolled diesel engines emit high concentrations of particulate matter (PM), nitrogen oxides (NO_x), and aldehydes and low concentrations of carbon monoxide and hydrocarbons (HEI Diesel Epidemiology Working Group 2002). DE contains many compounds that are considered toxic or carcinogenic, including aldehydes, aromatic compounds (e.g., benzene), 1,3-butadiene, polycyclic aromatic hydrocarbons (PAHs), nitro-PAHs, other forms of organic carbon (OC), sulfate, and metals. After emission, DE undergoes chemical and physical transformations, or "aging," in the atmosphere as well as dispersion and transport. The aging process depends on the environment into which the DE is emitted; the atmosphere contains many compounds, such as oxidizing and nitrating radicals, as well as organic and inorganic compounds from sources other than diesel engines. These compounds can influence the chemical composition and toxicity of DE as well as how long its various components remain in the atmosphere (U.S. Environmental Protection Agency [U.S. EPA] 2002).

A factor that complicates research on the health effects of DE is the substantive changes to diesel engine technology that have taken place in recent years as a result of more stringent emissions regulations, particularly in the United States and Europe. Regardless of which technology is being tested, however, limited information is available about the physical and chemical transformations of DE in the atmosphere and how these transformations might affect DE's toxicity. When the study described in this report was funded, information was available on the transformation of DE components exposed to irradiation or to reactive gases such as ozone (O_3) or NO_x, with a focus on the formation of mutagenic compounds (e.g., Pitts et al. 1978; Van Vaeck and Van Cauwenberghe 1984; Arey et al. 1989). Several studies had started to investigate the health effects associated with such alterations, including changes in mutagenicity and lung inflammation when DE-particle extracts were exposed to radiation or O_3 (Claxton and Barnes 1981; Stärk et al. 1985; Madden et al. 2000); additional toxicologic studies were also underway at the time (Doyle et al. 2004; Sexton et al. 2004; Kafoury and Kelley 2005).

In response to Request for Preliminary Applications 98-6, "Health Effects of Air Pollution," Dr. Barbara Zielinska of the Desert Research Institute in Reno, Nevada, submitted an application entitled "Atmospheric Transformation of Diesel Emissions." She proposed to study the effects of photochemical transformations on DE constituents and whether such changes in chemical and physical form would also be reflected in changes in toxicity. She proposed to study the gas- and particle-phase products of atmospheric transformations under various exposure conditions in an atmospheric reaction chamber, including in daylight or dark conditions (to vary the extent of photochemical reactions) as well as with the addition of O_3 and radical precursors. In addition to detailed chemical characterization of the atmospheres, she proposed to evaluate the biologic effects of samples collected under these aging conditions. The atmospheric aging experiments would be conducted at the European Photoreactor (EUPHORE) outdoor simulation chamber in Valencia, Spain; the toxicologic experiments would be conducted in collaboration with Dr. JeanClare Seagrave at the Lovelace Respiratory Research Institute in Albuquerque, New Mexico, and other colleagues.

The HEI Health Research Committee thought that Dr. Zielinska's approach to studying the photochemical transformations of DE and their potential effects on its toxicity was novel and likely to produce interesting results. The Committee recommended the proposed study for funding, with a strong recommendation that the investigators use a modern diesel engine.

The 3-year study "Atmospheric Transformation of Diesel Emissions" by Dr. Zielinska and colleagues began in March 2003. Total expenditures were $609,330. The draft Investigators' Report was received for review in June 2007. A revised report, received in July 2008, was accepted for publication in October 2008. During the review process, the HEI Health Review Committee and the investigators had the opportunity to exchange comments and to clarify issues in both the Investigators' Report and the Health Review Committee's Critique.

*A list of abbreviations and other terms appears at the end of the Investigators' Report.

SCIENTIFIC BACKGROUND

Primary DE PM is emitted directly from diesel-powered engines. Secondary DE PM is formed by condensation of the gaseous and semivolatile compounds emitted by diesel engines into droplets and onto existing particles. The majority of particle-associated DE is composed of carbonaceous material (i.e., OC and elemental carbon [EC]); a small fraction is composed of inorganic compounds and metals — although the nature of diesel PM is changing rapidly, with the development of new control technologies that might cause a shift toward the emission of noncarbonaceous particles (Khalek et al. 2009). The EC component of diesel PM is generally inert to atmospheric degradation by reaction with sunlight or reactive compounds in the atmosphere. The OC fraction adsorbed onto diesel PM is composed of high-molecular-weight compounds, such as PAHs, that are generally more resistant to atmospheric reactions than PAHs in the gas phase (U.S. EPA 2002). Gas-phase DE compounds react primarily with hydroxyl (OH) radicals, hydroperoxyl radicals, nitrate (NO_3) radicals, O_3, dinitrogen pentoxide (N_2O_5), and nitric acid (HNO_3) as well as other compounds, such as nitrous acid (HONO) and sulfuric acid; many of these reactions require or are facilitated by sunlight (Atkinson 1988).

Several studies have investigated the formation, reaction, and consumption of PAHs to evaluate the process and characteristics of the atmospheric transformations of DE. It has been shown, for example, that, in the presence of NO_x, OH radicals react with naphthalene and related gaseous compounds present in DE, leading to the formation of mutagenic nitro-PAHs (Pitts et al. 1978; Atkinson et al. 1987; Arey et al. 1989); that PAHs deposited on combustion-generated fine particles and on model substrates react with O_3 (Van Vaeck and Van Cauwenberghe 1984; Finlayson-Pitts and Pitts 1986; Pitts et al. 1986); and that, in the particle phase, the extent of the photodegradation of PAHs depends very much on the nature of the substrate to which they are adsorbed (Behymer and Hites 1985; Dunstan et al. 1989).

A factor that complicates research on DE and its potential health effects is the substantive changes to diesel engine technology that have taken place in recent years as a result of the introduction of new, more stringent regulation of emissions, particularly in the United States and Europe. The U.S. EPA's emission standard for NO_x for new heavy-duty trucks and buses, for example, was reduced from 10.7 grams per brake horsepower per hour (g/bhp-hr) in 1984 to 0.2 g/bhp-hr in 2007, and the PM standard was reduced from 0.6 g/bhp-hr in 1984 to 0.01 g/bhp-hr in 2007, with further reductions required by 2010; in addition, the amount of sulfur allowed in fuel was reduced to 15 ppm starting with model year 2007 (U.S. EPA 2001; HEI Panel on the Health Effects of Traffic-Related Air Pollution 2010). (Brake horsepower is a measure of an engine's horsepower without the loss in power caused by the gearbox, alternator, and other auxiliary components.) There is thus a need to evaluate newer diesel engine technologies, including their emissions (Khalek et al. 2009), the atmospheric processing of their emissions, and the corresponding health effects (Ris 2007).

There is ample evidence of adverse health effects resulting from exposure to diesel emissions, especially to those of older diesel engine technologies. DE components have been shown to be mutagenic in cell cultures, and exposure to DE might contribute to an increased risk of lung cancer. In addition, human and laboratory-animal studies have shown that short-term and long-term exposure to DE can produce irritation of the eyes and nose, airway resistance, and inflammatory responses (e.g., HEI Diesel Epidemiology Working Group 2002; U.S. EPA 2002; HEI Air Toxics Review Panel 2007; Hesterberg et al. 2009; HEI Panel on the Health Effects of Traffic-Related Air Pollution 2010).

The toxicity of DE is associated with its chemical composition, which depends in turn on the engine type and fuel used and on the operating conditions. Particles collected from different types of engines have been shown to differ in their toxicity (e.g., DeMarini et al. 2004; Singh et al. 2004). However, few studies have taken into account the role that exhaust gases play or how exhaust gases and particles interact with each other and with other compounds in the atmosphere. In some cases, the lifetime of toxic compounds can be reduced by atmospheric reactions; in other cases, toxic compounds that were not present before can be newly created. Early studies showed that exposing DE-particle extracts to sunlight and O_3 reduced the mutagenic effects of DE organic compounds in vitro (Claxton and Barnes 1981; Stärk et al. 1985). More recent studies showed that photochemical products of 1,3-butadiene and isoprene enhanced inflammatory responses in human epithelial cells in vitro compared with cells exposed to 1,3-butadiene and isoprene alone (Doyle et al. 2004, 2007) and that photochemically produced gaseous compounds contributed to the observed inflammatory responses (Sexton et al. 2004). Similarly, DE particles treated with O_3 led to enhanced inflammatory responses compared with untreated DE particles alone, both in human epithelial cells in vitro (Kafoury and Kelley 2005) and in rats exposed to DE particles by way of intratracheal instillation (Madden et al. 2000).

Most of the evidence summarized here was obtained with specific compounds present in DE or with particle

extracts obtained from older diesel engine technologies. Research on the toxicity of whole DE under more realistic conditions, including atmospheric aging, and expansion of the scope of the research to newer diesel technologies are needed. For the present study, Dr. Zielinska and her colleagues proposed to expose rodents to extracts of aged diesel particles and volatile organic compounds (VOCs) by way of intratracheal instillation in order to evaluate a comprehensive set of biologic endpoints — including mutagenicity, cytotoxicity, inflammation, structural and functional changes in the lung, and oxidative stress — using an approach similar to that used in previous studies of engine exhaust in their laboratory (Seagrave et al. 2002).

SPECIFIC AIMS

The overall objective of Dr. Zielinska and her colleagues was to investigate photochemical transformations of diesel emissions in the atmosphere. The investigators hypothesized that these transformations would result in a change in the toxicity of DE in vivo. Their two primary specific aims were as follows:

1. To characterize the gas- and particle-phase products of atmospheric transformations of diesel emissions under the influence of sunlight, O_3, OH radicals, and NO_3 radicals; and
2. To explore changes in the biologic effects of DE before and after the atmospheric transformations had occurred.

METHODS

REACTION CHAMBER

Atmospheric aging of DE was conducted at the EUPHORE outdoor simulation chamber facility in Valencia, Spain. EUPHORE has two simulation chambers, each consisting of a half-spherical Teflon bag with a volume of about 200 m^3 and a retractable cover that allows reactions to take place in daylight or in the dark. DE was generated on-site using a 2003-model-year 1.8-L Ford light-duty diesel engine that was run on a dynamometer at about 50% load. The engine used diesel fuel that contained 47 ppm sulfur and 15% aromatic compounds and was allowed to warm up before its DE was injected into the chamber. The duration and number of DE injections were adjusted to limit the concentrations of NO_x being introduced into the chamber (see Sampling Campaigns below) and to prevent overheating of the engine.

In addition to DE, several compounds were added to the atmospheric mixture to create various aging conditions (see EUPHORE Chamber Conditions below). The mixture was allowed to react for 3 to 5 hours, during which time the investigators monitored chamber concentrations of NO_x, reactive nitrogen oxides (NO_y), sulfur dioxide (SO_2), O_3, peroxyacetyl nitrate, HONO, formaldehyde (CH_2O), VOCs, and particle mass, size, number, and volume concentrations. The investigators also monitored the nitrogen dioxide (NO_2) photolysis rate (which is a function of latitude, season, time, and cloud cover), temperature, pressure, and relative humidity. After completion of the reactions, the chamber cover was closed (if open, i.e., during daylight conditions), and integrated air samples were collected overnight for detailed chemical analyses at the Desert Research Institute and in vivo toxicologic experiments at the Lovelace Respiratory Research Institute.

SAMPLING CAMPAIGNS

The investigators conducted three sampling campaigns, in January 2005, May 2005, and May to June 2006, with the intention of looking at seasonal differences. They chose months that were expected to have minimal cloud cover. During the first campaign (winter 2005), the investigators found that high NO_x concentrations from the engine were interfering with the experiments. (When high NO_x concentrations are present, any OH radicals or O_3 formed in daylight conditions reacts with nitric oxide [NO] to form NO_2 and HNO_3, thus preventing reactions that might otherwise have occurred between the OH radicals or O_3 and organic compounds present in the mixture.) The investigators therefore decided to develop a NO_x denuder to remove the majority of NO_x from the exhaust prior to injection into the chamber. This process would lower the NO_x concentrations in the chamber to levels similar to those that normally occur in the atmosphere. A particular challenge was to find an efficient method of removing NO_x without substantially altering the concentrations and properties of the PM in the exhaust. In the end, cobalt oxide was selected for use as an absorption material to capture NO_x from the exhaust stream.

After the NO_x denuder was used in the second campaign (summer 2005), the design was improved further to allow even more efficient removal of NO_x for use in the third, final campaign (summer 2006). Because of these substantive changes in the experimental design, the main presentation of results in the Investigators' Report focuses on data obtained with a NO_x denuder in the second and third campaigns; full results are presented in the Appendices. Between sampling campaigns, the engine was not used but remained mounted on the dynamometer. At the end of the project, the engine had been operated for about 100 hours.

EUPHORE CHAMBER CONDITIONS

The investigators tested a variety of experimental aging conditions. An overview of the conditions is provided in Critique Table 1 (for a complete list, see Table 3 in the Investigators' Report). A key goal was to assess the difference between aging in daylight and in dark (nighttime) conditions; daylight allows photo-oxidation to take place, which is especially important for the formation of O_3 and leads to different sets of chemical reactions. In addition, several compounds — such as individual VOCs, VOC mixtures, or precursors to reactive radicals — that are part of the real-world ambient atmosphere and would influence the chemical reactions were added to the test mixtures. The following conditions were tested:

1. *DE in the dark or in daylight.* These served as baselines to evaluate the effects of photo-oxidation on the formation of reaction products in the absence of any other compounds.
2. *DE with added NO_3-radical precursors.* This was achieved by injecting a sufficiently high concentration (1–2.5 ppm) of O_3 into the chamber in the dark to oxidize all NO to NO_2; the O_3 then reacted with the NO_2 to form N_2O_5 and NO_3.
3. *DE with added OH-radical precursors.* This was achieved by heating a glass tube with 30 mg paraformaldehyde and introducing evaporated CH_2O into the chamber; the CH_2O then acted as a precursor to the formation of OH radicals in daylight.
4. *DE with added toluene.* This was achieved by injecting 500 ppb toluene into the chamber in daylight; the toluene simulated the presence of VOCs in ambient air.
5. *DE with various added VOC mixtures.* These conditions were tested in summer 2006 only, when the investigators discovered that the NO_x denuder appeared to remove aromatic compounds from DE. Two different VOC mixtures were added: Mixture #1 consisted of *p*-cymene, 1,2-diethylbenzene, 1,2,4-trimethylbenzene, and isobutylbenzene (all in liquid form) as well as naphthalene and 1,2,4,5-tetramethylbenzene (both in solid form); it was added to the chamber in the dark, together with NO_3 radicals (accomplished by injecting O_3 into the chamber; see condition 2 above). Mixture #2 consisted of mixture #1 plus benzene and *o*-xylene (both in liquid form); it was added to the chamber in daylight, with or without OH radicals (by adding evaporated CH_2O to the chamber; see condition 3 above).

Critique Table 1. Overview of Experimental Conditions During Three Sampling Campaigns at the EUPHORE Chamber[a]

Experimental Conditions	Campaign #1 Winter 2005	Campaign #2 Summer 2005	Campaign #3 Summer 2006
NO_x denuder use	None	Original model	Improved model
Aging in the dark with denuder		Chamber blank (1) DE (2) DE with NO_3 radicals[b] (2)	DE (2) DE with NO_3 radicals[b] and VOC mixture #1[c] (1)
Without denuder[d]	DE (4) DE with NO_3 radicals[b] (5)		DE (3) DE with NO_3 radicals (1)
Aging in daylight with denuder		Chamber blank (1) DE (2) DE with OH radicals[e] (4) DE with toluene (2)	Chamber blank (2) DE (1) DE with OH radicals[e] (1) DE with VOC mixture #2[c] (1) DE with OH radicals[e] and VOC mixture #2[c] (1) DE with toluene (2)
Without denuder[d]		DE (1)	

[a] Based on Table 3 of the Investigators' Report. Numbers in parentheses indicate the number of experiments conducted for each condition. After completion of 3 to 4 hours of atmospheric reactions in the dark or in daylight, parallel samples were collected overnight for chemical analysis and for toxicity testing. Some of the replicate samples collected for toxicity testing were combined to increase the mass available for intratracheal instillation in rats or mice.

[b] O_3 was introduced into the chamber to induce the formation of NO_3 radicals.

[c] Two different VOC mixtures containing naphthalene and other organic compounds were introduced into the chamber.

[d] Data from experiments without a NO_x denuder were not used in the final comparisons of results.

[e] Formaldehyde vapor was introduced into the chamber to induce the formation of OH radicals.

SAMPLE COLLECTION

Samples for analysis of semivolatile organic compounds (SVOCs) were collected overnight using an XAD denuder (XAD is an adsorbent resin used in sampling cartridges) to capture gas-phase compounds, followed by a Teflon filter and XAD cartridge at a flow rate of 100 L/min. Parallel samples for toxicity testing were collected using Teflon filters followed by two XAD cartridges at a flow rate of 200 L/min. In addition, gas-phase VOCs were collected in canisters, and DE particles were collected on quartz-fiber filters for analysis of OC, EC, sulfate, and nitrate. Samples were shipped to the Desert Research Institute for chemical analysis and to the Lovelace Respiratory Research Institute for toxicologic experiments.

CHEMICAL ANALYSES

The investigators measured a large number of compounds known to be present in DE, including alkanes, PAHs, nitro-PAHs, and polar compounds, as well as hopanes and steranes that are known to be present in lubricating oil (for a complete lists of compounds, see Tables 5 through 9 of the Investigators' Report). To quantify the amount of compound detected, deuterated internal standards were added to the Teflon filters and XAD cartridges prior to extraction in a dichloromethane/hexane/methanol (1:1:1) mixture. Extracts were analyzed by electron-impact gas chromatography (GC) followed by ion trap mass spectrometry or by GC followed by quadrupole mass spectrometry; polar and nonpolar compounds were analyzed separately.

The investigators measured EC and OC by a thermal optical reflectance method. During the process of heating the quart filters, some organic compounds pyrolized; these were recorded as pyrolized OC. Using various temperature stages, four OC and three EC fractions were obtained. Nitrate and sulfate were measured by ion chromatography.

TOXICITY TESTING

The investigators conducted two separate series of toxicologic experiments. Series A was conducted in male F344 rats with samples collected during the first and second sampling campaigns. Series B was conducted in male BALB/c mice with samples collected during the third sampling campaign, because the sample masses collected during this campaign were insufficient for intratracheal instillation in rats (mice have a much lower body weight than rats). Each sample was administered in three doses (250, 500, and 750 µg per rat and 25, 50, and 75 µg per mouse). If there was not enough sample mass to test all three doses, only the highest dose was tested. Samples collected for instillation were composed of about 10% PM and 90% SVOCs.

Each series contained a negative control, consisting of the fluid used to instill the samples, and a positive control, consisting of diesel soot (NIST Standard Reference Material 2975, collected from a fork lift; 1 mg for rats and 0.1 mg for mice prepared in the same manner as the other samples). In addition, a number of field blanks, consisting of extracts from unexposed filters, were also tested.

The animals were killed 24 hours after intratracheal instillation. Blood and lung lavage samples were collected for evaluation of markers of inflammation. Lung sections were evaluated for signs of inflammation, cytotoxicity, and parenchymal changes. In addition, markers of oxidative stress and macrophage phagocytosis were evaluated in mouse lung tissue and lavage fluid cells, respectively. The approach used was similar to that used in previous studies by the investigators (Seagrave et al. 2002).

STATISTICAL ANALYSES

Analyses of chemical-composition results were descriptive. Outlier values were flagged and removed if found to be invalid. Results were evaluated, taking into account the measurement errors of individual compounds, based on the detection limits of the analytic methods.

For the analyses of toxicity outcomes, a statistical test was performed to determine whether outliers were significantly different from the other values, and the outliers were removed if the P value was < 0.01. Subsequently, dose–response relations were determined by linear regression for each sample and each endpoint. The slope of the linear regression was reported as the "potency score." A one-way analysis of variance (ANOVA) was used to compare the results for each endpoint for all exposure conditions (except the positive control). The ANOVA was followed by Newman–Keuls or Dunnett post hoc tests if a significant effect was observed. Additional statistical analyses of the data collected with the use of a denuder included pairwise comparison of potency scores using unequal-variance t tests. Examples of pairwise comparisons included DE aged in the dark versus DE aged in daylight, DE aged in the dark versus DE aged in the dark with added NO_3 precursors, and DE aged in daylight versus DE aged in daylight with added toluene.

OVERVIEW OF KEY RESULTS

NO_x CONCENTRATIONS WITH AND WITHOUT DENUDER

In the first sampling campaign, NO_x concentrations in the chamber ranged from 450 ppb to various out-of-range

values (see Appendix C of the Investigators' Report — available at *www.healtheffects.org*), which is much higher than the typical concentrations of 50 to 200 ppb found in ambient air. In daylight conditions, these high NO_x concentrations interfered with the chemical reactions in the chamber — as evidenced by the low amount of organic compounds formed. Once a denuder was installed, NO_x concentrations in the chamber were somewhat reduced (to 210–960 ppb in the second sampling campaign). Further development of the denuder technology yielded a much more efficient device, resulting in substantially lower NO_x concentrations in the third campaign (7–35 ppb). Because it would not be very meaningful to compare results from experiments with and without a NO_x denuder, the results discussed here focus on the experiments in the second and third campaigns, when a NO_x denuder was in fact used.

ATMOSPHERIC REACTIONS OF DIESEL EXHAUST

The investigators reported that most of the exposures in daylight as well as the exposures in the dark with added NO_3-radical precursors led to particle formation and increased concentrations of SVOCs. This was evident in the increased fraction of OC in the samples and the increased OC/EC ratios compared with atmospheres containing only DE. The addition of toluene or VOCs in daylight led to the highest increases in organic compounds, including the formation of pyrolized OC, which is indicative of the presence of highly polar or oligomeric organic compounds. The investigators reported increased concentrations of many organic compounds, such as 9-fluorenone and other oxy-PAHs; nitro-naphthalene and other nitro-PAHs; certain nitropyrenes and nitrofluoranthenes; and polar compounds, such as heptanoic acid and oxalic acid. In addition, exposures in daylight led to the formation of O_3 and formic acid.

Concentrations of methylnaphthalenes and related compounds were reduced with the addition of reactants, especially in daylight with the addition of OH-radical precursors, VOCs, or toluene. Concentrations of *n*-alkanes, *n*-alkylcyclohexanes, and iso-alkanes were also reduced. Such reduced concentrations indicate that the primary compounds had been depleted, by way of the formation of secondary organic compounds (such as compounds with increased polarity).

It should be noted that the results from the second and third sampling campaigns were qualitatively different, probably owing to the differences in efficiency between the original and the improved NO_x denuders. The concentrations of nitrates and sulfates observed with DE alone, for example, were higher in the second campaign; the concentrations of PAHs and alkanes were higher in the third campaign.

TOXICITY OF AGED DIESEL EXHAUST

Because samples from the second and third campaigns were tested in two different animal species (rats and mice, respectively), the results were difficult to compare. However, some general patterns appeared that were consistent across both species. The investigators observed the following:

- increased cytotoxicity as assessed by histopathologic changes and concentrations of protein in lavage fluid after the addition of toluene to DE in daylight;
- increased histopathologic indications of inflammation after the addition of OH-radical precursors or toluene to DE in daylight;
- increased concentrations of polymorphonuclear neutrophils (PMNs) in lavage fluid (also an indicator of inflammation) after the addition of OH-radical precursors to DE in daylight; and
- decreased concentrations of alkaline phosphatase (an indicator of parenchymal changes) with DE in daylight compared with dark conditions; however, concentrations of this enzyme increased after the addition of toluene to DE in daylight.

Other results were less consistent: Concentrations of protein in lavage fluid, for example, increased in rats exposed to DE aged in daylight but decreased in mice. In addition, the effects of adding OH-radical precursors to DE in daylight on concentrations of macrophages and total cells in lavage fluid were opposite in the two species. The investigators stated that the latter result might have been an indication of differences in cell-adhesion processes between rats and mice.

Markers of oxidative stress were analyzed only in mice and yielded mixed results. Significant changes were observed under certain exposure conditions but not others, and in some cases the changes were the opposite of what would have been expected. Concentrations of heme oxygenase-1, for example, increased after the addition of VOCs to DE in daylight but decreased after the addition of toluene to DE in daylight. In addition, concentrations of thiobarbituric-acid–reactive substances (TBARS) increased in lung tissue after the addition of OH-radical precursors to DE in daylight but decreased in blood plasma after the addition of NO_3-radical precursors and VOCs to DE in the dark or after the addition of OH-radical precursors, toluene, or VOCs to DE in daylight. The most consistent effect observed was an increase in oxidized-glutathione concentrations after the addition of OH-radical precursors, VOCs, or both to DE in daylight and after the aging of DE in daylight without additional compounds.

The investigators concluded that the addition of toluene and, to a lesser extent, OH-radical precursors to DE

in daylight increased the toxic potential of the samples compared with DE aged in daylight without additional compounds.

It should be noted that one of the DE samples collected in the first sampling campaign — without having used a NO_x denuder or adding any compounds — appeared quite toxic. After intratracheal instillation of this sample, four of five rats died and showed large responses in lavage and histopathologic parameters (as described in Appendix D of the Investigators' Report, available at *www.healtheffects.org*). The most potent sample in mice was also a sample collected without the use of a NO_x denuder.

REVIEW COMMITTEE EVALUATION

In its independent review of the study, the HEI Health Review Committee thought that Dr. Zielinska and colleagues had successfully conducted a complex study to characterize the atmospheric transformations of DE (from a 2003-model-year light-duty diesel engine) aged under the influence of daylight, O_3, two radicals, and various organic compounds and that the resulting report presented a number of novel results. The strengths of the study design included the use of state-of-the-art atmospheric chamber facilities in Spain; the use of a realistic set of atmospheric aging conditions; and the chemical analyses of a large number of organic compounds. Another strength was the assessment, in parallel with the chemical analyses, of changes in biologic effects in rodents exposed to DE samples collected before and after the atmospheric transformations. A minor criticism might be that the use of a light-duty engine could be considered less relevant to the United States, because it has a much lower percentage of light-duty diesel engines than Europe does.

The Committee agreed with the investigators' conclusion that exposing DE to daylight (with or without additional VOCs), as well as adding NO_3-radical precursors to DE in the dark, resulted in increased particle mass concentrations and the formation of secondary organic compounds, such as oxy-PAHs and nitro-PAHs. The Committee thought the investigators had used an appropriate set of analytic chemistry techniques for the majority of measurements of compounds in the particle or gas phases, including the use of deuterated compounds for calibration. The Committee thought the list of compounds analyzed was extensive but agreed with the investigators that future studies could further characterize the formation of secondary products by, for example, analyzing additional organic compounds in PM using liquid chromatography–mass spectrometry and by measuring additional carbonyls, such as glyoxal and acetaldehyde. The current study was somewhat limited in that it measured only one carbonyl (i.e., CH_2O).

The Committee commended the investigators' efforts to develop an efficient NO_x denuder but concluded that the additional work had led to a reduced number of experiments and a set of somewhat disparate results that remain predominantly descriptive and qualitative in nature. The results of the first sampling campaign, conducted without a NO_x denuder, were not representative of reactions that might take place in ambient air. In addition, results from the second and third sampling campaigns were difficult to compare because of the use of two different NO_x denuders and rodent species. Although the investigators were appropriately cautious in their interpretations, further research will be needed to obtain a more complete, systematic, and quantitative set of results.

As to the NO_x denuder technology, it should be noted that the more efficient denuder used during the third campaign also removed some VOCs and particles, which reduced the number of chemical reactions that could take place. It would have been helpful if the VOC and particle losses caused by the second denuder had been determined and quantified in more detail. The investigators adjusted for these losses by adding VOC mixtures to the chamber atmosphere. However, the addition to the chamber of naphthalene as a component of the VOC mixture rendered it difficult to estimate the extent of the atmospheric transformation (whether formation or depletion) of the naphthalene that was already present in the engine emissions.

The finding of relatively high NO_x concentrations in the chamber in the first sampling campaign reinforced the notion that NO_x emissions might increase (relative to other DE components) with some of the newer diesel engine technologies that remove particles from the exhaust but do not have additional NO_x controls. Evaluation of the health effects of these newer engine technologies will have to proceed cautiously, because high NO_2 concentrations might produce acute toxicity, masking health effects caused by other compounds in the exhaust. For this reason, recent health-effects studies of DE have included exposures to NO_2 alone as a control condition (e.g., Sawant et al. 2008; Riedl et al. 2010 in press) or have limited the maximum DE concentration to minimize the potential for acute health effects caused by the NO_2 (McDonald and Mauderly 2010, in press). The fact that in the current study some animals died after intratracheal instillation of samples collected without a NO_x denuder reinforces the importance of ongoing regulatory efforts to reduce both particle and NO_x emissions in diesel engine exhaust.

One of the limiting factors of this study was the variable number of replicate experiments. Some atmospheric aging conditions were tested only once; others were tested up to four times. It was thus difficult to assess the extent of variability in the formation of certain compounds within

and among the experimental conditions. The investigators' approach relied on comparisons of fully aged atmospheres, insofar as only one sample was collected at the end of the 3-to-5-hour aging periods. An alternative approach would have been to compare samples collected at the beginning and the end of an aging period.

When using an atmospheric chamber that is situated outdoors, variable cloud cover can cause variations in the amount of light reaching the chamber, thereby influencing the extent to which photochemistry might drive the chemical reactions. An indoor location would allow for perfectly controlled light conditions. However, the investigators minimized the possibility that cloud cover would affect their experiments by planning them for months of the year that have a maximum amount of sunshine at that location. They observed some variation in relative humidity and the temperature of the engine intake air (as described in Appendix A of the Investigators' Report) that might have been indicative of slight weather variations. Such day-to-day variations might explain some of the variability in the results. The investigators also measured the photolysis rate (which varies according to latitude, cloud cover, and other factors) but did not include these data in the report.

The study's assessment of the toxicity of aged DE samples was well designed. Samples to be tested were collected using filters and XAD cartridges so as to capture both particles and gaseous components, an important improvement over many older studies of DE that assessed the effects of particles only. The investigators observed increased inflammation under certain conditions; changes in biochemical measures correlated fairly well with changes in histopathology. The Committee noted that several endpoints were used as indicators of oxidative stress and that some of these have been shown to be more reliable than others. This could account for the apparent discrepancies between increases in heme oxygenase-1 expression and concentrations of oxidized glutathione (indicating increased oxidative stress) and a lack of change in concentrations of TBARS in the lung. In addition, rats and mice have different sets of cytochrome P450 and other major detoxification enzymes in airway epithelium, which could lead to differences in biologic responses to the organic compounds in engine exhaust. It remains difficult to draw firm conclusions other than that atmospheric aging of DE generally seemed to increase the toxicity of the samples. Further research will be needed to evaluate which of the atmospheric reaction products might be contributing to the increased toxicity.

The large set of data generated under variable conditions also posed challenges with regard to statistical analysis. The results of the chemical analyses, which included a large number of chemical compounds, remained largely descriptive. Analysis of the results of toxicity testing was challenging, not only because of the many atmospheric aging conditions tested and the fact that conditions were not consistent across the sampling campaigns, but also because of the use of the two different rodent species and the many biologic endpoints that were assessed. Such a complex experimental design would generally call for a multifactorial statistical analysis. The investigators decided to take a simplified approach by analyzing data obtained in rats and mice separately and by calculating separate potency scores that represented a dose–response relationship for each biologic endpoint. In a set of supplemental statistical analyses, the investigators made pairwise comparisons of selected exposure atmospheres, such as comparing DE aged in daylight with DE aged in the dark or comparing DE aged in daylight with DE aged in daylight with added toluene. Although multifactorial analyses would have been preferable, the Committee thought that this was a reasonable approach.

SUMMARY

This complex study generated a large set of data on the detailed chemical composition of DE samples collected under a variety of experimental conditions intended to simulate real-world atmospheric aging of DE. The investigators observed that atmospheric aging under certain conditions, such as in daylight (which facilitates photochemical reactions) or with the addition of radical precursors (which facilitates chemical reactions), led to the formation of particles and secondary organic compounds. Atmospheric aging generally also increased the toxicity of the samples, as indicated by increased concentrations of markers of inflammation and oxidative stress in exposed rodents. However, the results remain preliminary because of differences among the various sampling campaigns, including the use of NO_x denuders of different efficiencies, variations in the number of replicate samples collected, and the use of two different rodent species (rats and mice) to evaluate biologic endpoints. Although the investigators observed changes in chemical composition and toxicity under certain atmospheric aging conditions, it remains difficult to relate specific chemical-reaction products to increased toxicity. Further systematic research on the composition and toxicity of DE and other pollution mixtures after atmospheric transformation is needed to provide more quantitative answers. Importantly, such research should cover the most recent diesel engine technologies that comply with the 2007 and 2010 PM and NO_x standards in the United States and have much lower emissions compared with older technologies, including the 2003 engine used in this study.

ACKNOWLEDGMENTS

The Health Review Committee thanks the ad hoc reviewers for their help in evaluating the scientific merit of the Investigators' Report. The committee is also grateful to Debra Kaden for her oversight of the study and to Annemoon van Erp and Mei Wang for their assistance in preparing its Critique; to George Simonson for the science editing of this Report and its Critique; and to Virgi Hepner, Fred Howe, and Flannery McDermott for their roles in publishing this Research Report.

REFERENCES

Arey J, Zielinska B, Atkinson R, Aschmann SM. 1989. Nitroarene products from the gas-phase reactions of volatile polycyclic aromatic hydrocarbons with OH radical and N_2O_5. Int J Chem Kinet 21:775–799.

Atkinson R. 1988. Atmospheric transformations of automotive emissions. In: Air Pollution, the Automobile, and Public Health (Watson AY, Bates RR, Kennedy D, eds). National Academy Press, Washington DC.

Atkinson R, Arey J, Zielinska B, Aschmann SM. 1987. Kinetics and products of the gas-phase reactions of OH radicals and N_2O_5 with naphthalene and biphenyl. Environ Sci Technol 21:1014–1022.

Behymer TD, Hites RA. 1985. Photolysis of polycyclic aromatic hydrocarbons adsorbed on simulated atmospheric particulates. Environ Sci Technol 19:1004–1006.

Claxton LD, Barnes HM. 1981. The mutagenicity of diesel-exhaust particle extracts collected under smog-chamber conditions using the Salmonella typhimurium test system. Mutat Res 88:255–272.

DeMarini DM, Brooks LR, Warren SH, Kobayashi T, Gilmour MI, Singh P. 2004. Bioassay-directed fractionation and salmonella mutagenicity of automobile and forklift diesel exhaust particles. Environ Health Perspect 112: 814–819.

Doyle M, Sexton KG, Jeffries H, Bridge K, Jaspers I. 2004. Effects of 1,3-butadiene, isoprene, and their photochemical degradation products on human lung cells. Environ Health Perspect 112:1488–1495.

Doyle M, Sexton KG, Jeffries H, Jaspers I. 2007. Atmospheric photochemical transformations enhance 1,3-butadiene-induced inflammatory responses in human epithelial cells: The role of ozone and other photochemical degradation products. Chem Biol Interact 166:163–169.

Dunstan TDJ, Mauldin RF, Jinxian Z, Hipps AD, Wehry EL, Mamantov G. 1989. Adsorption and photodegradation of pyrene on magnetic, carbonaceous, and mineral subfractions of coal stack ash. Environ Sci Technol 23:303–308.

Finlayson-Pitts BJ, Pitts JNJ. 1986. Atmospheric chemistry: Fundamentals and experimental techniques. John Wiley & Sons, New York, NY.

HEI Air Toxics Review Panel. 2007. Mobile-Source Air Toxics: A Critical Review of the Literature on Exposure and Health Effects. Special Report 16. Health Effects Institute, Boston, MA.

HEI Diesel Epidemiology Working Group. 2002. Research Directions to Improve Estimates of Human Exposure and Risk from Diesel Exhaust. Special Report. Health Effects Institute, Boston, MA.

HEI Panel on the Health Effects of Traffic-Related Air Pollution. 2010. Traffic-Related Air Pollution: A Critical Review of the Literature on Emissions, Exposure, and Health Effects. Special Report 17. Health Effects Institute, Boston, MA.

Hesterberg TW, Long CM, Bunn WB, Sax SN, Lapin CA, Valberg PA. 2009. Non-cancer health effects of diesel exhaust: A critical assessment of recent human and animal toxicological literature. Crit Rev Toxicol 39:195–227.

Kafoury RM, Kelley J. 2005. Ozone enhances diesel exhaust particles (DEP)-induced interleukin-8 (IL-8) gene expression in human airway epithelial cells through activation of nuclear factors-κB (NF-κB) and IL-6 (NF-IL6). Int J Environ Res Public Health 2:403–410.

Khalek IA, Bougher TL, Merritt PM. 2009. Phase 1 of the Advanced Collaborative Emissions Study. CRC Report: ACES Phase 1. Coordinating Research Council. Alpharetta, Georgia.

Madden MC, Richards JH, Dailey LA, Hatch GE, Ghio AJ. 2000. Effect of ozone on diesel exhaust particle toxicity in rat lung. Toxicol Appl Pharmacol 168:140–148.

McDonald JD, Mauderly JM. 2010. Advanced Collaborative Emissions Study Phase 3A: Characterization of engine-exposure system operation and potential animal exposure atmospheres. Health Effects Institute, Boston MA. In press.

Pitts JN Jr, Paur HR, Zielinska B, Arey J, Winer AM, Ramdahl T, Mejia V. 1986. Factors influencing the reactivity of polycyclic aromatic hydrocarbons absorbed on filters and ambient POM with ozone. Chemosphere 15:675–685.

Pitts JN Jr, Van Cauwenberghe KA, Grosjean D, Schmid JP, Fitz DR, Belser WL, Knudson GP, Hynds PM. 1978.

Atmospheric reactions of polycyclic aromatic hydrocarbons: Facile formation of mutagenic nitro derivatives. Science 202:515–519.

Riedl MA, Diaz-Sanchez D, Linn WS, Gong H Jr, Clark KW, Effros RM. 2010. Exacerbation of Allergic Inflammation in the Lower Respiratory Tract by Diesel Exhaust Particles. Health Effects Institute, Boston MA. In press.

Ris C. 2007. U.S. EPA health assessment for diesel engine exhaust: A review. Inhal Toxicol 19 Suppl 1:229–239.

Sawant AA, Cocker DR 3rd, Miller JW, Taliaferro T, Diaz-Sanchez D, Linn WS, Clark KW, Gong H Jr. 2008. Generation and characterization of diesel exhaust in a facility for controlled human exposures. J Air Waste Manag Assoc 58:829–837.

Seagrave J, McDonald JD, Gigliotti AP, Nikula KJ, Seilkop SK, Gurevich M, Mauderly JL. 2002. Mutagenicity and in vivo toxicity of combined particulate and semivolatile organic fractions of gasoline and diesel engine emissions. Toxicol Sci 70:212–216.

Sexton KG, Jeffries HE, Jang M, Kamens RM, Doyle M, Voicu I, Jaspers I. 2004. Photochemical products in urban mixtures enhance inflammatory responses in lung cells. Inhal Toxicol 16 Suppl 1:107–114.

Singh P, DeMarini DM, Dick CA, Tabor DG, Ryan JV, Linak WP, Kobayashi T, Gilmour MI. 2004. Sample characterization of automobile and forklift diesel exhaust particles and comparative pulmonary toxicity in mice. Environ Health Persp 112:820–825.

Stärk G, Stauff J, Miltenburger HG, Stumm-Fischer I. 1985. Photodecomposition of 1-nitropyrene and other direct-acting mutagens extracted from diesel-exhaust particulates. Mutat Res 155:27–33.

U.S. Environmental Protection Agency. 2001. Control of Air Pollution from New Motor Vehicles: Heavy-Duty Engine and Vehicle Standards and Highway Diesel Fuel Sulfur Control Requirements; Final Rule. 40 CFR Parts 69, 80, and 86. Fed Regist 66: 5002–5193. Available from *www.gpo.gov/fdsys/pkg/FR-2001-01-18/pdf/01-2.pdf*.

U.S. Environmental Protection Agency. 2002. Health Assessment Document for Diesel Engine Exhaust. EPA 600/8-90/057F. National Center for Environmental Assessment, Office of Research Development. Washington, DC. Available from *http://nepis.epa.gov*.

Van Vaeck L, Van Cauwenberghe K. 1984. Conversion of polycyclic aromatic hydrocarbons on diesel particulate matter upon exposure to ppm levels of ozone. Atmos Environ 18:323–328.

RELATED HEI PUBLICATIONS: PARTICULATE MATTER AND DIESEL EXHAUST

Number	Title	Principal Investigator	Date*
Research Reports			
145	Effects of Concentrated Ambient Particles and Diesel Engine Exhaust on Allergic Airway Disease in Brown Norway Rats	J.R. Harkema	2009
138	Health Effects of Real-World Exposure to Diesel Exhaust in Persons with Asthma	J. Zhang	2009
136	Uptake and Inflammatory Effects of Nanoparticles in a Human Vascular Endothelial Cell Line	I.M. Kennedy	2009
135	Mechanisms of Particulate Matter Toxicity in Neonatal and Young Adult Rat Lungs	K.E. Pinkerton	2008
134	Black-Pigmented Material in Airway Macrophages from Healthy Children: Association with Lung Function and Modeled PM_{10}	J. Grigg	2008
129	Particle Size and Composition Related to Adverse Health Effects in Aged, Sensitive Rats	F.F. Hahn	2003
128	Neurogenic Responses in Rat Lungs After Nose-Only Exposure to Diesel Exhaust	M.L. Witten	2005
126	Effects of Exposure to Ultrafine Carbon Particles in Healthy Subjects and Subjects with Asthma	M.W. Frampton	2004
124	Particulate Air Pollution and Nonfatal Cardiac Events		2005
	Part I. Air Pollution, Personal Activities, and Onset of Myocardial Infarction in a Case–Crossover Study	A. Peters	
	Part II. Association of Air Pollution with Confirmed Arrhythmias Recorded by Implanted Defibrillators	D. Dockery	
120	Effects of Concentrated Ambient Particles on Normal and Hypersecretory Airways in Rats	J.R. Harkema	2004
118	Controlled Exposures of Healthy and Asthmatic Volunteers to Concentrated Ambient Particles in Metropolitan Los Angeles	H. Gong Jr.	2003
117	Peroxides and Macrophages in Toxicity of Fine Particulate Matter	D.L. Laskin	2003
112	Health Effects of Acute Exposure to Air Pollution	S.T. Holgate	2003
	Part I. Healthy and Asthmatic Subjects Exposed to Diesel Exhaust		
	Part II. Healthy Subjects Exposed to Concentrated Ambient Particles		
110	Particle Characteristics Responsible for Effects on Human Lung Epithelial Cells	A.E. Aust	2002
107	Emissions from Diesel and Gasoline Engines Measured in Highway Tunnels		
	Part I. Real-World Particulate Matter and Gaseous Emissions From Motor Vehicles in a Highway Tunnel	A.W. Gertler	2002
	Part II. Airborne Carbonyls from Motor Vehicle Emissions in Two Highway Tunnels	D. Grosjean	2002
106	Effects of Combined Ozone and Air Pollution Particle Exposure in Mice	L. Kobzik	2001

Continued

** Reports published since 1999.*
Copies of these reports can be obtained from the Health Effects Institute and many are available at pubs.healtheffects.org.

RELATED HEI PUBLICATIONS: PARTICULATE MATTER AND DIESEL EXHAUST

Number	Title	Principal Investigator	Date*
105	Pathogenomic Mechanisms for Particulate Matter Induction of Acute Lung Injury and Inflammation in Mice	G.D. Leikauf	2001
104	Inhalation Toxicology of Urban Ambient Particulate Matter: Acute Cardiovascular Effects in Rats	R. Vincent	2001
101	Epithelial Penetration and Clearance of Particle-Borne Benzo[*a*]pyrene	P. Gerde	2001
96	Acute Pulmonary Effects of Ultrafine Particles in Rats and Mice	G. Oberdörster	2000
91	Mechanisms of Morbidity and Mortality from Exposure to Ambient Air Particles	J.J. Godleski	2000
Special Reports			
17	A Critical Review of the Health Effects of Traffic-Related Air Pollution		In Press
	Research Directions to Improve Estimates of Human Exposure and Risk from Diesel Exhaust		2002
	Diesel Emissions and Lung Cancer: Epidemiology and Quantitative Risk Assessment		1999
HEI Communications			
10	Improving Estimates of Diesel and Other Emissions for Epidemiologic Studies		2003
7	Diesel Workshop: Building a Research Strategy to Improve Risk Assessment		1999
HEI Program Summaries			
	Research on Diesel Exhaust and Other Particles		2003
	Research on Diesel Exhaust		1999
	Research on Particulate Matter		1999
HEI Perspectives			
	Understanding the Health Effects of Components of the Particulate Matter Mix: Progress and Next Steps		2002

** Reports published since 1999.*
Copies of these reports can be obtained from the Health Effects Institute and many are available at pubs.healtheffects.org.

HEI BOARD, COMMITTEES, and STAFF

Board of Directors

Richard F. Celeste, Chair *President, Colorado College*

Sherwood Boehlert *Of Counsel, Accord Group; Former Chair, U.S. House of Representatives Science Committee*

Enriqueta Bond *President Emeritus, Burroughs Wellcome Fund*

Purnell W. Choppin *President Emeritus, Howard Hughes Medical Institute*

Michael T. Clegg *Professor of Biological Sciences, University of California–Irvine*

Jared L. Cohon *President, Carnegie Mellon University*

Stephen Corman *President, Corman Enterprises*

Gowher Rizvi *Vice Provost of International Programs, University of Virginia*

Linda Rosenstock *Dean, School of Public Health, University of California–Los Angeles*

Henry Schacht *Managing Director, Warburg Pincus; Former Chairman and Chief Executive Officer, Lucent Technologies*

Warren M. Washington *Senior Scientist, National Center for Atmospheric Research; Former Chair, National Science Board*

Archibald Cox, Founding Chair *1980–2001*

Donald Kennedy, Vice Chair Emeritus *Editor-in-Chief Emeritus,* Science; *President Emeritus and Bing Professor of Biological Sciences, Stanford University*

Health Research Committee

Mark J. Utell, Chair *Professor of Medicine and Environmental Medicine, University of Rochester Medical Center*

Kenneth L. Demerjian *Ray Falconer Endowed Chair, Director and Professor, Atmospheric Sciences Research Center and Department of Atmospheric and Environmental Sciences, University at Albany, State University of New York*

Joe G.N. Garcia *Lowell T. Coggeshall Professor of Medicine, University of Chicago*

Uwe Heinrich *Professor, Medical School Hannover; Executive Director, Fraunhofer Institute for Toxicology and Experimental Medicine, Hannover, Germany*

Grace LeMasters *Professor of Epidemiology and Environmental Health, University of Cincinnati College of Medicine*

Sylvia Richardson *Professor of Biostatistics, Department of Epidemiology and Public Health, Imperial College School of Medicine, London, United Kingdom*

Richard L. Smith *Mark L. Reed Distinguished Professor of Statistics, University of North Carolina–Chapel Hill*

James A. Swenberg *Kenan Distinguished Professor of Environmental Sciences, Department of Environmental Sciences and Engineering, University of North Carolina–Chapel Hill*

Ira B. Tager *Professor of Epidemiology, School of Public Health, University of California–Berkeley*

HEI BOARD, COMMITTEES, and STAFF

Health Review Committee

Homer A. Boushey, Chair *Professor of Medicine, Department of Medicine, University of California–San Francisco*

Ben Armstrong *Reader in Epidemiological Statistics, Public and Environmental Health Research Unit, Department of Public Health and Policy, London School of Hygiene and Tropical Medicine, United Kingdom*

Michael Brauer *Professor, School of Environmental Health, University of British Columbia, Canada*

Bert Brunekreef *Professor of Environmental Epidemiology, Institute of Risk Assessment Sciences, University of Utrecht, the Netherlands*

Mark W. Frampton *Professor of Medicine and Environmental Medicine, University of Rochester Medical Center*

Stephanie London *Senior Investigator, Epidemiology Branch, National Institute of Environmental Health Sciences*

William N. Rom *Sol and Judith Bergstein Professor of Medicine and Environmental Medicine and Director of Pulmonary and Critical Care Medicine, New York University Medical Center*

Armistead Russell *Georgia Power Distinguished Professor of Environmental Engineering, School of Civil and Environmental Engineering, Georgia Institute of Technology*

Lianne Sheppard *Professor of Biostatistics, School of Public Health, University of Washington–Seattle*

Officers and Staff

Daniel S. Greenbaum *President*
Robert M. O'Keefe *Vice President*
Rashid Shaikh *Director of Science*
Barbara Gale *Director of Publications*
Jacqueline C. Rutledge *Director of Finance and Administration*
Helen I. Dooley *Corporate Secretary*

Kate Adams *Staff Scientist*
Aaron J. Cohen *Principal Scientist*
Maria G. Costantini *Principal Scientist*
Philip J. DeMarco *Compliance Manager*
Hope Green *Editorial Assistant (part time)*
L. Virgi Hepner *Senior Science Editor*
Sarah Katz *Research Associate*
Anny Luu *Administrative Assistant*
Francine Marmenout *Senior Executive Assistant*
Flannery Carey McDermott *Editorial Assistant*
Sumi Mehta *Senior Scientist*
Nicholas Moustakas *Policy Associate*
Tiffany North *Research Associate*
Hilary Selby Polk *Science Editor*
Sarah Rakow *Science Administrative Assistant*
Robert A. Shavers *Operations Manager*
Geoffrey H. Sunshine *Senior Scientist*
Annemoon M.M. van Erp *Senior Scientist*
Katherine Walker *Senior Scientist*

HEALTH
EFFECTS
INSTITUTE

101 Federal Street, Suite 500
Boston, MA 02110, USA
+1-617-488-2300
www.healtheffects.org

RESEARCH
REPORT

Number 147
April 2010